



**Michigan  
Technological  
University**

Michigan Technological University  
**Digital Commons @ Michigan Tech**

---

Dissertations, Master's Theses and Master's Reports

---

2022

## REVERSE CATIONIC FLOTATION OF HEMATITE

Natalia Parra Alvarez

*Michigan Technological University, nparra@mtu.edu*

Copyright 2022 Natalia Parra Alvarez


---

### Recommended Citation

Parra Alvarez, Natalia, "REVERSE CATIONIC FLOTATION OF HEMATITE", Open Access Dissertation, Michigan Technological University, 2022.

<https://doi.org/10.37099/mtu.dc.etr/1395>

Follow this and additional works at: <https://digitalcommons.mtu.edu/etr>

 Part of the [Other Chemical Engineering Commons](#)

REVERSE CATIONIC FLOTATION OF HEMATITE

By

Natalia Parra Alvarez

A DISSERTATION

Submitted in partial fulfillment of the requirements for the degree of

DOCTOR OF PHILOSOPHY

In Chemical Engineering

MICHIGAN TECHNOLOGICAL UNIVERSITY

2022

© 2022 Natalia Parra Alvarez

This dissertation has been approved in partial fulfillment of the requirements for the Degree of DOCTOR OF PHILOSOPHY in Chemical Engineering.

Department of Chemical Engineering

Dissertation Advisor: *Dr. S. Komar Kawatra*

Committee Member: *Dr. Rebecca G. Ong*

Committee Member: *Dr. Tony N. Rogers*

Committee Member: *Dr. Gowtham*

Department Chair: *Dr. Pradeep K. Agrawal*

# Table of Contents

List of Figures .....	vii
List of Tables .....	xiii
Author Contribution Statement.....	xv
Acknowledgements.....	xvii
Abstract.....	xviii
1 General Introduction .....	1
1.1 References .....	3
2 Iron Ore Flotation Review .....	4
2.1 Abstract .....	4
2.2 Flotation Process Description.....	4
2.3 Electrical Double Layer and Zeta Potential .....	5
2.4 Iron Ore Flotation Pathways.....	6
2.4.1 Direct Flotation of Iron Ore .....	7
2.4.1.1 Process Overview.....	7
2.4.1.2 Common Reagents in Direct Flotation of Iron Ore .....	8
2.4.2 Reverse Flotation of Iron Ore .....	8
2.4.2.1 Reverse Anionic Flotation .....	9
2.4.2.2 Reverse Cationic Flotation.....	14

2.5	Importance of Water Chemistry in Flotation .....	23
2.6	Conclusions .....	24
2.7	References .....	26
3	Recreating the Iron Ore Flotation Process in the Laboratory .....	37
3.1	Abstract .....	37
3.2	Introduction .....	38
3.3	Materials and Methods .....	45
3.3.1	Chemical reagents .....	45
3.3.2	Hematite ore sample collection and sampling methods.....	46
3.3.3	Water analysis and preparation.....	49
3.3.3.1	ICP Tests .....	49
3.3.3.2	Titration Tests .....	50
3.3.3.3	“Feed water” Preparation.....	52
3.3.4	Grinding.....	52
3.3.5	Size Distribution Analysis .....	53
3.3.6	Selective Flocculation and Dispersion (desliming) .....	54
3.3.7	Iron Content Determination .....	55
3.3.8	Reverse Cationic Flotation.....	57
3.4	Results and Discussion.....	58
3.4.1	Water Analysis and Preparation.....	58
3.4.2	Grinding.....	59
3.4.3	Selective Flocculation and Dispersion (desliming) .....	61

3.4.4	Reverse Cationic Flotation.....	65
3.4.5	Conclusion .....	68
3.4.6	References.....	70
4	Partially Substituting Amine with Frothers to Improve Iron Ore Flotation.....	73
4.1	Abstract .....	73
4.2	Introduction .....	74
4.2.1	Amine Collectors in Flotation.....	76
4.2.2	Frothers in Flotation.....	81
4.2.3	Frothing Ability of Amines and Frothers.....	85
4.3	Materials .....	89
4.4	Methods .....	91
4.4.1	Baseline of Flotation Experiments.....	91
4.4.2	Maximum Tolerable Froth Dosage Determination.....	92
4.4.3	Flotation Tests by Partially Replacing Amine with a Frother .....	93
4.5	Results and Discussion.....	93
4.5.1	Baseline of Flotation Experiments.....	93
4.5.2	Maximum Tolerable Froth Dosage Determination.....	94
4.5.3	Flotation Tests by Partially Replacing Amine with a Frother .....	95
4.6	Conclusions .....	98
4.7	References .....	98
5	Specifically Adsorbed Ions in the Reverse Cationic Flotation of Iron Ore .....	105
5.1	Abstract .....	105

5.2	Introduction .....	106
5.3	Materials .....	113
5.4	Methods .....	115
5.4.1	Sample Preparation .....	115
5.4.2	Flotation Tests and Iron Content Analysis.....	117
5.4.3	Zeta Potential Analysis .....	118
5.4.4	Settling Tests.....	118
5.5	Results and Discussion .....	119
5.5.1	Flotation and Entrainment Analysis.....	120
5.5.2	Zeta Potential Analysis .....	126
5.5.3	Settling Tests.....	131
5.6	Conclusions .....	135
5.7	References .....	136
6	Hydration of Hematite .....	141
6.1	Abstract .....	141
6.2	Introduction .....	141
6.3	Materials and Methods .....	143
6.4	Results and Discussion.....	145
6.5	Conclusion.....	150
6.6	References .....	150
A	Copyright documentation.....	151

## List of Figures

Figure 3.1: Simplified flotation-scavenger circuit at Plant A.....	42
Figure 3.2: Fine and low-grade hematite ore beneficiation process flowsheet (Mariani and Nelson, 1993; Keranen, 1986; Haselhuhn and Kawatra, 2015).....	42
Figure 3.3: Sampling locations at the iron ore concentrator plant. Location #1: Deslime thickener underflow, right before starch addition. Samples at this location had a $40.95 \pm 0.6\%$ grade and a particle size of $12.09 \mu\text{m}$ at 80% passing. Location #2: Autogenous mill screen underflow, right before dispersant addition. Samples at this location had a $32.32 \pm 0.7\%$ grade and a particle size of 0.8 mm at 80% passing. Collection dates included.....	47
Figure 3.4: Rotary riffle splitter at the Michigan Technological University laboratory....	48
Figure 3.5: X-Ray diffraction results for the hematite ore used in this investigation. Quartz: 65.15%, Hematite: 21.45%, Magnesioferrite: 7.7%, Goethite: 5.7%. .....	49
Figure 3.6: EDTA complexometric titration laboratory setup for total water hardness determination. ....	51
Figure 3.7: Color change as titration is performed carefully with the EDTA solution. When the indicator-ion complex is present the solution is pink, and when the indicator-ion complex is not present the solution is blue. ....	51
Figure 3.8: Grinding mill at Michigan Technological University laboratory.....	53
Figure 3.9: Microtrac SRA 9200 at Michigan Technological University laboratory. ....	54



Figure 3.10: Desliming cell at Michigan Technological University laboratory. ....	55
Figure 3.11: Calibration curve for iron content analysis. ....	57
Figure 3.12: Flotation cell at Michigan Technological University laboratory. ....	58
Figure 3.13: Particle size at 80% passing at four different grinding times without dispersant addition. ....	60
Figure 3.14: Particle size distribution after grinding for 50 minutes in the rod mill at a pH of 10.5 and 3 lb/ton of dispersant.....	61
Figure 3.15: Grade and recovery curve for desliming tests at a constant starch dosage of 0.1 lb/ton and varying dosages of dispersant presented as labels in the plot.....	62
Figure 3.16: Grade and recovery curve for desliming tests at a constant dispersant dosage of 3 lb/ton and varying dosages of starch presented as labels in the plot. ....	63
Figure 3.17: Grade and recovery curve for the desliming process at various dispersant and starch dosages listed in Table 4. The error bars indicate the 95% confidence interval. The best performance was observed at 3 lb/ton of dispersant and 0.0635 lb/ton of starch with a grade of $40.20 \pm 0.30\%$ Fe and recovery of $74.78 \pm 2.06\%$ . .....	65
Figure 3.18: Grade and recovery curve for the flotation process at a constant starch dosage (1.5 lb/ton) and various ether amine dosages presented as labels in the plot. ....	66
Figure 3.19: Grade and recovery curve for the flotation process at a constant ether amine dosage (1.5 lb/ton) and various starch dosages presented as labels in the plot. ....	67

Figure 3.20: Grade and recovery curve for the laboratory flotation circuit with one rougher stage and five scavenger stages. ....	68
Figure 4.1: Plateau border depiction.....	75
Figure 4.2: Primary, secondary, tertiary, and quaternary amine representation. ....	77
Figure 4.3: Bubble coalescence mechanism. The mechanism by which two bubbles merge into one single bubble during contact. ....	85
Figure 4.4: XRD results for the hematite sample used. Quartz: 65.15%, Hematite: 21.45%, Magnesioferrite: 7.7%, Goethite: 5.7%. ....	90
Figure 4.5: Visual transition from no frother dosage to the maximum tolerable frother dosage at which the froth starts overflowing without scraping. ....	92
Figure 5.1: Divalent ions complexes with the hydroxyl groups in the [100] plane of hematite.....	110
Figure 5.2: Zeta Potential of hematite ore at increasing concentrations of Magnesium, Calcium, Barium, and Strontium. ....	111
Figure 5.3: Sampling location at the iron ore concentrator plant: autogenous mill screen underflow, right before dispersant addition. Particle size: 0.8 mm at 80% passing. ....	114
Figure 5.4: X-Ray diffraction for the hematite ore used. Quartz: 65%, Hematite: 21% .	114
Figure 5.5: Chemical analysis of calcium and magnesium throughout grinding, desliming, and flotation in the laboratory setup. ....	120

Figure 5.6: Entrainment tests for hematite ore at various concentrations of calcium. For these tests, the magnesium concentration added was 0 ppm. ....122

Figure 5.7: Grade/Recovery curve at various concentrations of calcium. For these tests, the magnesium concentration added was 0 ppm. Slight reductions in zeta potential can cause flocculation of slimes thereby increasing recovery. Higher concentrations of calcium coat surfaces and activate both silicates and hematite for starch adsorption. The optimum flotation performance was obtained at 45 ppm calcium. Past this dosage both grade and recovery decreased.....123

Figure 5.8: Entrainment tests for hematite ore at various concentrations of magnesium. For these tests, the calcium concentration added was 0 ppm. ....124

Figure 5.9: Grade/Recovery curve at various concentrations of magnesium. For these tests, the calcium concentration added was 0 ppm. Slight reductions in zeta potential can cause flocculation of slimes thereby increasing recovery. Higher concentrations of magnesium coat surfaces and activate both silicates and hematite for starch adsorption. The optimum flotation performance was obtained at 7 ppm magnesium. Past this dosage both grade and recovery decreased. ....125

Figure 5.10: Zeta potential of flotation feed sample conditioned with increasing concentrations of magnesium or calcium at a pH of 10.5 (no starch added). Concentration expressed in ppm. ....128

Figure 5.11: Zeta potential of flotation feed sample conditioned with increasing concentrations of magnesium or calcium, followed by 1.5 lb/ton of starch at a pH of 10.5. Concentration expressed in ppm.....129

Figure 5.12: Zeta potential of flotation feed sample conditioned with increasing concentrations of magnesium or calcium at a pH of 10.5 (no starch added). Concentration expressed in molarity (mmol/L).....130

Figure 5.13: Zeta potential of flotation feed sample conditioned with increasing concentrations of magnesium or calcium, followed by 1.5 lb/ton of starch at a pH of 10.5. Concentration expressed in molarity (mmol/L).....131

Figure 5.14: Settling tests for a fully hydrated iron ore at 10.5 pH with varying concentrations of calcium and starch. Calcium activates the starch for adsorption and increases flocculation of particles. ....132

Figure 5.15: Settling tests for a fully hydrated iron ore at 10.5 pH with varying concentrations of magnesium and starch. Magnesium activates the starch for adsorption and increases flocculation of particles. ....133

Figure 5.16: Settling tests for a fully hydrated iron ore at 10.5 pH conditioned with 1.5 lb/ton of starch and increasing calcium concentrations. An increase in calcium will not change the settling rate of solids significantly.....134

Figure 5.17: Settling tests for a fully hydrated iron ore at 10.5 pH conditioned with 1.5 lb/ton of starch and increasing magnesium concentrations. As magnesium increases, it affects the adsorption of starch to the ore. ....135

Figure 6.1: Zeta potential of hematite in a sodium bicarbonate/sodium carbonate buffer solution over a period of 48 hours. Initial pH of 10.43 and final pH of 10.27. ...146

Figure 6.2: Zeta potential of hematite in an ammonium hydroxide/ammonium chloride buffer solution over a period of 24 hours. Initial pH of 10.95 and final pH of 9.18. ....147

Figure 6.3: Zeta potential of hematite in a solution containing sodium hydroxide (NaOH) mixed with sodium chloride (NaCl) over a period of 1 hour. Initial pH of  $9.9 \pm 0.1$  and final pH of  $9.3 \pm 0.2$ . ....148

Figure 6.4: Zeta potential of silica in a solution containing sodium hydroxide (NaOH) mixed with sodium chloride (NaCl) over a period of 1 hour. Initial pH of  $10.1 \pm 0.05$  and final pH of  $7.8 \pm 0.8$ . ....149

## List of Tables

Table 2.1: Anionic and cationic flotation summary (Based on Zhang et al., 2021). .....	25
Table 3.1: Grinding, desliming, and flotation performance targets provided by Plant A..	44
Table 3.2: Water hardness comparison between Houghton’s city water, flotation process water at the plant, and the feed water used for recreating the flotation process at Michigan Tech for one batch of experiments. ....	59
Table 3.3: Particle size at 80% passing after grinding for 50 minutes at a pH of 10.5 both without dispersant addition and with 3 lb/ton of dispersant. ....	60
Table 3.4: Grade and recovery values for the desliming process at various dispersant and starch dosages. It was determined that 3 lb/ton of dispersant and 0.0635 lb/ton of starch yielded grade and recovery values within the targets established for this process. This reagent combination was performed in triplicate for statistical accuracy. ....	64
Table 3.5: Summary of results of grinding, desliming and flotation in the laboratory.....	69
Table 4.1: Aryl amines, alkyl amines, and alkyl-arid amines classification.....	78
Table 4.2: CCC and DFI values for MIBC and PPG 1012 (Gupta et al., 2007).....	90
Table 4.3: Dosage determination for partial amine replacement with MIBC.....	94
Table 4.4: Dosage determination for partial amine replacement with PPG 1012 .....	94
Table 4.5: Flotation results after partially substitution the ether amine collector with MIBC frother .....	95

Table 4.6: Flotation results after partially substitution the ether amine collector with PPG1012 frother .....	96
Table 5.1: Ionic species concentration in process water at various locations in an iron ore concentration plant (Haselhuhn and Kawatra, 2015).....	108
Table 5.2: Water chemistry comparison between municipal water available at Michigan Tech, flotation process water at the plant, and the feed water used for grinding and desliming at the Michigan Tech Laboratory.....	116
Table 5.3: Summary of flotation performance with only deionized water and at optimal dosages of calcium and magnesium separately and combined.....	126
Table 6.1: Zeta potential variability of hematite in 50 ml of deionized water at increasing ionic strength conditions controlled by NaCl additions. Tests performed in triplicate. ....	144

# Author Contribution Statement

This dissertation includes previously reviewed and published material. Full citations are as follows:

## Chapter 1:

Chapter 1 was completely rewritten and modified by the author of this dissertation. Most of the content was obtained and properly cited from the following paper:

Zhang, X., Gu, X., Han, Y., **Parra-Álvarez, N.**, Claremboux, V., and Kawatra, S. K., 2021, “Flotation of Iron Ores: A Review”, *Mineral Processing and Extractive Metallurgy Review*, DOI: 10.1080/08827508.2019.1689494

## Chapter 5:

Reprinted with permission from **N. Parra-Álvarez**, H. J. Haselhuhn, V. Claremboux & S. K. Kawatra (2021) Specifically Adsorbed Ions in the Reverse Cationic Flotation of Iron Ore, *Mineral Processing and Extractive Metallurgy Review*, DOI:

10.1080/08827508.2021.2018314.

Author contributions:

### Parra-Álvarez

Experimental work with exception of data shown in Figures 5.1 and 5.2, analysis and interpretation of data, writing of the paper, responsible for submission and review of journal article.

### Haselhuhn

Experimental work and interpretation of data presented in Figures 5.1 and 5.2, paper review, and editing.



Claremboux

Analysis and interpretation of data, paper review, and editing.

Kawatra

Research guidance, paper review, and editing.

**Chapter 6:**

Reprinted with permission from **Parra-Álvarez, N.**, Claremboux, V., and Kawatra, S. K., 2022, “Hydration of Hematite,” Mineral Processing and Extractive Metallurgy Review (planned for submission in the near future)

Author contributions:

Parra-Álvarez

Experimental design, experimental work and data collection, analysis and interpretation of data, writing of the paper, responsible for submission and review of journal article.

Claremboux

Experimental design, analysis and interpretation of data, paper review, and editing.

Kawatra

Research guidance, paper review, and editing.

## **Acknowledgements**

First of all, I would like to thank my advisor, Dr. S. Komar Kawatra, for all his support, guidance, and advice over the past few years. Without him this work would not have been possible. I would also like to thank my research group for all their help and support. I would like to extend my thanks to Cleveland Cliffs and Solvay for providing materials, advice, and part of the funding for my work.

My deepest gratitude goes to my parents, Adriana Alvarez Vesga and Juan Carlos Parra Osorio, my brother Sebastian, and my grandparents, Jesus, Sofia, Enrique, and Ruby for always believing in me and supporting me throughout this journey. Finally, I would like to thank God for giving me strength and guidance along the way.

## Abstract

The reverse cationic flotation of hematite is the most common method to process hematite ores. The goal of this research is to understand the impact of fundamental water and surface effects to enable the optimization of the flotation process. At present, reverse cationic flotation is performed using a single chemical as both collector and frother. Excessive amounts of frother or collector should lead to diminished performance. This research investigates this phenomenon by replacing some of the collector with frothers. It was found that flotation recovery can be improved up to 2.5wt% via 10% replacement with methyl isobutyl carbinol (MIBC). Since most frothers are less expensive than the amine collector, there is a possibility of reducing cost of reagents and increasing profits in industry.

There is a large body of literature on the impact of calcium on the flotation process. However, despite magnesium and calcium often being treated as interchangeable in literature and practice, magnesium's smaller atomic size suggests that its behavior in flotation should be stronger. This research investigates the effect of calcium and magnesium in the adsorption of starch onto the hematite. We have found that initially both ions are beneficial to the process but as the magnesium concentrations increase, it becomes detrimental to flotation. These results make it clear that magnesium is not a one-for-one replacement of calcium in iron ore flotation, and should be accounted for and, if necessary, controlled separately.

Lastly, the time it takes for the hematite to become fully hydrated may play a role in flotation. If the hydration of fresh surfaces takes place during the ½ to 2 hours that the

hematite is expected to reside in the concentration process, then this could have a significant impact in flotation. In this research, the time scale of the hydration of pure hematite was determined to be on the order of 5 to 20 minutes, which tells us that in a plant-scale operation, it is very likely that the hematite is completely hydrated before it reaches flotation. These findings demonstrate improved understanding of reverse cationic flotation, which leads to a set of clear process recommendations.

# 1 General Introduction

The objective of this dissertation is to gain a deeper understanding of the intricacies of the reverse cationic flotation process to enable process optimization. In particular, this research seeks to highlight key points which are 1) novel, i.e. unrecognized or underrecognized in the literature, 2) likely to have a critical impact on the flotation process, 3) which can identify key points of the flotation process which can be further improved upon. This work both helps to refine our understanding of the fundamentals of flotation while allowing for clear and meaningful recommendations for industrial practice.

Though the flotation of iron ore first began in America in 1931 (Zhang et al., 2021) and received considerable attention, there are still many aspects of flotation which are addressed through empirical observation and experience alone. For instance, local hematite beneficiation plants have noticed that high levels of water hardness led to poor flotation performance due to poor rejection of impurities but did not have a scientific explanation for this effect. Another example is the role of the hydration of the fresh hematite surface sites produced during crushing and grinding. These surface sites are known to react with water. However, it is unclear from the literature that these fresh surface sites have any impact on flotation because it may be that by the time the ore has traversed the plant from comminution to flotation, they have all completely hydrated. This dissertation seeks to provide scientific explanations to these and other parts of the flotation process.

Chapter 2 of this dissertation serves as an introductory chapter for this research. It is a review of the iron ore flotation process including the three iron ore flotation pathways and the reagents used for each process. This chapter also covers the importance of the desliming process prior to reverse cationic flotation and the function of the reagents used during this operation. Other factors that affect flotation and deslime such as zeta potential and water chemistry are briefly introduced in this section.

Chapter 3 describes recreating the iron ore flotation process in the laboratory for baseline experiments, and develops the standard operating procedures for this research. In this section, laboratory process conditions for grinding, desliming and flotation were determined with the goal of obtaining a final flotation concentrate comparable to the beneficiation plant's concentrate. These conditions or parameters include water chemistry, grinding time, reagent dosages, conditioning times, and step by step procedures.

In Chapter 4 the idea of partially replacing the amine collector with a frother is developed. Most flotation processes use collectors and frothers to selectively float minerals. This is not the case in reverse cationic flotation of hematite, where ether amine acts as both the collector and the frother. Partially replacing amine with a frother enables greater control of the frothing characteristics of the process while also providing an opportunity to reduce overall reagent cost. This section evaluates the use of different frothers in flotation to improve the overall iron recovery in the process and minimize reagent costs.

Chapter 5 explores the impact of water chemistry stemming from different amounts of calcium and magnesium in the flotation of iron ore. This section proposes and develops evidence to support that the smaller atomic size of magnesium causes it to interact more strongly and less selectively with the surface of the iron ore. At very low concentrations both calcium and magnesium help to improve the adsorption of starch to hematite, but the stronger interaction of magnesium lead to magnesium becoming detrimental to the overall separation process at far lower concentrations than calcium does.

Similarly, Chapter 6 investigates the importance of hematite hydration in flotation.

Experimental work was performed primarily seeking to answer the question of how long it takes to hydrate hematite. By establishing that on average hydration will take less time than it will take for the freshly ground ore to travel from the grinding process to the flotation process, it can be ruled out as a variable of concern for process optimization.

## **1.1 References**

- Zhang, X., Gu, X., Han, Y., Parra-Álvarez, N., Claremboux, V., and Kawatra, S. K., 2021, “Flotation of Iron Ores: A Review”, Mineral Processing and Extractive Metallurgy Review, DOI: 10.1080/08827508.2019.1689494

## **2 Iron Ore Flotation Review**

### **2.1 Abstract**

Several researchers have studied the flotation of iron ore and the variety of reagents that are used in this process. This chapter is a detailed review of iron ore flotation, including general aspects of the flotation process, the three different flotation pathways in iron ore and the reagents used, the electrical double layer and the importance of water chemistry in froth flotation. Additionally, this chapter explores the main advantages and disadvantages of direct flotation, reverse anionic flotation, and reverse cationic flotation. The main purpose of this chapter aside from serving as an introductory section for the entire research is to provide a detailed review of the current status of iron ore flotation to be used as a guide for future developments and process improvements.

### **2.2 Flotation Process Description**

In mineral processing, froth flotation is a separation method based on differences in surface properties. Particularly differences in the level of hydrophobicity or water affinity. In flotation a slurry is placed in a cell with an impeller that stirs and injects bubbles from the bottom of the cell. As bubbles rise to the surface due to buoyancy, hydrophobic particles adsorb to them and float to the surface where a froth is created. This froth is continuously removed until the desired separation is achieved. Meanwhile, the hydrophilic particles remain in the pulp or liquid phase until they are removed as an underflow product.



Most minerals found in natural ore reserves do not have sufficient differences in hydrophobicity to be separated. For this reason, surfactants known as collectors are added to the system to increase the hydrophobicity of a selected mineral. Furthermore, surfactants known as frothers are typically added to maintain the strength and stability of the air bubbles so that they do not collapse as soon as they are in contact with particles and the size and froth properties can be controlled. Depending on the process, other surfactants known as modifiers need to be added to the system. Modifiers include a broad range of surfactants such as dispersants, flocculants, pH modifiers, activators, among other which will be described in later sections (Nakhaei and Irannajad, 2018).

One of the most important modifiers used in iron ore flotation is the pH modifier which is in charge of controlling the pH of the slurry throughout the process. The pH of the slurry is a critical parameter in all flotation systems since it defines the surface charge of particles and determines the adsorption mechanisms between mineral particles and surfactants. The surface charge of particles can be better understood with the concept of the electrical double layer and zeta potential.

## **2.3 Electrical Double Layer and Zeta Potential**

The interaction between particles, water, and surfactants greatly depends on the electrostatic effects. These effects can be measured as the zeta potential in any charged particle in suspension. When a particle is suspended in a liquid, an immobile layer of a specific thickness is formed around it. This layer denominated as the “boundary layer” can be divided into two electrostatic regions: stern layer and diffuse layer. The stern layer is the first layer formed around the mineral surface. It is described as one layer of ions

charged oppositely to the surface charge. Depending on the charge of the stern layer, the diffuse layer can be partially negative or positive. The stern layer and diffuse layer together constitute the so called electrical double layer. After the immobile boundary layer comes a boundary known as the slipping plane. Past this point the liquid will no longer move with the particle but with the bulk fluid. The zeta potential is defined as the electrostatic potential at the slipping plane. (Carlson and Kawatra, 2013; Hunter, 1993)

The pH is one of the main factors that establishes the zeta potential of a mineral surface. As the pH changes, the concentration of hydroxide anions and hydronium cations is affected, thus provoking changes on the zeta potential (Zhang et al., 2021). Typically, surfaces tend to carry a positive charge at low pH values and a negative charge at high pH values. The isoelectric point (IEP) is the pH value where the zeta potential is neutral. This value varies based on the type of mineral. As a reference an IEP of 2.65 (pH) has been recorded for a quartz sample while an IEP of 6.5 (pH) has been recorded for a hematite sample (Zhang et al., 2021). This means that below a pH of 2.65 both quartz and hematite would carry a positive charge and above a pH of 6.5 both minerals would carry a negative charge. Hence, the pH of the solution is key to determining the type and concentration of reagents needed in the process.

## **2.4 Iron Ore Flotation Pathways**

Flotation can be divided into two general pathways: direct flotation and reverse flotation. The main difference between these two pathways is the way that the valuable product is recovered. In direct flotation the valuable iron material is recovered in the froth product

whereas in reverse flotation it is recovered in the sinks or underflow product. A detailed description and common reagents used in each pathway are described below.

## **2.4.1 Direct Flotation of Iron Ore**

### *2.4.1.1 Process Overview*

In direct flotation the iron is floated with the help of a collector while the gangue material is recovered in the underflow product. This process was originally developed in the U.S. by Hanna Mining and American Cyanamid around the 1930's and the 1940's, and implemented in processing plants located in Michigan and Minnesota around the 1950's (Zhang et al., 2021; Filippov et al., 2014). This process can be performed in various flotation media, but alkaline and acidic media are the most common. The direct flotation route with an alkaline media has been used by the Humbolt concentrator (U.S), the Donganshan concentrator (China), and the Republic mine (U.S) (Zhang et al., 2021). For this process sodium carbonate is used to maintain a pH of 9-10, and fatty acids such as a combination of oleic, linoleic, and rosin acids are added as collectors (Iwasaki, 1983; Houot, 1983; Zhang et al., 2021). This process is not sensitive to slimes or fine silica particles but there are some separation limitations due to the surface similarities between the iron and the gangue materials (Zhang et al., 2021).

The main advantage of the acidic media compared to the alkaline media is that the iron and the gangue have very different surface charges resulting in a better performance (Bunge et al., 1977). This method has been used by the Groveland mine (U.S), and the Qidashan concentration (China) (Houot, 1983; Yong, 2005; Zhang et al., 2021). Unlike the alkaline media, this process is very sensitive to slimes as the negatively charge

ultrafine material can coat the iron particles and inhibit separation (Zhang et al., 2021). The Maanshan Mine Research Institute in China compared the direct flotation process with alkaline media to the acidic media and concluded that even though the flotation performance is greater in the acidic media, the need for desliming and higher concentrations of collector makes it costlier (Zhang et al., 2021). Due to the low grades and high reagent consumption the direct flotation pathway for iron ores is not commonly practiced nowadays.

#### *2.4.1.2 Common Reagents in Direct Flotation of Iron Ore*

The direct flotation of iron ore was performed with anionic collectors such as fatty acid, hydroxamates, and petroleum sulfonates (Zhu et al., 2016; Zhang et al., 2021). Other surfactants used included soaps, resin acids, alkyl sulfonates, and alkyl sulfates (Liu et al., 2007; Zhang et al., 2021). The direct flotation of iron ore was replaced years ago by reverse flotation due to complications with gangue depression among other factors.

#### **2.4.2 Reverse Flotation of Iron Ore**

In reverse flotation the gangue material is floated while the iron is recovered in the underflow product. This pathway can be divided into two groups based on the type of collector used during the process. In reverse anionic flotation an anionic collector is used to collect positively charged quartz whereas in reverse cationic flotation a cationic collector is used to collect negatively charged quartz. While anionic flotation is more popular in China, cationic flotation is commonly used in the U.S and other western countries (Zhang et al., 2021; Filippov et al., 2014).

#### *2.4.2.1 Reverse Anionic Flotation*

In the reverse anionic flotation process, positively charged silica is floated with the help of anionic collectors while the iron concentrate is recovered in the underflow. Due to the low IEP values of silica minerals, these particles are only positively charged at acidic conditions (Zhang et al., 2021). However, the reverse anionic flotation process is typically performed at alkaline conditions (pH of 11-12). In this process, calcium and magnesium cations are added as activators to the system to change the surface charge of silica from negative to positive while the iron is depressed with a starch depressant (Zhang et al., 2021). The benefits of this process include lower desliming requirements and in some cases lower reagent cost as the fatty acid collectors used can be obtained from paper plants waste (Forsmo et al., 2008; Zhao et al., 2012; Zhang et al., 2021). Reverse anionic flotation of iron ore was first developed in the U.S. by Hanna Mining and American Cyanamid using iron ore deposits from Lake Superior (Zhang et al., 2021; Filippov et al., 2014). During this process, desliming is not required. Instead, the silica is activated with calcium chloride and the iron oxide is depressed with dextrin (Zhang et al., 2021). The anionic collector used is known as Acintol A2 mainly composed of tall oil and the pH of the slurry is maintained around 11.5 adjusted with caustic soda (Zhang et al., 2021). When this method was developed the grades obtained averaged 60.3% iron and 6% silica. However, in the U.S. this process was replaced by the reverse cationic flotation process due to the high cost of reagents and filtration problems (Filippov et al., 2014; Zhang et al., 2021).

Nowadays the reverse anionic flotation process is not very common in the U.S but it is very popular in China (Yuan et al., 2007; Zhang et al., 2021). The Anshan-type iron ore constitutes 55% of the iron ore reserves in China. About 40% of this ore is characterized by low grades and complex mineralogy (Han et al., 2006; Sun, 2006; Zhang et al., 2021). This type of ore is processed in various Chinese concentrator plants such as the Qidashan concentrator, the Sijiayin mine, the Yuanjiacun concentrator and the Gongchangling concentrator by a process composed of grinding, gravity separation, magnetic separation, and reverse anionic flotation (Zhang et al., 2021). Typically, calcium oxide is used as an activator, corn starch as a depressant, and a modified fatty acid as a collector, while maintaining a pH of 11.5 with caustic soda (Zhang et al., 2021). Depending on the ore characteristics the steps prior to flotation are adjusted.

#### *2.4.2.1.1 Common Reagents in Reverse Anionic Flotation*

##### *2.4.2.1.1.1 Anionic Collectors*

The dissociation of anionic collectors in water results in a negative surface charge which is attracted to positive surface charges. The anionic collectors in iron ore flotation can be classified into two groups: carboxylic acids and their salts, and alkyl sulfonates and their salts (Zhang and Dai, 2012; Zhang et al., 2021). The most common example of carboxylic acids are fatty acids such as sodium oleates and oleic acids (Zhang and Dai, 2012). Similarly, sodium petroleum sulfonate is the most common collector in the alkyl sulfonates category (Zhang and Dai, 2012).

The larger the carbon chain of the fatty acid, the stronger its collecting power (Zhang et al., 2021). However, fatty acids with long carbon chains can become insoluble, thus no

longer useful in flotation (Quast, 2006). The effectivity of a fatty acid is also dependent on the pH of the slurry. At alkaline conditions long-chained fatty acids can be more effective than short-chained fatty acids. For instance, Quast (2006) observed that dodecanoic acid is more effective at pH values higher than 5, while octanoic acid is more effective at pH values lower than 7.

Abaka-Wood et al. (2017) tested sodium oleate, alkyl hydroxamic acid, and sodium dodecylsulfate in the flotation of hematite and monazite. The best recovery with sodium oleate was obtained at a pH of 9. In the case of sodium dodecylsulfate a high pH value was beneficial up to pH 10, and with alkyl hydroxamic acid a pH range of 7-9 was ideal. A higher recovery of monazite was obtained with sodium oleate whereas a higher recovery of iron was obtained with sodium dodecylsulfate (Abaka-Wood et al., 2017; Zhang et al., 2021).

Recently in China, anionic collectors with the RA series have been developed with tar oil and a combination of unchlorinated and chlorinated oleic acid and fatty acids (Luo et al., 2015; Zhang et al., 2021). Collectors such as RA-315 have been tested with Gongchangling and Donganshan iron ores and results show good selectivity and collecting power (Luo et al., 2015). A benefit of these RA series collectors is their low prices, low toxicity, and good performance (Luo et al., 2015).

#### *2.4.2.1.1.2 Activators in Reverse Anionic Flotation*

In some cases, collectors cannot adsorb naturally onto the desired mineral surfaces. Activators are added to promote the adsorption of the collector onto the surface by modifying surface charges. Reverse anionic flotation is typically performed at alkaline

conditions; thus, both the collector and the mineral surfaces are negatively charged.

Because the collector adsorbs onto the surface mainly via electrostatic interactions, it is necessary to activate the mineral surface by making it positively charged.

Most quartz minerals require polyvalent metal cations such as  $\text{Fe}^{2+}$ ,  $\text{Mg}^{2+}$ , and  $\text{Ca}^{2+}$  for activation (Zhang et al., 2021). The most common activator in the reverse anionic flotation of iron ore is calcium oxide (CaO). The activation power of calcium oxide greatly depends on the pH of the slurry. At pH values over 11, calcium hydroxide ( $\text{Ca}(\text{OH})^+$ ) is more common and leads to a strong silica activation (Zhang et al., 2021).

However, at pH values lower than 11, calcium cations ( $\text{Ca}^+$ ) are more common leading to a weak activation of silica (Zhang et al., 2021).

#### *2.4.2.1.1.3 Depressants in Reverse Anionic Flotation*

In flotation, depressants are used to lower the hydrophobicity of particles or inhibit collector adsorption onto particles that are not desired in the froth product. In reverse anionic and cationic flotation, the iron particles are depressed with the help of depressants such as starch, dextrin, carboxymethylcellulose (CMC), or guar (Nakhaei and Irannajad, 2018). Among these, starch is the most popular depressant as it has low cost, high availability, and is effective (Nakhaei and Irannajad, 2018). Starch is a polymer formed naturally by plants for energy storage. The main sources for industrial starch include corn, potato, rice, cassava, wheat, and others (Perez and Bertoft, 2010).

Most industrial starches contain 70-80% amylopectin, 20-30% amylose, and less than 1% proteins and lipids (Nakhaei and Irannajad, 2018). Amylopectin is a branched structure composed of amylose straight chains of glucose monomers. Hydrogen bonds link



amylose and amylopectin together. The site spacing between the hydroxyl groups of these molecules matches the average hydroxyl group of hematite, which explains one of the mechanisms of starch adsorption onto hematite (Haselhuhn, 2015; Zhang et al., 2021).

Pavlovic and Brandao (2003) tested the depressant behavior of amylose, amylopectin, starch, maltose and glucose on silica and hematite. It was determined that amylose, amylopectin, and starch depress both silica and hematite, though the last two depressed silica more than amylose (Pavlovic and Brandao, 2003). The main reason why amylose is the least effective flocculant is due to its linear structure compared to the branched structure of amylopectin. A study performed by Iwasaki and Lai (1965) determined that when starch has high contents of amylopectin it adsorbs more readily to the hematite compared to amylose. However, 20-30% amylose is still desirable in industrial starch as it has low depression effects on silica compared to amylopectin, making starch more selective towards hematite (Zhang et al., 2021).

The depressant behavior of starch is also dependent on pH. Ma and Bruckard (2010) observed a low starch affinity for kaolinite, a silicate clay mineral, at high pH values. Meanwhile, below a 9 pH, the surface of kaolinite carries a more positive charge which adsorbs more readily to the starch surface. This shows the importance of performing reverse anionic and cationic flotation at high pH conditions.

Another depressant known in the iron industry is carboxymethylcellulose (CMC).

Poperechnikova et al. (2017) tested a modified CMC with iron ore and obtained final concentrates with iron grades greater than 68%. However, an increase in iron losses was

observed when using CMC compared to starch, as well as an increase in reagents cost (Poperechnikova et al., 2017). Similarly, Turrer and Peres (2010) compared the depression effect of various CMC, guar gum, humic acid, and lignosulphonates depressants and concluded that only CMC and guar gum achieved a similar flotation performance than with only starch due to the glucopyranose rings that they all have in common. Even with the ongoing tests and development of new depressants for iron ore, starch is still the most common depressant used in reverse anionic and cationic flotation of iron ore.

#### *2.4.2.2 Reverse Cationic Flotation*

This process was developed by the U.S Bureau of Mines and is the most common flotation route used in the U.S and other western countries (Zhang et al., 2021; Filippov et al., 2014). This process is principally found in the U.S, Canada, Brazil, Chile, Russia and India (Lima et al., 2013; Peres et al., 2009). Because a cationic collector is used, the quartz particles need to be negatively charged. However, quartz is negative except during very acidic conditions so this process can theoretically be performed in a broad pH range (Zhang et al., 2021). Typically, this process is performed at alkaline pH conditions so the iron and silica particles can remain dispersed from each other during the separation process. At alkaline conditions the hematite usually carries a negatively charged surface, so for the cationic collector to selectively adsorb onto the silica, a depressant needs to be added to inhibit collector adsorption onto the hematite.

In the U.S, Tilden Mine performs selective flocculation and dispersion followed by reverse cationic flotation using an unneutralized primary ether amine collector, corn

starch as a flocculant and depressant, caustic soda as a pH modifier, and sodium polyacrylates as a dispersant (Villar and Dawe, 1975; Zhang et al., 2021). The ore processed at this location is very unique as it is very fine with a size of 25  $\mu\text{m}$  at 80% passing and very low-grade ( $\sim 30\%$  Fe) (Villar and Dawe, 1975). The final concentrate averages 64-67% iron grade, and 5% quartz (Zhang et al., 2021).

In the Sept-Iles concentrator in Canada the final concentrate contains a 64% iron grade, and 4.5% silica after going through a circuit composed of eight rougher cells, three cleaners, four primary scavengers, and four secondary scavengers (Gagnon, 1981). In Brazil, there are around ten different concentrators that perform reverse cationic flotation of iron ore with hematite ore from the Iron Quadrangle (Peres et al., 2009). In the Candelaria's mine in Chile, the copper tailings containing iron ore (2-10%) are mixed with a magnetite ore of approximately 40% grade obtain from Mina de Los Colorados and treated in Planta Magnetite with a process that consists on magnetic separation, grinding, desliming, and reverse cationic flotation which results in a final concentrate of 66% grade (Oyarzun, 2013).

The Mikhailovsk plant (MMPP) in Russia concentrates the ore with magnetic separation followed by reverse cationic flotation (Varicheva et al., 2017; Zhang et al., 2021). The final product in this plant averages 69.7% iron grade (Varicheva et al., 2017; Zhang et al., 2021). In India, the slimes or tailings from alumina plants undergo reverse cationic flotation of iron along with magnetic separation or hydrocyclones (Jain et al., 2013; Kumar et al., 2010; Zhang et al. 2019).

In summary, the reverse cationic flotation of iron ore is the most common process used in the iron ore industry nowadays. However, China is the exception, where the reverse anionic flotation process is very popular. There is not much data available to explain why China prefers the anionic route, but it may be related to the ore mineralogy and reagents availability (Zhang et al., 2021). Plants that follow the reverse cationic flotation process usually process very fine ores that require desliming prior to flotation. Because desliming requires a high level of dispersion, it is very common to be followed by cationic flotation as high levels of dispersion are also desired (Zhang et al., 2021).

#### *2.4.2.2.1 Desliming Process*

The desliming process consists on separating slimes or ultrafine gangue particles (mainly silica) from coarser iron minerals. Desliming is a very important step in the reverse cationic flotation as slimes increase the consumption of reagents and lower the flotation efficiency (Lima et al., 2012; Zhang et al., 2021). In the iron ore industry, slimes are defined as particles finer than 10  $\mu\text{m}$  and in some instances particles finer than 20  $\mu\text{m}$  (Krishnan and Iwasaki, 1984). If the slimes are not removed prior to flotation and a dispersive state is not maintained, these ultrafine silica particles can adsorb to coarser iron ore particles and prevent separation. Additionally, slimes can adsorb to air bubbles reducing mineral attachment and cause problems in filtration (Edwards et al., 1980; Iwasaki, 2000). Due to the large surface area of slimes, they can adsorb and consume more reagents during the process (Lima et al., 2012).

Overall, slimes negatively impact the flotation process. Studies like Filippov et al. (2010) show that removing particles below 20  $\mu\text{m}$  prior to flotation increase the selectivity of the

reverse cationic flotation process. There are several techniques to remove slimes, but the most common include the use of hydrocyclones or thickeners (Zhang et al., 2021).

Studies such as Mohanty and Das (2010) and Jena et al. (2015) show how to select and design hydrocyclones based on the process characteristics. Each process may require unique vortex finder diameters, inlet pressures, type and concentration of reagents, among other parameters (Mohanty and Das, 2010).

The use of hydrocyclones and thickeners to remove slimes are considered as conventional techniques (Zhang et al., 2021). However, a more common technique in the iron ore industry is the selective flocculation and dispersion technique. This process consists on ensuring a high dispersion of ultrafine silica particles by maintaining alkaline conditions meanwhile a flocculant such as starch is added to selectively flocculate the hematite particles. The alkaline conditions are generally maintained with caustic soda, but the addition of dispersants such as sodium silicates and tripolyphosphates are recommended to control dispersion (Zhang et al., 2021). Selective flocculation and dispersion helps remove slimes while reducing iron losses which is a major problem when using conventional techniques (Colombo, 1980; Colombo and Frommer, 1976).

This technique is used in the U.S. by Tilden Mine where a low grade (~30% iron) and fine ore (~25  $\mu\text{m}$ ) hematite ore undergoes selective flocculation and dispersion prior to flotation to improve the grade up to 40% iron (Zhang et al., 2021). This process heavily relies on water chemistry as high concentrations of divalent cations are known to be detrimental to the process (Haselhuhn et al., 2012). Heerema et al. (1982) determined that even low concentrations of calcium ions (0.001 M) in the process water can cause low

selectivity. Data shows decreasing grades from 48.5% to a maximum of 32% iron in the presence of calcium ions (Heerema et al., 1982).

#### *2.4.2.2.2 Common Reagents in Reverse Cationic Flotation*

##### *2.4.2.2.2.1 Cationic Collectors*

The dissociation of cationic collectors in water results in a positive surface charge which is attracted to negative surface charges. Amines constitute the majority of cationic collectors used in reverse cationic flotation. Initially, fatty amines such as dodecylamine were used in iron ore, but later they were replaced by ether amine collectors due to the low selectivity, and poor collection power of dodecylamine (Ma, 2012). There are several investigations that compare the effectivity of different cationic collectors in iron ore. The main conclusion is that the proper selection of a cationic collector greatly depends in the ore mineralogy and process conditions.

Papini et al. (2001) compared the use of ether monoamines, ether diamines, fatty amines, and condensates in the reverse cationic flotation of silica from iron ore obtained from the Iron Quadrangle in Brazil. It was determined that for that specific ore, ether monoamine resulted in the best performance, followed by ether diamines (Papini et al., 2001). Fatty acids and condensates showed poor selectivity for this process (Papini et al., 2001). It is important to note that ether diamines have been reported to be more effective than ether monoamines when dealing with coarser ores (Nakhaei and Irannajad, 2018).

Other researchers have investigated the use of quaternary ammonium collectors. For instance, Weng et al. (2013) developed a quaternary ammonium reagent composed of hydrocarbon tails and ester bonds which was tested with a Chinese magnetite ore. Results

showed an increasing the collecting power, a greater temperature range, and better frothing patterns than a dodecylamine chloride collector (Weng et al., 2013; Zhang et al., 2021). Similarly, Sahoo et al. (2015) tested a quaternary ammonium salt composed of a mixture of hydrocarbon chains (C8 and C10) with a nitrogen functional group (Zhang et al., 2021). After testing this collector with an indian hematite ore, an iron grade and recovery of 65% and 60% respectively were obtained (Sahoo et al., 2015; Zhang et al., 2021).

Gemini surfactants have recently been tested by Huang et al. (2014) and Nakhaei and Irannajad (2018) for use in reverse cationic flotation. The use of ethane-1,2-bis(dimethyldodecylammonium bromide) (EBAB) gemini surfactant resulted in a higher iron grade and a lower silica content than tests performed with a conventional cationic reagent known as DAC (dodecylammonium chloride).

Aside from the continuing development of cationic collectors in the iron ore industry, ether amines are still the most common collectors used. Among the most common commercial ether amines found in iron ore plants in western countries include Aerosurf MG584, Aerosurf MG 98, Armac CES342, Aerosurf MG70A3, MG83A, and M98A3 (Nakhaei and Irannajad, 2018).

#### *2.4.2.2.2 Depressants in Reverse Cationic Flotation*

Just as in the reverse anionic flotation, starch is the most common iron ore depressant in the reverse cationic flotation. The theory and studies described in Section 2.4.2.1.1.3 apply for this section as well. Research specifically performed for the reverse cationic flotation of iron ore include the one by Kar et al. (2013) who compared the depression

effect of soluble starch, corn starch, potato starch, and rice starch using a dodecylamine collector. The best performance was obtained by soluble starch which resulted in the best hematite depression followed by corn starch, rice starch, and finally potato starch which obtained the lowest hematite depression (Kar et al., 2013). Potato starch and rice starch resulted in the lowest silica depression though not enough to show a better performance than soluble starch (Kar et al., 2013). The maximum starch adsorption was observed between 5-9 pH (Kar et al., 2013).

#### *2.4.2.2.2.3 Frothers in Reverse Cationic Flotation*

In the reverse cationic flotation, frothers are rarely added separately as the typical amine collectors used have frothing characteristics at alkaline conditions. Houot (1983) mentions that propylene glycols and certain alcohols have been used in the U.S such as methyl isobutyl carbinol (MIBC) which is a weak frother often utilized in the flotation of magnetite (Zhang et al., 2021). Even though the use of separate frothers is not very common in the reverse cationic flotation of iron, researchers are investigating the possibility of partially replacing the ether amine collector with a frother in order to improve the flotation efficiency.

In flotation, solids can be recovered in the froth via true flotation or entrainment.

Entrainment happens when both silica and iron oxide particles suspended in the water are trapped by bubbles and transferred to the froth (Nykänen et al., 2018). Iron entrainment is a great cause of low recoveries in the concentrate, thus it is of great importance to control it. Froth structure and stability is one of the main factors that affects entrainment (Pita, 2015; Dobby, 2002). The problem lies on controlling the froth dosage without reducing



the collector power necessary to float the hydrophobic material. By partially replacing the amine collector with a frother it might be possible to independently control the frothing and collecting properties separately and reduce entrainment (Zhang et al., 2021).

Silva et al. (2008) performed laboratory and industrial tests at Vargem Grande iron ore concentrator in Brazil. In these tests, the 20-30% neutralized ether amine collector was partially replaced with a frother composed of a blend of alcohols, esters, and aldehydes. It was determined that a 10% amine replacement with the chosen frother improved the iron recovery from 67.96% to 80.78% and the grade from 64.92% to 65.43%. Other researchers have performed similar studies; however, further studies are required to determine which frothers work best and what is the effect of different ore mineralogy. Chapter 4 of this dissertation discusses this topic in depth.

#### *2.4.2.2.2.4 Dispersants in Reverse Cationic Flotation*

In the reverse cationic flotation, dispersants are used to maintain dispersion of particles during the desliming process. Dispersion of fine silica particles is particularly important to achieve separation. The most common dispersants used in industry include sodium silicate, sodium carbonate, sodium hydroxide, sodium tripolyphosphate, sodium hexametaphosphate, sodium henicosapolyphosphate, and ethylenediaminetetraacetic acid (Haselhuhn, 2015). Studies show that sodium silica is effective at dispersing kaolinite only at acidic conditions (Ma, 2011). Considering that the reverse cationic flotation of iron ore is performed at alkaline conditions, sodium silica is not the most ideal dispersant for kaolinite (Ma, 2011). On the contrary, polyacrylic acid and sodium polyphosphate are effective at up to 10.5 pH (Ma, 2011).

#### 2.4.2.2.2.5 *Flocculants in Reverse Cationic Flotation*

In the reverse cationic flotation, flocculants are used to accomplish selective flocculation during the desliming process. Flocculants help create larger flocs of iron particles that can settle faster with the purpose of reducing the amount of iron in the tailing's product during desliming. Starch is the most common flocculant in iron ore, however, humate, and polyacrylamide have also been used for this purpose (Zhang et al., 2021). Starch is widely used as a depressant in flotation, however, this natural polymer plays a very important role during desliming. Starch can form hydrogen bonds and complexes with the surface of the iron allowing it to be a selective flocculant. In the U.S, the Tilden mine successfully performs selective flocculation and dispersion with corn starch (Zhang et al., 2021).

It has been reported that the amylopectin component of starch is in charge of the flocculating action due to its branched structure and high molecular weight, while amylose improves the selectivity of separation by suppressing the action of the amylopectin due to the co-adsorption of these molecules (Weissenborn, 1996; Zhang et al., 2021). Natural starch usually contains a 1:3 ratio of amylose to amylopectin which seems to be optimal for the selective flocculation of iron (Zhang et al., 2021).

The use of other flocculants in iron ore have been studied by several authors. For instance, Ng et al. (2015), proposed the use of temperature-sensitive polymers such as poly(N-isopropylacrylamide) (PNIPAM) which is highly hydrophilic, soluble in water, and with strong dispersing abilities below 32°C, and is highly hydrophobic and tends to precipitate above 32°C (Ng et al., 2015). The advantage of this reagent compared to

polyacrylamide flocculants is that the hydrophobic flocculation is reversible with temperature changes and it can be used as a flocculant, dispersant, or collector by adjusting the temperature (Ng et al., 2015). The high selectivity of this reagent allows it to flocculate iron particles larger than 20  $\mu\text{m}$  in contrast to the flocculation ability of sodium oleate (Ng et al., 2015).

Tripathy et al. (2001) studied the flocculating action of sodium alginate-g-polyacrylamide grade VI (SAG-VI) polymer and observed a similar performance to commercially available flocculants, and concluded that neutral flocculants are better at flocculating iron ore slimes with small particles compared to slimes with large particles. Furthermore, Kemppainen et al. (2016) studied the flocculating action of anionic cellulose nanofibers such as sulfonated cellulose nanofibers (ADAC) and dicarboxylic acid (DCC). It was found that between a pH of 5-10, both surfactants selectively flocculated the hematite while there was minimum interaction with quartz (Kemppainen et al., 2016).

## **2.5 Importance of Water Chemistry in Flotation**

Water chemistry control is unique for each individual process. The reverse cationic flotation process is especially sensitive to water chemistry parameters such as the presence of specifically adsorbed ions such as calcium and magnesium in the process. The effect of these ions in flotation depends on the ore mineralogy, reagents used, among other factors (Tang and Wen, 2018). In some instances, calcium and magnesium have been found to promote flotation performances, yet most of the time they are known to be detrimental to flotation. In anionic reverse flotation, calcium and magnesium ions help activate the silica for collector adsorption (Cao et al., 2013; Ruan et al., 2018; Fuerstenau

and Palmer, 1976). However, in cationic reverse flotation high concentrations of calcium and magnesium result in lower grade and recoveries (Fuerstenau and Palmer, 1976; Lelis et al., 2019; Lelis et al., 2020). The effect of these ions in reverse cationic flotation is further explored in Chapter 5.

Some methods to control divalent cations concentrations in the process include chemical complexation and precipitation. The most common chemicals used for complexation are ethylenediaminetetraacetic acid (EDTA), sodium hexametaphosphate (SHMP), and sodium tripolyphosphate (STPP) (Manukonda and Iwasaki, 1987; Arol and Iwasaki, 1987). Some dispersants added during the process are also known to sequester divalent ions and help control the water chemistry. Precipitating calcium with carbonates or other ultrasonic techniques have been reported to be effective for water chemistry control (Iwasaki, 2000).

## **2.6 Conclusions**

- Reverse flotation is the most favorable pathway for iron ore flotation. Due to the low grades and high reagent consumption the direct flotation pathway for iron ores is not commonly practiced nowadays.
- Choosing between cationic and anionic reverse flotation greatly depends on the characteristics of the ore and reagent's availability. The U.S. and other western countries typically prefer cationic flotation whereas China mostly operates following the reverse anionic flotation pathway.
- The main advantages and disadvantages of anionic and cationic flotation are summarized as follows:

Table 2.1: Anionic and cationic flotation summary (Based on Zhang et al., 2021).

	<b>Advantages</b>	<b>Disadvantages</b>
<b>Cationic Reverse Flotation</b>	<ul style="list-style-type: none"> <li>• Higher flotation rates.</li> <li>• Simpler reagent systems.</li> <li>• Simpler operation.</li> <li>• Low temperatures allowed.</li> </ul>	<ul style="list-style-type: none"> <li>• High slimes sensitivity.</li> <li>• Foaming properties that uncontrolled can cause lower grades.</li> <li>• Higher toxicity with a negative environmental impact.</li> </ul>
<b>Anionic Reverse Flotation</b>	<ul style="list-style-type: none"> <li>• Low slimes sensitivity.</li> <li>• Lower cost of anionic collectors compared to cationic collectors.</li> <li>• High selectivity due to use of quartz activators with iron depression effects such as calcium activators.</li> </ul>	<ul style="list-style-type: none"> <li>• High quantities of activator required which makes the overall cost of reagents higher than the cationic route.</li> <li>• High process temperatures required.</li> <li>• Filtration issues have been reported.</li> </ul>

- Desliming step is crucial for cationic flotation and greatly recommended for anionic flotation. Excessive amounts of slimes may cause low selectivity and very high reagents consumption. Selective flocculation and dispersion is the most common technique for slimes removal.
- There are many novel surfactants in iron ore flotation especially in the areas of collectors and depressants. However, there is still a need for further investigation of less toxic cationic collectors with more controllable frothing properties (higher efficiency). Chapter 4 of this dissertation explores the option of partially substituting amine collectors with frothers for greater performance and cost savings.
- To understand and further optimize flotation processes it is important to study the role of the zeta potential of minerals and water chemistry sensitivity in flotation.

## 2.7 References

- Abaka-Wood, G. B., Addai-Mensah, J., and Skinner, W., 2017. “A study of flotation characteristics of monazite, hematite, and quartz using anionic collectors,” *International Journal of Mineral Processing*, 158:55–62. doi:10.1016/j.minpro.2016.11.012.
- Arol, A. I., and Iwasaki, I., 1987. “Control of montmorillonite via complexation and ultrasonics in the selective flocculation of iron ores,” *Mining, Metallurgy & Exploration*, 4 (2):82–87. doi:10.1007/BF03403448.

- Bunge, F. H., Morrow, J. B., and Trainor, L. W., 1977. “Developments and realizations in the flotation of iron ores in North America,” *Iron, XIIIth IMPC*, Sao Paulo.
- Carlson, J. J., and Kawatra, S. K., 2013. “Factors affecting zeta potential of iron oxides,” *Mineral Processing and Extractive Metallurgy Review*, 34(5), pp. 269-303.
- Cao, Z., Zhang, Y., and Cao, Y., 2013. “Reverse flotation of quartz from magnetite ore with modified sodium oleate,” *Mineral Processing and Extractive Metallurgy Review*, 34(5), pp. 320-330. DOI: 10.1080/08827508.2012.675531.
- Colombo, A. F., and Frommer, D. W., 1976. “Cationic flotation of mesabi range oxidized taconite,” *In Flotation A.M. Gaudin memorial volume*, ed. M. C. Fuerstenau, 1285–304. USA: SME-AIME.
- Colombo, A. F., 1980. “Selective flocculation and flotation of iron bearing materials,” *In Fine particles processing*, ed. P. Somasundaran, Vol. 2, 1034–56. New York: SME-AIME.
- Dobby, G., 2002. “Column flotation. In Mineral processing plant design, practice and control,” ed. A. L. Mular, D. N. Halbe, and D. J. Barratt, 1239–52. Littleton: SME Inc.
- Edwards, C. R., Kipkie, W. B., and Agar, G. E., 1980. “The effect of slime coatings of the serpentine minerals, chrysotile and lizardite, on pentlandite flotation,” *International Journal of Mineral Processing*, 7(1):33–42. doi:10.1016/0301-7516(80)90035-6.

- Filippov, L. O., Filippova, I. V., and Severov, V. V., 2010. “The use of collectors mixture in the reverse cationic flotation of magnetite ore: The role of Fe-bearing silicates,” *Minerals Engineering*, 23 (2):91–98.  
doi:10.1016/j.mineng.2009.10.007.
- Filippov, L. O., Severov, V. V., and Filippova, I. V., 2014. “An overview of the beneficiation of iron ores via reverse cationic flotation,” *International Journal of Mineral Processing*, 127:62–69. doi:10.1016/j.minpro.2014.01.002.
- Forsmo, S. P. E., Forsmo, S. E., Björkman, B. M. T., and Samskog, P. O., 2008. “Studies on the influence of a flotation collector reagent on iron ore green pellet properties,” *Powder Technology*, 182:444–52. doi:10.1016/j.powtec.2007.07.015.
- Fuerstenau, M. C., and Palmer, B. R., 1976. “Anionic flotation of oxides and silicates,” *Society of Mining Engineers of AIME, Mineral Processing Division, Gaudin, A. M., Fuerstenau, M. C., Eds.; American Institute of Mining, Metallurgical, and Petroleum Engineers*, New York, NY, USA, pp. 148-196.
- Gagnon, B., 1981. “Iron ore company of Canada Zv concentrator flowsheet description and process development,” *Superintendent Sept-Iles*.
- Han, Y., Yuan, Z., Li, Y., and Chen, B., 2006. “Advances in mineral processing technology of China metallic mine and its development orientation,” *Metal Mine*, 1:34–52. (in Chinese).
- Haselhuhn, H. J., 2015. “The dispersion and selective flocculation of hematite ore,” *Michigan Technological University*.



- Haselhuhn, H. J., Carlson, J. J., and Kawatra, S. K., 2012. “Water chemistry analysis of an industrial selective flocculation dispersion hematite ore concentrator plant,” *International Journal of Mineral Processing*, 102:99–106. doi:10.1016/j.minpro.2011.10.002.
- Heerema, R. H., Lipp, R. J., and Iwasaki, I., 1982. “Complexation of calcium ion in selective flocculation of iron ores,” *Trans. SME-AIME* 272:1879–84.
- Houot, R., 1983. “Beneficiation of iron ore by flotation-review of industrial and potential applications,” *International Journal of Mineral Processing*, 10 (3):183–204. doi:10.1016/0301-7516(83)90010-8.
- Huang, Z., Zhong, H., Wang, S., Xia, L., Zou, W., and Liu, G., 2014. “Investigations on reverse cationic flotation of iron ore by using a Gemini surfactant: Ethane-1, 2-bis (dimethyl-dodecyl-ammonium bromide),” *Chemical Engineering Journal*, 257:218–28. doi:10.1016/j.cej.2014.07.057.
- Hunter, R. J., 1993. “Introduction to Modern Colloid Science,” Oxford, NY, *Oxford University Press*.
- Iwasaki, I., 1983. “Iron ore flotation, theory and practice,” *Mining Engineering*, 35:622–31.
- Iwasaki, I., 2000. “Iron ore beneficiation in the USA: Past and future,” 4–5. *USA: University of Minnesota*.
- Iwasaki, I., and Lai, R. W., 1965. “Starches and starch products as depressants in soap flotation of activated silica from iron ores,” *Trans. AIME*. 232:364–71.

- Jain, V., Rai, B., Waghmare, U. V., Tammishetti, V., and Pradip, 2013. “Processing of alumina-rich iron ore slimes: Is the selective dispersion–flocculation–flotation the solution we are looking for the challenging problem facing the Indian iron and steel industry?” *Indian Institute of Metals*, 66:447–56. doi:10.1007/s12666-013-0287-1.
- Jena, S. K., Sahoo, H., Rath, S. S., Rao, D. S., Das, S. K., and Das, B., 2015. “Characterization and processing of iron ore slimes for recovery of iron values,” *Mineral Processing and Extractive Metallurgy Review*, 36(3):174–82. doi:10.1080/08827508.2014.898300.
- Kar, B., Sahoo, H., Rath, S. S., and Das, B., 2013. “Investigations on different starches as depressants for iron ore flotation,” *Minerals Engineering*, 49:1–6. doi:10.1016/j.mineng.2013.05.004.
- Kemppainen, K., Suopajarvi, T., Laitinen, O., Ämmälä, A., Liimatainen, H., and Illikainen, M., 2016. “Flocculation of fine hematite and quartz suspensions with anionic cellulose nanofibers,” *Chemical Engineering Science*, 148:256–66. doi:10.1016/j.ces.2016.04.014.
- Krishnan, S. V., and Iwasaki, I., 1984. “Pulp dispersion in selective desliming of iron ores,” *International Journal of Mineral Processing*, 12 (1–3):1–13. doi:10.1016/0301-7516(84)90019-X.
- Kumar, T. V. V., Rao, D. S., Subba Rao, S., Prabhakar, S., and Bhaskar Raju, G., 2010. Reverse flotation studies on an Indian low grade iron ore slimes. *International Journal of Engineering Science and Technology*, 2(4):637–48.

- Lelis, D. F., da Cruz, D. G., and Lima, R. M. F., 2019, “Effects of calcium and chloride ions in iron ore reverse cationic flotation: Fundamental studies,” *Mineral Processing and Extractive Metallurgy Review*. Issue 6, Vol. 40, pp. 402-409.
- Lelis, D. F., Lima, R. M. F., Rocha, G. M., and Leão, V. A., 2020, “Effect of magnesium species on cationic flotation of quartz from hematite,” *Mineral Processing and Extractive Metallurgy Review*. Doi: 10.1080/08827508.2020.1864362
- Lima, N. P., Peres, A. E. C., and Marques, M. L. S., 2012. “Effect of slimes on iron ores flotation,” *International Journal of Mining Engineering and Mineral Processing*, 1 (2):43–46. doi:10.5923/j.mining.20120102.04.
- Lima, N. P., Valadão, G. E. S., and Peres, A. E. C., 2013. “Effect of amine and starch dosages on the reverse cationic flotation of an iron ore,” *Minerals Engineering*, 45:180–84. doi:10.1016/j.mineng.2013.03.001.
- Liu, J., Zhang, J., and Liu, J., 2007. “Status quo of iron ores flotation reagent,” *China Mining Magazine*, 16 (2):106–08. (in Chinese).
- Luo, B., Zhu, Y., Sun, C., Li, Y., and Han, Y., 2015. “Flotation and adsorption of a new collector  $\alpha$ -Bromodecanoic acid on quartz surface,” *Minerals Engineering*, 77:86–92. doi:10.1016/j.mineng.2015.03.003.
- Ma, M., 2012. “Froth flotation of iron ores,” *International Journal of Mining Engineering and Mineral Processing*, 1 (2):56–61. doi:10.5923/j.mining.20120102.06.

- Ma, X., and Bruckard, W. J., 2010. “The effect of pH and ionic strength on starch-kaolinite interactions,” *International Journal of Mineral Processing*, 94:111–14. doi:10.1016/j.minpro.2010.01.004.
- Manukonda, V. R., and Iwasaki, I., 1987. “Control of calcium ion via chemical precipitation-ultrasonic treatment in selective flocculation,” *Mining, Metallurgy & Exploration*, 4 (4):217–22. doi:10.1007/BF03402696
- Mohanty, S., and Das. B., 2010. “Optimization studies of hydrocyclone for beneficiation of iron ore slimes,” *Mineral Processing & Extractive Metallurgy Review*, 31 (2):86–96. doi:10.1080/08827500903397142.
- Nakhaei, F., and Irannajad, M., 2018. “Reagents types in flotation of iron oxide minerals: A review,” *Mineral Processing and Extractive Metallurgy Review*, 39 (2):89–124. doi:10.1080/08827508.2017.1391245.
- Ng, W. S., Sonsie, R., Forbes, E., and Franks, G. V., 2015. “Flocculation/flotation of hematite fines with anionic temperature-responsive polymer acting as a selective flocculant and collector,” *Minerals Engineering*, 77:64–71. doi:10.1016/j.mineng.2015.02.013.
- Nykänen, V. P. S., Braga, A. S., Pinto, T. C. S., Matai, P. H., Lima, N. P., Leal Filho, L. S., and Monte, M. B., 2018. “True flotation versus entrainment in reverse cationic flotation for the concentration of iron ore at industrial scale,” *Mineral Processing and Extractive Metallurgy Review*, 1–11. doi:10.1080/08827508.2018.1514298.

- Oyarzun, F. C., 2013. “Modificaciones del proceso de flotación inversa de hierro en celdas neumáticas de Planta Magnetita,” *Valparaíso, Chile: Pontificia Universidad Católica de Valparaíso, Facultad de Ingeniería*. (In Spanish).
- Papini, R. M., Brandao, P. R. G., and Peres, A. E. C., 2001. “Cationic flotation of iron ores: Amine characterization and performance,” *Mining, Metallurgy & Exploration*, 18 (1):5–9. doi:10.1007/BF03402863.
- Pavlovic, S., and Brandao, P. R. G., 2003. “Adsorption of starch, amylose, amylopectin and glucose monomer and their effect on the flotation of hematite and quartz,” *Minerals Engineering*, 16 (11):1117–22. doi:10.1016/j.mineng.2003.06.011.
- Peres, A. E. C., Araujo, A. C., El-Shall, H., Zhang, P., and Abdel-Khalek, N. A., 2009. “Plant practice: Nonsulfide minerals,” *In Froth flotation: A century of innovation*, Ch. 5, ed. M.C. Fuerstenau, G.J. Jameson, and R.-H. Yoon, 857–61. Colorado: SME.
- Perez, S., and Bertoft, E., 2010. “The molecular structures of starch components and their contribution to the architecture of starch granules: A comprehensive review,” *Starch Journal: Biosynthesis, Nutrition, Biomedical*, 62 (8): 389-420. DOI: 10.1002/star.201000013.
- Pita, F. A., 2015. “True flotation and entrainment of kaolinitic ore in batch tests,” *Mineral Processing & Extractive Metallurgy Review*, 36:213–25. doi:10.1080/08827508.2014.928619.

- Poperechnikova, O. Y., Filippov, L. O., Shumskaya, E. N., and Filippova, I. V., 2017. “Intensification of the reverse cationic flotation of hematite ores with optimization of process and hydrodynamic parameters of flotation cell,” *Journal of Physics: Conference Series*, 879:1–8.
- Quast, K., 2006. “Flotation of hematite using C6–C18 saturated fatty acids,” *Minerals Engineering*, 19 (6–8):582–97. doi:10.1016/j.mineng.2005.09.010.
- Ruan, Y., Zhang, Z., Luo, H., Xiao, C., Zhou, F., and Chi, R., 2018. “Effects of metal ions on the flotation of apatite, dolomite and quartz,” *Minerals*, 8, 141.
- Sahoo, H., Rath, S. S., Jena, S. K., Mishra, B. K., and Das, B., 2015. “Aliquat-336 as a novel collector for quartz flotation,” *Advanced Powder Technology*, 26 (2):511–18. doi:10.1016/j.apr.2014.12.010.
- Silva, R. R., Correa De Araujo, A., and Farias De Oliveira, J., 2008. “Frother assisted amine flotation of iron ores,” *2nd International Iron Symposium*, São Luís, Maranhão, Brazil.
- Sun, B., 2006. “Progress in China’s beneficiation technology for complex refractory iron ore,” *Metal Mine*, 3:11–13. (in Chinese).
- Tang, M., and Wen, S., 2018. “Effects of cations/anions in recycled tailing water on cationic reverse flotation of iron oxides,” *Minerals*, 9, 161. Doi: 10.3390/min9030161
- Tripathy, T., Bhagat, R. P., and Singh, R. P., 2001. “The flocculation performance of grafted sodium alginate and other polymeric flocculants in relation to iron ore

slime suspension,” *European Polymer Journal*, 37 (1):125–30.

doi:10.1016/S0014-3057(00)00089-6.

- Turrer, H. D. G., and Peres, A. E. C., 2010. “Investigation on alternative depressants for iron ore flotation,” *Minerals Engineering*, 23 (11–13):1066–69. doi:10.1016/j.mineng.2010.05.009.
- Varicheva, A. V., Ugarova, A. A., Efendieva, N. T., Kretovb, S. I., Lavrinenkoc, A. A., Soludukhind, A. A., and Puzakovb. P. V., 2017. “Innovative solutions in iron ore production at Mikhailovsky Mining and Processing Plant,” *Journal of Mining Sciences*, 53 (5):925–37.
- Villar, J. W., and Dawe, G. A., 1975. “The Tilden mine-a new processing technique for iron ore,” *Mining Congress Journal*, 61 (10):40–48.
- Weissenborn, P. K., 1996. “Behaviour of amylopectin and amylose components of starch in the selective flocculation of ultrafine iron ore,” *International Journal of Mineral Processing*, 47 (3–4):197–211. doi:10.1016/0301-7516(95)00096-8.
- Weng, X., Mei, G., Zhao, T., and Zhu, Y., 2013. “Utilization of novel ester-containing quaternary ammonium surfactant as cationic collector for iron ore flotation,” *Separation and Purification Technology*, 103:187–94. doi:10.1016/j.seppur.2012.10.015.
- Yong, Y., 2005. “Processing state and technology progress of iron ore in China,” *Conservation and Utilization of Mineral Resources*, 6:102–06. (in Chinese).
- Yuan, Z., Han, Y., and Yin, W., 2007. “Status quo and development orientation of China’s refractory ore resource utilization,” *Metal Mine*, 1:01. (in Chinese).

- Zhang, C., and Dai, H., 2012. “Current situation and future development of the collector for reverse flotation of iron ore,” *Multipurpose Utilization of Mineral Resources*, 2:3–6. (in Chinese).
- Zhang, X., Gu, X., Han, Y., Parra-Álvarez, N., Claremboux, V., and Kawatra, S. K., 2021, “Flotation of Iron Ores: A Review”, *Mineral Processing and Extractive Metallurgy Review*, DOI: 10.1080/08827508.2019.1689494
- Zhao, C., Yahui, Z., and Yongdan, C., 2012. “Reverse flotation of quartz from magnetite ore with modified sodium oleate,” *Mineral Processing and Extractive Metallurgy Review*, 34 (5):320–30.
- Zhou, T., 2017. “Research and application utilization status of the iron ore flotation reagents,” *Modern Mining*, 6:98–102. (in Chinese).
- Zhu, Y., Luo, B., Sun, C., Liu, J., Sun, H., Li, Y., and Han, Y., 2016. “Density functional theory study of  $\alpha$ -Bromolauric acid adsorption on the  $\alpha$ -quartz (1 0 1) surface,” *Minerals Engineering*, 92:72–77. doi:10.1016/j.mineng.2016.03.007.



## **3 Recreating the Iron Ore Flotation Process in the Laboratory**

### **3.1 Abstract**

Prior to performing any optimization tests on the iron ore flotation process, it is important to have a laboratory process baseline or “control test” as a point of reference. This chapter summarizes the steps that were followed to define a laboratory procedure where the iron ore flotation process is recreated. The main goal was to obtain a final flotation concentrate similar to that obtained at the plant where the samples were collected, with a grade of 63-64% Fe and an iron recovery of approximately 60%. This procedure was divided in three steps: grinding, desliming, and flotation. For each of these steps, parameters such as water chemistry, grinding time, reagent dosages, conditioning times, and step by step procedures were defined. Results showed that the iron ore flotation process at the plant where the samples were collected can be recreated in the laboratory by grinding 500 grams of ore for 50 minutes, desliming with 3 lb/ton of anionic polyacrylamide dispersant and 0.0625 lb/ton of starch flocculant, and floating with 1.5 lb/ton of starch depressant and 1.5 lb/ton of ether amine, while maintaining the pH of the slurry at 10.5 with sodium hydroxide throughout the process. Following these parameters, flotation tests including one rougher stage and one stage of scavenging yielded a final concentrate with a grade of  $63.0 \pm 0.6\%$  Fe and an iron recovery of  $60.5 \pm 0.8\%$ .

## 3.2 Introduction

Most iron ore reserves found in the U.S. are composed mainly of low-grade hematite ores (~30% grade) that need to be concentrated prior to shipping to blast furnace facilities (Haselhuhn and Kawatra, 2015). In low-grade ores it is very common to find gangue minerals very attached to the iron minerals, requiring grinding to liberate the valuable material (DeVaney, 1985). The particle size at which the iron mineral is liberated is called “liberation size”. In the Lake Superior Iron Ore District in the U.S. the liberation size is considered very fine compared to other iron ore plants in the world. At the iron ore facility where the samples for this research were collected, the liberation size is approximately 25  $\mu\text{m}$  at 80% passing (Zhang et al., 2019). This particular material, characterized as low-grade and fine hematite ore, requires a specific process of beneficiation composed of selective flocculation and dispersion followed by the reverse cationic flotation of iron ore (Zhang et al., 2019).

The main objective of this PhD dissertation is to find ways to optimize the iron ore concentration process by explaining certain process behaviors, testing new reagents, and analyzing the ore surface properties in a more profound way. However, before any of these studies can be performed it is important to define a laboratory procedure that would recreate the iron ore flotation process with grade and recovery targets similar to those obtained at the processing plant during a stable run. Once a standard procedure is developed which includes set reagent dosages, water chemistry, grinding and conditioning times, among other parameters, then optimization tests can be performed. This chapter covers the process followed to recreate the iron ore flotation process in the

laboratory with a main reference given by the iron ore plant where the samples were collected. This plant is going to be denominated as Plant A during this chapter.

The iron ore beneficiation process typical of processing plants that treat low-grade and fine ores can be divided in four main steps: comminution, concentration, filtration, and pelletization. The comminution step consists of all the crushing and grinding steps required to reach the specific liberation size of the ore. In most mines, the primary crushers are placed near the open pits so that the crushed ore can be transported to the concentrator plant via belt conveyors (DeVaney, 1985). Primary crushing usually includes a gyratory crusher or a jaw crusher (Johansson et al., 2017). The former has been more popular in the last years because it allows the trucks to dump material at various sides of the crusher unlike the jaw crusher which only has one input location (DeVaney, 1985). In Plant A, a gyratory crusher of 60 x 109 in, driven by a 1,000-hp motor, with a closed side setting of 9 in, and a design capacity of 2,800 tph is used near the open pit (Keranen et al., 1985). The crushed ore is transported in a 72-in belt conveyor at a rate of 2,970 tph to a storage building with a capacity of 200,000 t (Keranen et al., 1985). Usually after the primary crushers the ore needs to be ground finer. In some facilities it is common to have a sequence of secondary gyratory crushers, and a cone-crusher to reduce the particle size to near 1-in. Then, grinding is performed with rod mills followed by ball or pebble mills. In the past year the use of autogenous mills has replaced the gyratory and cone crushers as well as the rod mills, which has brought significant improvements and cost savings to the comminution process. (DeVaney, 1985)

In Plant A, six autogenous mills 27-ft in diameter and 14 ½-ft in effective length are used. Each mill has a rated capacity of 226 ltph, driven by 5,720-hp dual synchronous motors. After this process, caustic soda is added as a pH modifier and a dispersant is added for the desliming process. The function of these reagents will be described later on. After reagents addition, the slurry is fed to two pebble mills (15 ½-ft in diameter and 40-ft in compartment length, driven by a 2,800 hp motor) and vibrating screens. The -3 +1 ¼-in material is used as grinding media in the pebble mill, while the -1 ¼ + 5/8-in material known as the “critical size” material is directed to an intermediate crusher composed of 7-ft short head cone crushers adjusted to 1/4-in setting after which the product is redistributed to the primary mills. The -5/8-in +2 mm material is recycled back to the mill while the - 2mm material is directed to the cyclone-pebble mill circuit composed of nine 15-in cyclones. The particle size of the cyclone overflow is monitored continuously for size control. The cyclone overflow is transported to the concentration step. (Keranen et al., 1985)

The hematite concentration process in Plant A consists of selective flocculation and dispersion (also called desliming) followed by reverse cationic flotation (Villar and Dawe, 1975). After comminution, corn starch is added through a 9x9-ft conditioner tank to a 55-ft diameter deslime thickener (Keranen et al., 1985). This process is performed at a pH of 10.5-11 which is controlled with sodium hydroxide (NaOH) (Zhang et al., 2019). The dispersant added during grinding disperses the ultrafine silica (slimes) while the starch selectively flocculates the hematite. The slimes (tailings) are recovered in the thickener overflow while the hematite concentrate is recovered in the thickener

underflow. The deslime thickener underflows from the 12 thickeners are placed in the flotation feed distributor which is in charge of distributing an equal load of slurry to six flotation feed conditioners, where the starch is added and conditioned for approximately 2 minutes (Keranen et al., 1985).

The slurry is then transferred to a flotation circuit composed of six different lines, each with 25,500-ft<sup>3</sup> flotation cells including 10 rougher cells, 5 primary scavenger cells, 4 secondary scavenger cells, 3 tertiary scavenger cells, and 3 quaternary scavenger cells (Keranen et al., 1985). Figure 3.1 shows a simple diagram of the flotation-scavenger circuit. Ether amine partially neutralized is added as a collector and a frother at the feed box and again in cell 6 (Keranen et al., 1985). The froth product of the rougher cell is sent to the scavenger sequence where the froth product is floated over and over again to improve the recovery of the concentrate. The froth product from the last scavenger cell is eliminated as tailings, and the underflow product from the rougher cell is considered as the final concentrate (Keranen et al., 1985). After flotation the concentrate follows filtration and pelletization. These two processes are outside of the scope of this research thus they will not be described in detail. A simplified process flow diagram of Plant A is depicted in Figure 3.2.

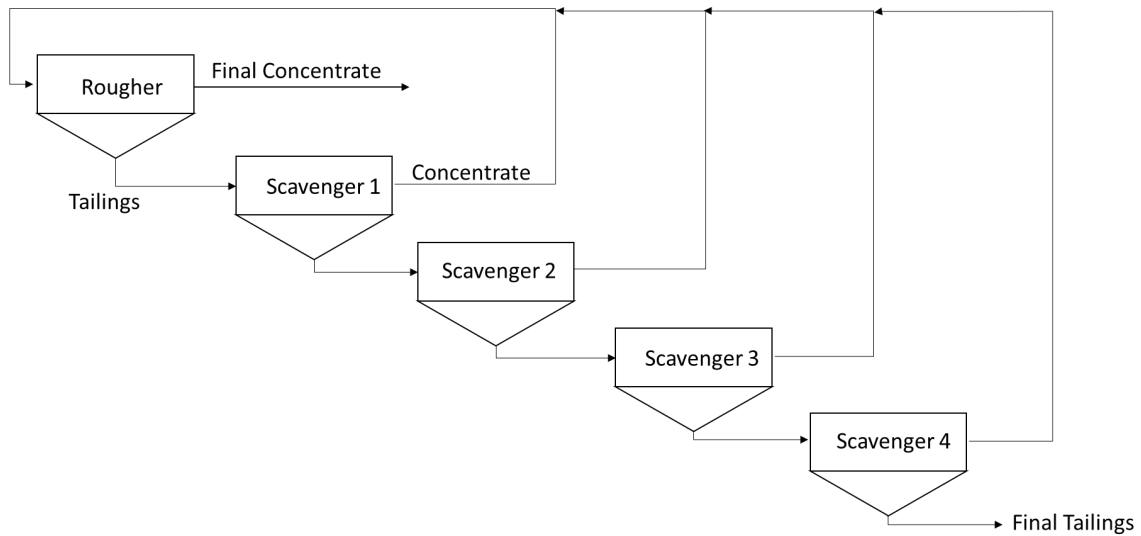


Figure 3.1: Simplified flotation-scavenger circuit at Plant A

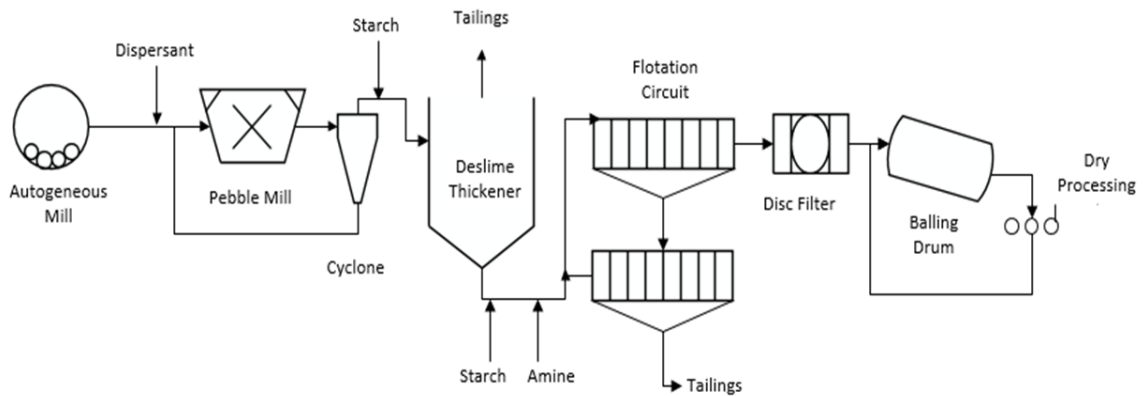


Figure 3.2: Fine and low-grade hematite ore beneficiation process flowsheet (Mariani and Nelson, 1993; Keranen, 1986; Haselhuhn and Kawatra, 2015).

In froth flotation, reagents can be divided in three groups: frothers, collectors, and modifiers (Nagaraj and Ravishankar, 2007). In iron ore flotation there are various modifiers used, including pH modifiers, dispersants, flocculants, and depressants, all with a unique function in the process. Sodium hydroxide (NaOH) is used as a pH modifier to maintain the pH of the process at 10.5-11. This is crucial in the process as the pH of the

slurry defines the surface charge of minerals in solution. A high pH helps maintain dispersion of particles and enhances reagents selectivity (Green and Colombo, 1984). The dispersion action of the pH modifier is not enough to maintain electrostatic repulsion between particles during selective flocculation and dispersion (desliming), thus a modifier referred as a dispersant is used in the process. Even though the main function of this reagent is to disperse the fine silica particles from the hematite, the dispersant also helps maintain the water quality during the process as it can sequester polyvalent cations before they adsorb to the ore and cause changes in the surface properties (Green and Colombo, 1984). Typical dispersants include sodium silicates, sodium polyphosphates, and sodium polyacrylates, the latter being the most common one used in Plant A since 2015 as stated by Zhang et al. (2019).

In addition to dispersants, during the desliming process flocculants are used to selectively flocculate or create larger compounds or flocs of hematite particles so they settle faster and can be recovered in the thickener underflow (Green and Colombo, 1984). Corn starch is the most common flocculant used in this process (Filippov et al., 2014). Industrial corn starch is a natural polymer that contains 20-30% amylose, 70-80% amylopectin, and less than 1% lipids and proteins (Nakhaei and Irannajad, 2018). The starch molecules are insoluble in cold water and for it to function as a flocculant it needs to undergo a gelatinization process where the starch is heated in water and causticized before used (Yang and Wang, 2017).

Corn starch is also used as a depressant in flotation. The main difference between its function as a flocculant and a depressant is that the latter is used to prevent collector

adsorption onto the hematite so that only the silica is floated while the hematite settles to the bottom of the cell. After the starch is added in the process, ether amine partially neutralized is added as both a frother and a collector (Zhang et al., 2019). The main function of a frother is to control froth formation and stability, while the collector is used to selectively increase the hydrophobicity of particles so they can be floated during the process. Ether amine is known as a cationic collector, which means that it will be attracted to minerals that are negatively charged (Zhang et al., 2019). Because hematite has already being depressed by the starch, ether amine ideally only adsorbs to silica particles. Partially substituting the ether amine with a frother could be beneficial to the process, but this will be discussed in a different chapter.

The objective of this chapter is to define a procedure to recreate the iron ore flotation process at Plant A in the laboratory to have it as a reference (“control test”) when optimization experiments are performed. For this purpose, particles size, iron grade, and recovery targets at different stages of the process were provided by process engineers at Plant A (Cleveland Cliffs, Personal communication, 2018). Table 3.1 summarizes these process targets.

Table 3.1: Grinding, desliming, and flotation performance targets provided by Plant A



<b>Process Variable</b>	<b>Process Target</b>
Grinding process – Final size distribution	25 $\mu\text{m}$ at 80% passing
Desliming process – Concentrate grade and recovery	Grade: 40-45% Recovery: 70-80%
Flotation process – Concentrate grade and recovery	Grade: 63-64% Recovery: 60%

### **3.3 Materials and Methods**

#### **3.3.1 Chemical reagents**

A 10% sodium hydroxide (NaOH) solution was prepared with sodium hydroxide acquired from Sigma Aldrich. This solution was used as a pH modifier during grinding, desliming, and flotation experiments. A 10% dispersant solution was prepared using an anionic polyacrylamide (Cyquest 3223 antiprecipitant) dispersant provided by Solvay. This solution was added during the grinding process to disperse the fine silica particles during desliming. Acid modified corn starch provided by Cleveland Cliffs was used both as a flocculant during desliming (0.3% solution) and as a depressant during flotation (3% solution). The starch was gelatinized and causticized in the lab by cooking with deionized

water on a hot plate at 240°C for 30 minutes followed by the addition of 0.5 ml of NaOH diluting further with more deionized water until the desired solution was obtained.

Finally, a 1% ether amine solution was used as the collector/frother in flotation. This solution was prepared with a primary ether monoamine 30% neutralized with acetic acid which was also provided by Solvay.

### **3.3.2 Hematite ore sample collection and sampling methods**

The hematite ore was collected at an iron ore concentration facility nearby. The samples were collected at two different locations in the processing plant as depicted in Figure 3.3. At first, samples were collected in the deslime thickener underflow right before starch addition (Location #1). The sample collection was then switched to Location #2, right after primary grinding and right before dispersant addition. The main reasons why the collection location was changed is because in Location #1 surface active reagents such as dispersant and flocculant are present in the sample, which can alter the surface properties and cause discrepancies in the experimental work. Additionally, ore aging was a concern with samples from Location #1. The advantage of Location #2 is that one more step of grinding is required in the laboratory before every experiment, guaranteeing fresh surface sites at the start of the process. These and other advantages of collecting the samples in Location #2 are discussed by Haselhuhn and Kawatra (2015).

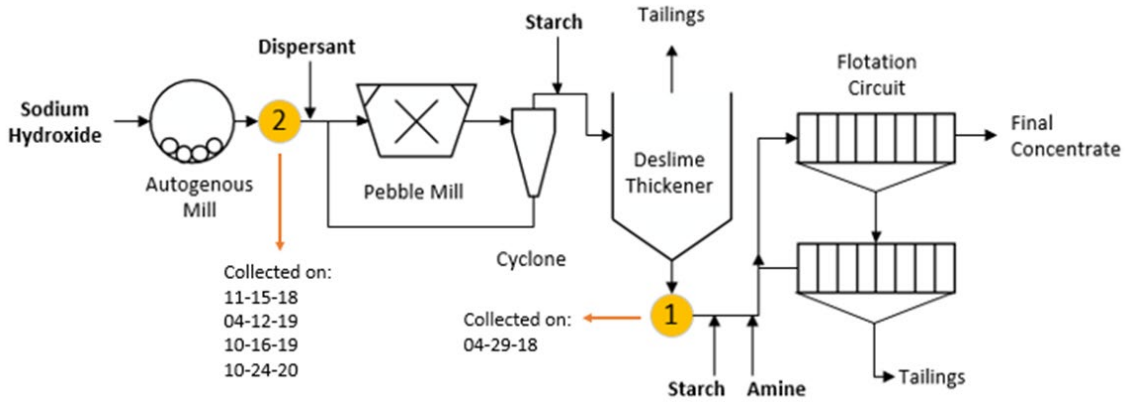


Figure 3.3: Sampling locations at the iron ore concentrator plant. Location #1: Deslime thickener underflow, right before starch addition. Samples at this location had a  $40.95 \pm 0.6\%$  grade and a particle size of  $12.09 \mu\text{m}$  at 80% passing. Location #2: Autogenous mill screen underflow, right before dispersant addition. Samples at this location had a  $32.32 \pm 0.7\%$  grade and a particle size of 0.8 mm at 80% passing. Collection dates included.

All the samples were collected in 5-gallon buckets using a cross-flow sample cutter. Once the samples were transported from the plant to the Michigan Tech laboratory, some of the water from the buckets was siphoned out and the rest of the slurry from each bucket were combined into one big bucket. Then the slurry was split into approximately 6000-gram samples following the “grab sampling method” where the material is divided into several samples by randomly grabbing small amounts from the big bucket. Afterwards, the samples were frozen and stored for future use. When more hematite ore was needed for experiments, one ~6000-gram bag was emptied on a tray and dried in the oven at  $106^\circ\text{C}$ . Then, the sample was further split using the rotary riffle splitter shown in Figure 3.4 into approximately twelve 500-gram representative samples.



Figure 3.4: Rotary riffle splitter at the Michigan Technological University laboratory.

Since Location #2 was determined as the ideal collection location in the plant, only this samples were used during the experimental work described in the rest of this project. An X-Ray Diffraction (XRD) analysis of the hematite ore from this location is shown in Figure 3.5. Results show that 65.15% of the sample is composed of quartz, 21.45% of hematite, 7.7% of magnesioferrite, and 5.7% of goethite.

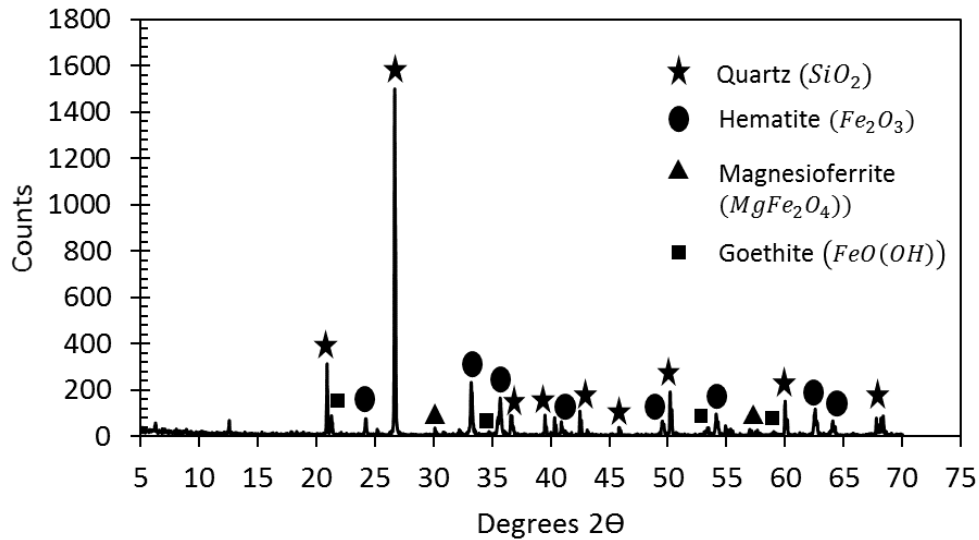


Figure 3.5: X-Ray diffraction results for the hematite ore used in this investigation.

Quartz: 65.15%, Hematite: 21.45%, Magnesioferrite: 7.7%, Goethite: 5.7%.

### 3.3.3 Water analysis and preparation

#### 3.3.3.1 ICP Tests

Water chemistry is a very important parameter in desliming and flotation. Especially the calcium and magnesium concentrations. To recreate the iron ore beneficiation process in the laboratory, it was decided to use a similar water hardness to that of the plant where the samples were collected. First, ICP tests were performed to determine the calcium and magnesium concentrations in a sample of Houghton's city water and in a sample of the flotation water used at the plant. These tests were performed with the help of the Michigan Technological University Forest Ecology Stable Isotope Laboratory. The analysis was performed using a Perkin Elmer Optima 7000DV ICP-OES. The samples were acidified with nitric acid prior to analysis, and all QC samples passed ( $\pm 10\%$ ).

### 3.3.3.2 *Titration Tests*

Titration tests were performed to determine the total water hardness in both samples. The method followed was based on Day and Underwood (1991a) complexometric titration procedure. The method consists of adding 50 ml of either the standard calcium chloride solution or the sample with unknown water hardness into a 250 ml Erlenmeyer flask. Then, 5 ml of ammonia-ammonium chloride buffer solution is added to maintain a pH of 10. Subsequently, 5 drops of the Eriochrome Black T indicator are added. This indicator forms a complex with calcium and magnesium ions in solution. When the ion complex is present the solution is pink, and when the ion complex is not present the solution is blue. The EDTA (ethylenediaminetetraacetic acid) solution is placed in the burette. This is a very large compound that also forms a complex with calcium and magnesium ions. As EDTA is added to the Erlenmeyer flask, the ion complex with the indicator is replaced by the ion complex with EDTA. The titration setup is depicted in Figure 3.6. Titration is performed carefully with the EDTA solution until the color of the solution changes from pink to blue as shown in Figure 3.7. The EDTA volume change is used to calculate the EDTA solution concentration when the standard calcium chloride solution is used, or the total water hardness ( $\text{CaCO}_3$  concentration) when an unknown water sample is used.

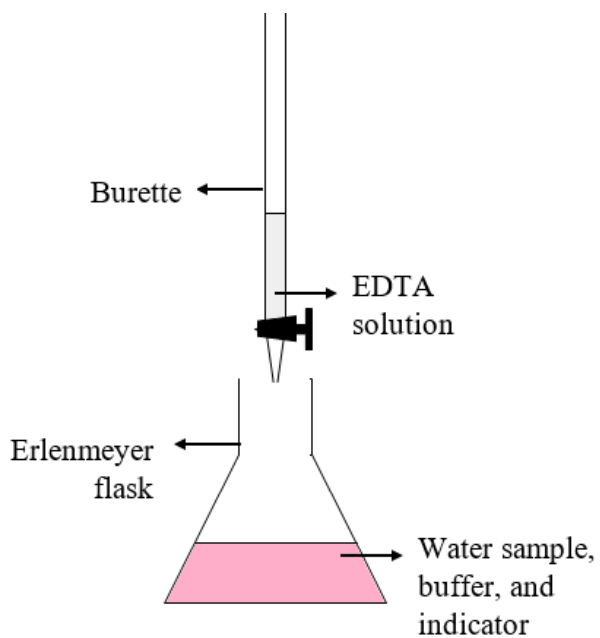


Figure 3.6: EDTA complexometric titration laboratory setup for total water hardness determination.



Figure 3.7: Color change as titration is performed carefully with the EDTA solution.

When the indicator-ion complex is present the solution is pink, and when the indicator-ion complex is not present the solution is blue.

### 3.3.3.3 “Feed water” Preparation

Houghton’s city water has a much greater water hardness than the flotation water used at the plant (data showed in results section). For this reason, it was recommended by plant engineers to mix Houghton’s city water with deionized water to achieve a lower water hardness concentration comparable to the plant. Because the water hardness in Houghton’s city water can vary significantly over a period of time due to weather changes and other factors, the titration procedure was performed on the specific city water sample for every batch of water prepared. A simple dilution equation was used to determine mixing ratios to reach a water hardness of approximately 15-20 mg/L of  $\text{CaCO}_3$ . Once the water was mixed ICP tests were then performed to determine the exact calcium and magnesium concentrations present.

### 3.3.4 Grinding

First, 500 grams of hematite ore were mixed with deionized water to prepare a hematite slurry of 60% solids. Then, the slurry was adjusted to a pH of 10.5 with sodium hydroxide (NaOH) and a desired amount of the anionic polyacrylamide dispersant was added. Once conditioned, the slurry was placed in the grinder along with the grinding rods and was sealed. Then the grinder was placed in the mill for different periods of time to determine how much time is needed to reach a particle size distribution of approximately 25  $\mu\text{m}$  at 80% passing. After grinding, the samples were filtered, dried at 106°C overnight, and sent to size distribution analysis. Figure 3.8 shows the grinding mill used.



Initially, grinding tests at 30, 40, 50, and 60 minutes were performed without dispersant addition. The time that resulted in a particle size closer to 25  $\mu\text{m}$  at 80% passing was selected as the set grinding time for the desliming tests. Once a set dispersant dosage was determined during desliming, further grinding tests were performed to determine if the particle size was affected by the addition of dispersant at a constant grinding time.



Figure 3.8: Grinding mill at Michigan Technological University laboratory

### 3.3.5 Size Distribution Analysis

The size distribution analysis was performed using a Microtrac SRA 9200 particle sizer (see Figure 3.9). Each measurement was performed in triplicate for statistical accuracy. The Microtrac analysis consisted on dispersing a representative sample of the material in water and sending it through the path of a light beam. The light scattered as the particles pass through the light beam is measured by photodetector arrays which convert the scatter light to electrical signals that are then analyzed by the Microtrac processor. The signal results are then converted to a size distribution plot based on the Fraunhofer Diffraction, and/or Mie Scattering theory (Nai-Ning et al., 1992). This method is further described in the ASTM B822-17 (“Standard Test Method for Particle Size Distribution of

Metal Powders and Related Compounds by Light Scattering”) (ASTM, 2017). A large light scatter indicates the presence of small particles and a small light scatter indicates the presence of large particles (Microtrac, 2007).



Figure 3.9: Microtrac SRA 9200 at Michigan Technological University laboratory.

### **3.3.6 Selective Flocculation and Dispersion (desliming)**

To recreate this process in the lab, a 10-liter cell was used as depicted in Figure 3.10. Two reagents are used during this process: anionic polyacrylamide dispersant and corn starch flocculant. Note that the desired amount of dispersant is added before the ore is ground. Then, the ground ore is placed in the cell and mixed with feed water to prepare a 7% solids slurry which is adjusted to a pH of 10.5 with sodium hydroxide (NaOH). At this point, the desired concentration of corn starch (0.3% solution) is added and the slurry is conditioned for 1 minute with the help of a plastic mixer. Once the solution is conditioned, the mixer is turned off and the slurry is let to settle for 30 seconds. The ultra-fine dispersed silica is siphoned out, while the hematite concentrate settles down. After siphoning, the concentrate product is filtered with a pressure filter and dried

overnight at 106°C. The dried ore is then analyzed for iron content using the method described below.

Tests were performed at various dispersant and corn starch dosages in order to determine the combination of reagents that would yield grade and recovery values between 40-45% and 70-80% respectively. All tests were performed one time. Once one combination of reagents was within the grade and recovery targets it was repeated 3 times for reproducibility.

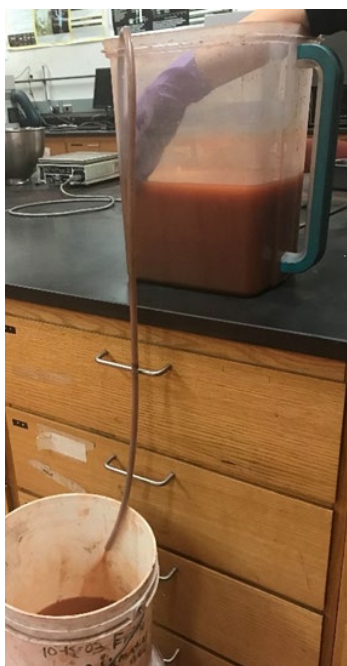


Figure 3.10: Desliming cell at Michigan Technological University laboratory.

### **3.3.7 Iron Content Determination**

The iron content analysis was performed using a UV-VIS spectrophotometer. First, an exact mass of ore is recorded to 0.1mg and is digested with hydrochloric acid (HCl) for 30 minutes. Then the sample is diluted to 100 ml with distilled water and an aliquot of

solution (0.100 ml) measured with a micropipette is placed in a 50 ml volumetric flask. Next, ammonium acetate is added as a buffer, and an excess of hydroxylamine hydrochloride is added to reduce all  $\text{Fe}^{+3}$  ions to  $\text{Fe}^{+2}$ . Then an excess of 1,10-phenanthroline is added as an indicator which gives an orange-red color to the solution when exposed to  $\text{Fe}^{+2}$  ions (Day and Underwood, 1991b). The absorbance of the solution at 510 nm is proportional to the iron content of the ore sample. Measurements were performed in triplicate for statistical accuracy.

For the calibration procedure, 0 ppm, 1 ppm, 2 ppm, and 4 ppm dilutions of a 1000 ppm iron AAS standard were prepared. An aliquot of these dilutions was added to a 50 ml flask and the same procedure was followed as described above. The absorbance of each solution was measured and a calibration curve of absorbance at 510 nm against the exact iron concentration (ppm) was plotted as shown in Figure 3.11. The calibration constants obtained were  $A=0.213$  and  $B=-0.0046$ . These constants were applied to the Beer-Lambert's law to determine the iron concentration of a solution with a known absorbance at a specific wavelength (Day and Underwood, 1991b).

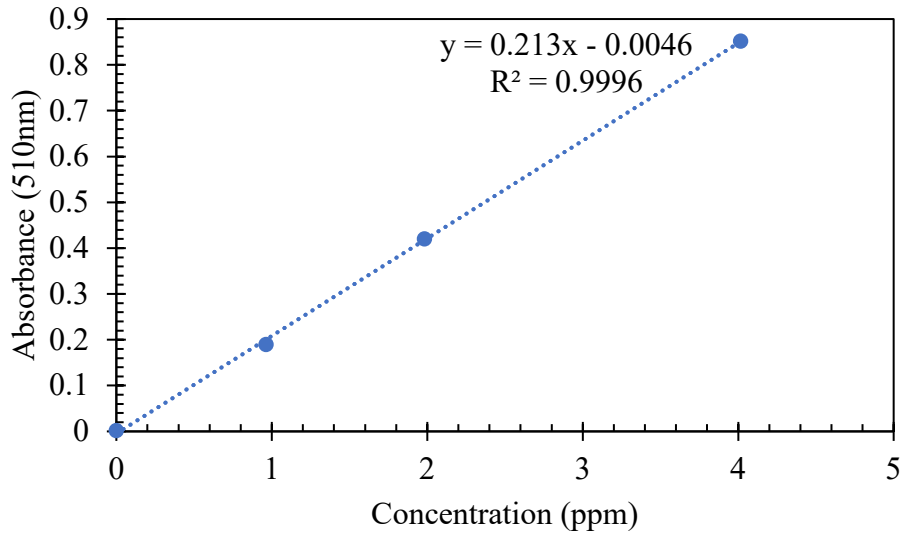


Figure 3.11: Calibration curve for iron content analysis.

### 3.3.8 Reverse Cationic Flotation

The flotation process was recreated in the lab with a 2-liter Denver flotation cell as depicted in Figure 3.12. First, the concentrate product from the desliming process is placed in the flotation cell and feed water is added to prepare a 15% solids slurry. Sodium hydroxide (NaOH) is added to adjust the pH to 10.5. Then the desired amount of corn starch (3% solution) is added and conditioned for 3 minutes, followed by the addition of the desired amount of ether amine (1% solution) and conditioning for 1 more minute. Once all the reagents are added, the air is turned on and the froth is scraped off onto a tailings pan, while the hematite concentrate is recovered in the flotation cell. After the material is separated, both products are filtered, dried, and sent for iron content analysis following the process described above.

Tests were performed at various amine and starch concentrations to determine the combination of these two reagents that would yield a grade and recovery of

approximately 63-64% and 60% respectively. Each test was performed in triplicate for statistical accuracy. Additionally, scavenging tests were performed in triplicate by floating the froth product five times in a row without any further addition of reagents. The final products were filtered, dried, and analyzed following the same process described above.



Figure 3.12: Flotation cell at Michigan Technological University laboratory.

## 3.4 Results and Discussion

### 3.4.1 Water Analysis and Preparation

Table 3.2 shows the ICP and titration results for the calcium and magnesium concentrations of a Houghton's city water sample, the plant's flotation water sample, and the water sample after mixing deionized water with Houghton's city water (referred as feed water in the table). As it was mentioned earlier, water hardness can vary significantly between days. Thus, the Houghton's city water column in the table varied

between batches and it was used to determine the exact mixing ratio of city water and deionized water required to reach a water hardness similar to the plant's flotation water.

Table 3.2: Water hardness comparison between Houghton's city water, flotation process water at the plant, and the feed water used for recreating the flotation process at Michigan Tech for one batch of experiments.

	<b>Houghton's City Water</b>	<b>Plant's Flotation Water</b>	<b>Feed Water used in MTU Lab</b>
Calcium (mg/L)	63.4	3.2	7.5
Magnesium (mg/L)	13.4	1.4	1.5
Total Water Hardness (mg/L of CaCO <sub>3</sub> )	298.9±5	18.7±0.02	16.6±0.0

### 3.4.2 Grinding

Figure 3.13 shows the particle size at 80% passing at four different grinding times without dispersant addition. As it is expected, the particle size decreases as the grinding time increases. After grinding for 50 minutes, the particle size obtained was  $24.21 \pm 0.16 \mu\text{m}$  at 80% passing. From the four grinding times studied, 50 minutes was the grinding time that yield a particle size closer to the liberation size of the ore ( $25 \mu\text{m}$  at 80% passing).

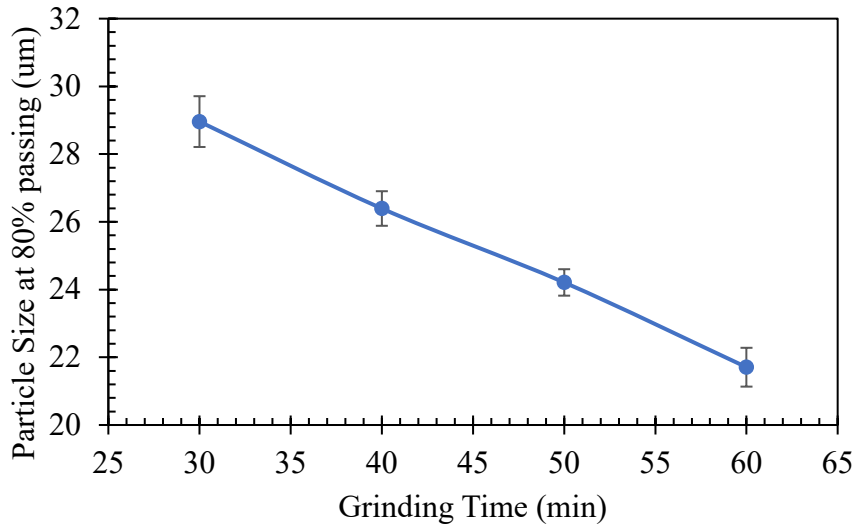


Figure 3.13: Particle size at 80% passing at four different grinding times without dispersant addition.

In iron ore processing plants, it is common for the dispersant to be added during the grinding process (Haselhuhn et al., 2015). Thus, during this project the dispersant is also added before grinding in the rod mill. Table 3.3 shows how the particle size changes with the addition of the dispersant while maintaining all the other parameters constant. The dispersant is known to decrease energy consumption during grinding because the ultrafine slime coating on particles is dispersed facilitating breakage, but this does not necessarily lead to faster grinding unless the energy input rate is constant. The complete particle size distribution after grinding for 50 minutes in the rod mill at a pH of 10.5 and 3 lb/ton of dispersant is shown in Figure 3.14.

Table 3.3: Particle size at 80% passing after grinding for 50 minutes at a pH of 10.5 both without dispersant addition and with 3 lb/ton of dispersant.



<b>Dispersant Dosage</b>	<b>Particle Size at 80% passing (um)</b>	<b>95% confidence</b>
0 lb/ton	24.21	0.39
3 lb/ton	25.57	0.30

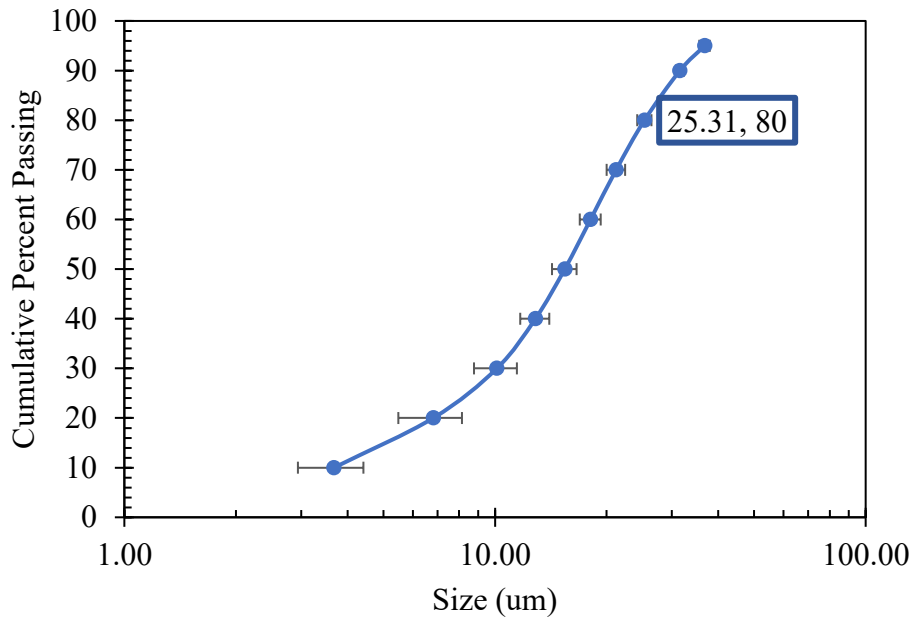


Figure 3.14: Particle size distribution after grinding for 50 minutes in the rod mill at a pH of 10.5 and 3 lb/ton of dispersant.

### 3.4.3 Selective Flocculation and Dispersion (desliming)

Figure 3.15 shows the grade and recovery curve for desliming tests at a constant starch dosage of 0.1 lb/ton and varying dosages of dispersant. Even though this data is based on one replicate, a pattern is observed. This data cannot be used for direct analysis of results

but it helps as a guide of what combination of reagents can yield the performance desired. As the dispersant dosage increases with a constant starch dosage, the grade increases by approximately 4% whereas the iron recovery decreases by approximately 20%. The iron recovery decreases significantly but, in this instance, it is more important to have a grade improvement as the lowest recovery observed (71.97%) is still within the performance targets (70-80%). This data suggests that a dispersant dosage of 3 lb/ton could potentially result in the desired performance.

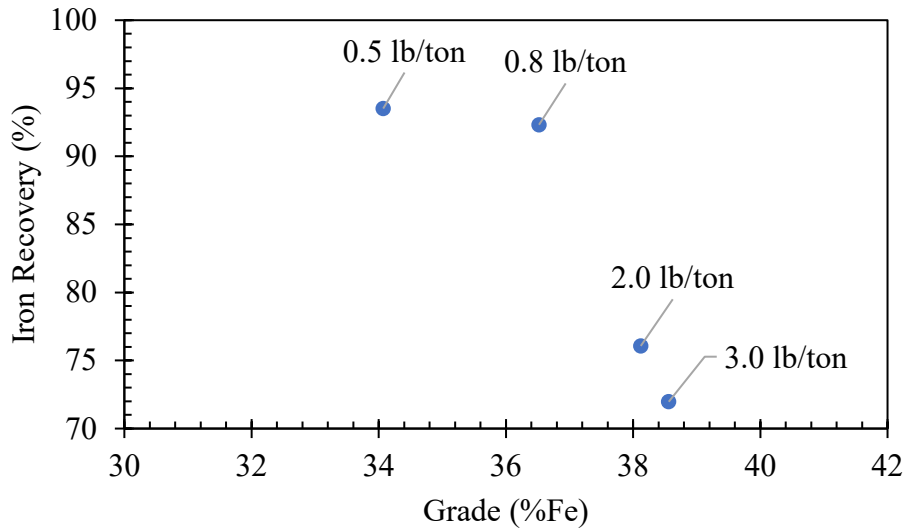


Figure 3.15: Grade and recovery curve for desliming tests at a constant starch dosage of 0.1 lb/ton and varying dosages of dispersant presented as labels in the plot.

Figure 3.16 shows the grade and recovery curve for desliming tests at a constant dispersant dosage of 3 lb/ton and varying dosages of starch. Just as the case of Figure 3.15, this data corresponds to one replicate per experiment so it can only be used as an approximate pattern indication and not as final results. It is observed that as the starch dosage decreases at a constant dispersant dosage, the grade and recovery both increase by

approximately 2%. This change is not as drastic as the changes observed in Figure 3.15 because the variation of starch dosage was not as broad as the dispersant dosage variation when the starch was constant. This data suggests that a starch dosage of 0.0625 lb/ton could potentially result in the desired performance.

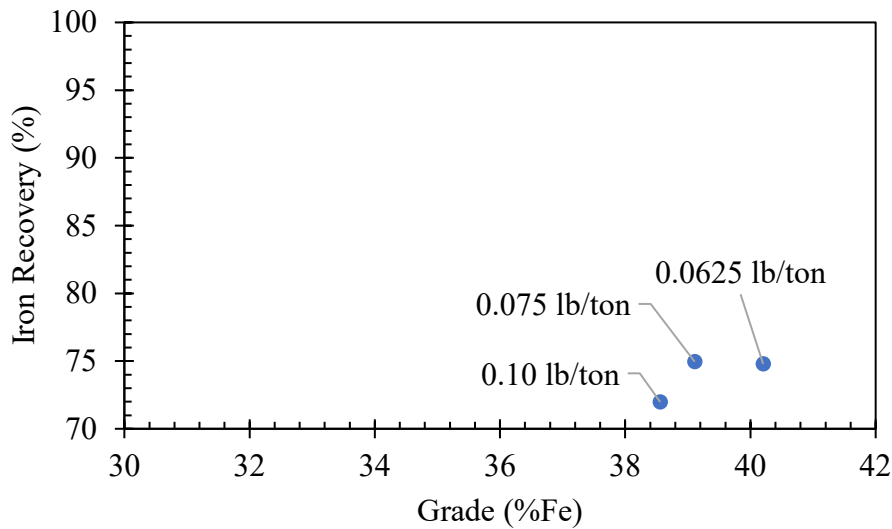


Figure 3.16: Grade and recovery curve for desliming tests at a constant dispersant dosage of 3 lb/ton and varying dosages of starch presented as labels in the plot.

Table 3.4 and Figure 3.17 summarize the grade and recovery results obtained from all the different combinations of dispersant and starch dosages. As it is observed, only the combination of reagents that approximated the desliming targets was performed in triplicate. The other combinations were not replicated because the main purpose of this test was not to optimize reagent addition but to determine one combination of reagents that would perform similarly as the desliming process in an iron ore concentration plant. Additionally, we were limited in material and reagents and decided to save them for the flotation tests which is the main focus of this research. As observed in the table, a

dispersant dosage of 3 lb/ton and a starch dosage of 0.0625 lb/ton resulted in a grade of  $40.20 \pm 0.30\%$  Fe and a recovery of  $71.97 \pm 2.06\%$ . Note that the targets for the desliming process were 40-45% grade and 70-80% iron recovery.

Table 3.4: Grade and recovery values for the desliming process at various dispersant and starch dosages. It was determined that 3 lb/ton of dispersant and 0.0635 lb/ton of starch yielded grade and recovery values within the targets established for this process. This reagent combination was performed in triplicate for statistical accuracy.

<b>Dispersant (lb/ton)</b>	<b>Starch (lb/ton)</b>	<b>Grade (%Fe)</b>	<b>95% confidence interval</b>	<b>Recovery (%)</b>	<b>95% confidence interval</b>
0.20	0.20	34.01	--	99.64	--
0.50	0.10	34.07	--	93.51	--
0.80	0.03	32.48	--	94.20	--
0.80	0.10	36.52	--	92.32	--
0.80	0.065	36.31	--	80.90	--
2.00	0.10	38.12	--	76.07	--
2.00	0.20	36.20	--	75.61	--
3.00	0.10	38.56	--	71.97	--
3.00	0.075	39.11	--	74.95	--
3.00	0.0625	40.20	0.30	74.78	2.06

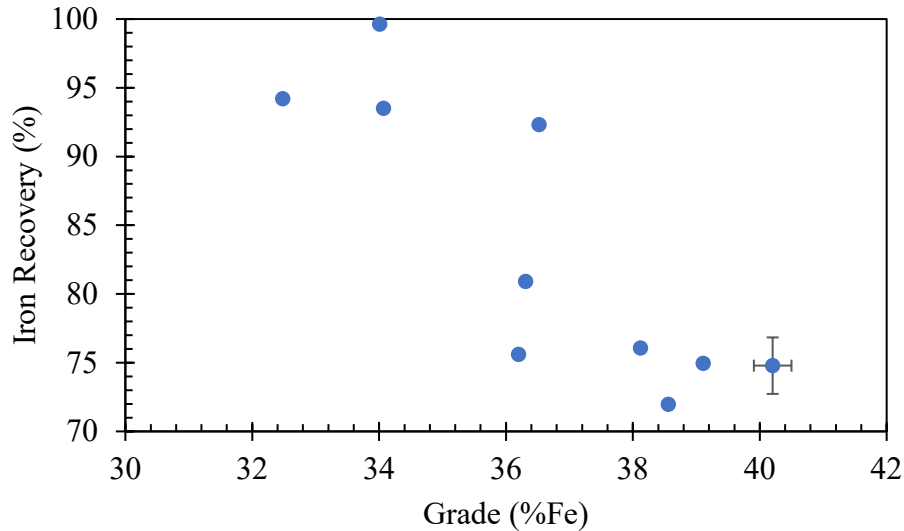


Figure 3.17: Grade and recovery curve for the desliming process at various dispersant and starch dosages listed in Table 4. The error bars indicate the 95% confidence interval. The best performance was observed at 3 lb/ton of dispersant and 0.0635 lb/ton of starch with a grade of  $40.20 \pm 0.30\%$  Fe and recovery of  $74.78 \pm 2.06\%$ .

### 3.4.4 Reverse Cationic Flotation

Figure 3.18 shows the grade and recovery curve for the flotation process at a constant starch dosage (1.5 lb/ton) and various ether amine dosages. As the ether amine concentration increases at a constant starch dosage, the grade increases but the recovery decreases. This is a typical behavior for a grade and recovery plot. An increase in the amine concentration improves the flotation of hydrophobic silica, thus improving the grade of the hematite concentrate. However, because amine acts as both collector and frother, an increase in the amine concentration increases the production of froth and can provoke an increase in the level of entrainment of hematite, meaning that more hematite particles can

be trapped in between bubbles and transferred to the froth product, which explains why there is a reduction on the iron recovery in the concentrate.

Figure 3.19 shows the grade and recovery curve for the flotation process at a constant ether amine dosage (1.5 lb/ton) and various starch dosages. As the starch concentration increases at a constant amine dosage, the grade decreases but the recovery increases. The more starch is added, the greater the depression of particles and the higher the recovery. However, an excess of starch can also cause a decrease in the grade as less material is being floated by the ether amine and more silica is ending up in the concentrate.

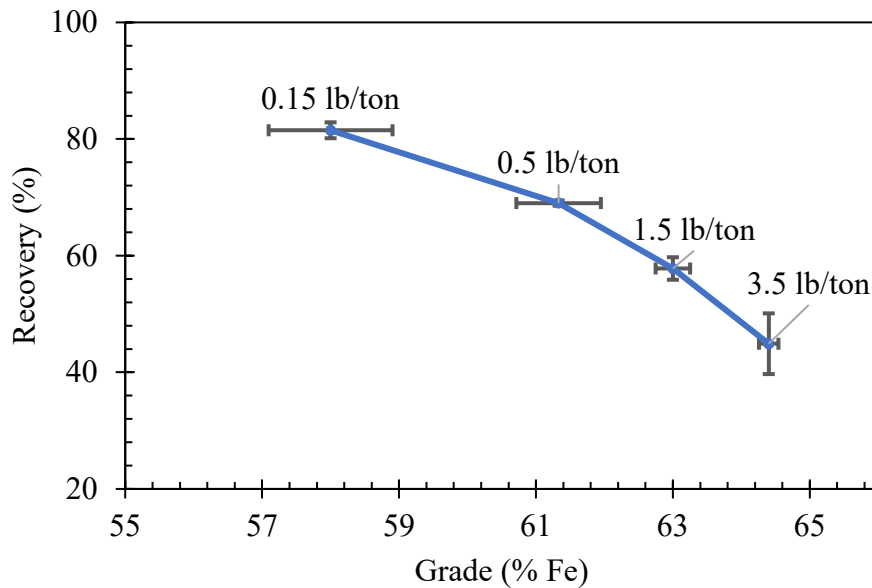


Figure 3.18: Grade and recovery curve for the flotation process at a constant starch dosage (1.5 lb/ton) and various ether amine dosages presented as labels in the plot.

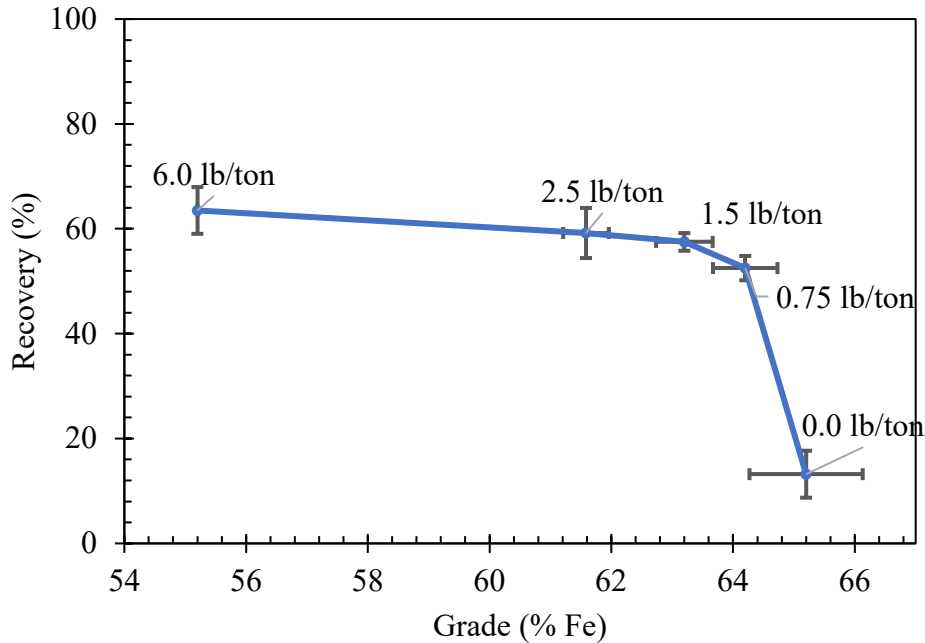


Figure 3.19: Grade and recovery curve for the flotation process at a constant ether amine dosage (1.5 lb/ton) and various starch dosages presented as labels in the plot.

Based on the data obtained, the best flotation performance was attained by adding 1.5 lb/ton of ether amine and 1.5 lb/ton of starch. With this reagent's dosage combination, a grade of  $63.4 \pm 1.8\%$  Fe and a recovery  $56.7 \pm 2.8\%$  were obtained. Note that this data represents a single stage rougher flotation. The recovery can be further improved by adding scavenging stages were the froth is floated again until the desired recovery is obtained. Figure 3.20 shows experimental results of adding scavenging stages in the laboratory. It was determined that one stage of scavenging improves the recovery by approximately 10% and lowers the grade by approximately 0.5%. From these results it is concluded that adding one stage of scavenging in the laboratory is enough to reach the grade and recovery targets desired. With 1.5 lb/ton of ether amine and 1.5 lb/ton of starch and one stage of scavenging, the grade and recovery obtained were  $63.0 \pm 0.6\%$  Fe and

60.5 ± 0.8% respectively. Adding extra scavenging stages in the laboratory did not prove to be helpful, as the grade starts to appear below the grade target necessary in flotation.

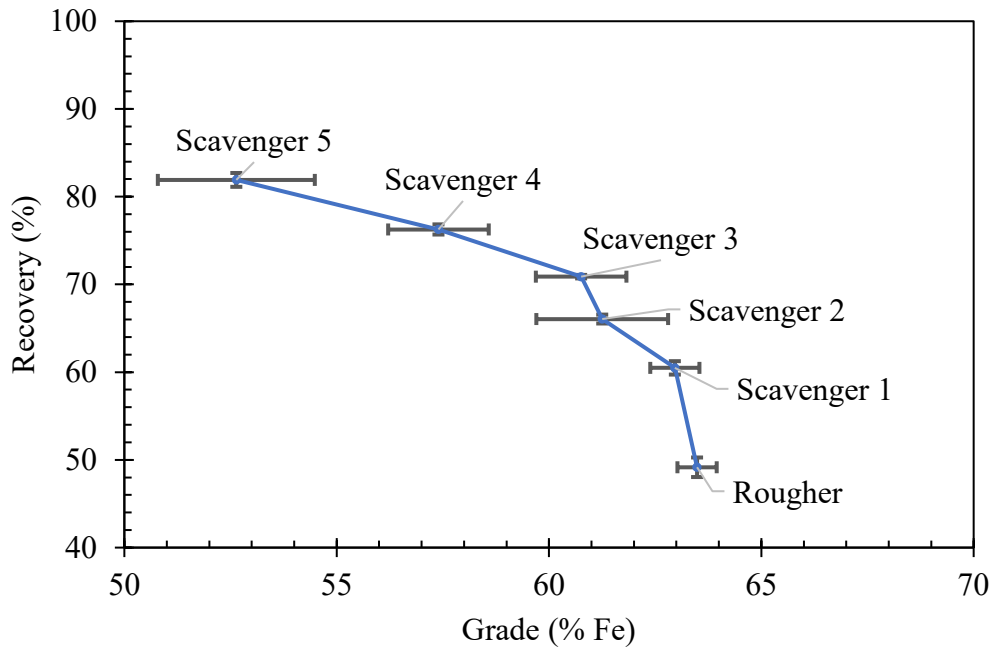


Figure 3.20: Grade and recovery curve for the laboratory flotation circuit with one rougher stage and five scavenger stages.

### 3.4.5 Conclusion

A laboratory procedure was developed to recreate the iron ore flotation process at Plant A. This procedure consisted on grinding 500 grams of ore for 50 minutes to reach a liberation size of approximately 25  $\mu\text{m}$  at 80% passing, desliming with 3 lb/ton of dispersant and 0.0625 lb/ton of starch flocculant, and floating with 1.5 lb/ton of starch depressant, and 1.5 lb/ton of ether amine collector/frother 30% neutralized. The whole process needs to be performed at a pH of 10.5 adjusted with sodium hydroxide (NaOH). It was concluded that one stage of scavenging in flotation could improve the recovery of



the laboratory results while maintaining an iron grade within the desired range. Table 3.5 provides a summary of the targets for each process and the results obtained at the Michigan Technological University laboratory. This data, along with the laboratory procedure determined can now be used as a reference to perform process optimization tests in the laboratory.

Table 3.5: Summary of results of grinding, desliming and flotation in the laboratory.

	<b>Plant Targets</b>	<b>Michigan Tech Lab Results</b>	<b>Method / Findings</b>
Grinding Process Initial size: 0.8 mm	25 $\mu\text{m}$ at 80% passing	25.57 $\pm$ 0.3 $\mu\text{m}$ at 80% passing	Achieved by grinding for 50 minutes in the rod mill with dispersant.
Desliming Process	Grade: 40-45% Recovery: 70-80%	Grade: 40.2 $\pm$ 0.5% Recovery: 76.2 $\pm$ 4.0%	Optimum dosages: 3 lb/ton Dispersant (anionic polyacrylamide) 0.0625 lb/ton Flocculant (corn starch)
Single Stage – Flotation Process	Grade: 63-64% Recovery: 60%	Grade: 63.4 $\pm$ 1.8% Recovery: 56.7 $\pm$ 2.8%	Optimum dosages: 1.5 lb/ton Depressant (corn starch) 1.5 lb/ton Collector (Ether Monoamine)

### 3.4.6 References

- ASTM, 2017. “ASTM-B822-17, Standard test method for particle size distribution of metal powders and related compounds by light scattering,” *ASTM International*, West Conshohocken, PA, U.S.
- Day, R. A., and Underwood, A. L., 1991a. “Quantitative analysis,” In *Complexometric Titrations*, 6th ed. Englewood Cliffs, NJ: Prentice Hall. pp. 201-208.
- Day, R. A., and Underwood, A. L., 1991b. “Quantitative analysis,” In *Determination of iron with 1,10-Phenanthroline*, 6th ed. Englewood Cliffs, NJ: Prentice Hall. pp. 645-646.
- DeVaney, F. D. 1985. “Ore preparation and concentration methods,” In *SME mineral processing Handbook*, ed. N. L. Weiss. Section 20. New York: Society of Mining Engineers of the American Institute of Mining, Metallurgical and Petroleum Engineers, Inc. pp. 20:4.
- Filippov, L. O., Severov, V. V., and Filippova, I. V., 2014. “An overview of the beneficiation of iron ores via reverse cationic flotation,” *International Journal of Mineral Processing*, 127, pp. 62-69.
- Green, R. E., and Colombo, A. F., 1984. “Dispersion-Selective Flocculation-Desliming Characteristics of Oxidized Taconites,” *Bureau of Mines Report of Investigations*.

- Haselhuhn, H. J., and Kawatra, S. K., 2015. “Effects of Water Chemistry on Hematite Selective Flocculation and Dispersion,” *Mineral Processing and Extractive Metallurgy Review*. 36:5, 305-309. DOI: 10.1080/08827508.2014.978318
- Johansson, M., Bengtsson, M., Evertsson, M., and Hulthen, E., 2017. “A fundamental model of an industrial-scale jaw crusher,” *Minerals Engineering*, Vol. 105, pp. 69-78.
- Keranen, C.U., 1986. “Reagents Preparation, Distribution and Feeding Systems at the Tilden Mine,” *Design and Installation of Concentration and Dewatering Circuits. Society for Mining, Metallurgy and Exploration*, pp. 308-319.
- Keranen, C. U., Ivelson, A. T., and Lindroos, E. W., 1985. “Plants using flotation,” *SME Mineral Processing Handbook*, ed. N. L. Weiss. Section 20. New York: Society of Mining Engineers of the American Institute of Mining, Metallurgical and Petroleum Engineers, Inc. pp. 20:30-20:33.
- Mariani, R. D., and Nelson, A. T., 1993. “Silica Flotation at the Tilden Mine,” *Society for Mining, Metallurgy & Exploration*.
- Microtrac, 2007. “Total Solutions in Particle Characterization,” Sync
- Nagaraj, D.R., and Ravishankar, S.A. 2007. “Flotation reagents—A critical overview from an industry perspective,” *In Froth Flotation: A Century of Innovation*. Edited by M.C. Fuerstenau, G.J. Jameson, and R.-H. Yoon. Littleton, CO: SME. pp. 375–424.

- Nakhaei, F., and Irannajad, M., 2018. “Reagents types in flotation of iron oxide minerals: a review,” *Mineral Processing and Extractive Metallurgy Review*. 39:2. pp. 89-124.
- Nai-Ning, W., Hong-Jian, Z., and Xian-Huang, Y., 1992. “A versatile Fraunhofer diffraction and Mie scattering based laser particle sizer,” *Advanced Powder Technology*, Vol. 3, Issue 1., pp. 7-14.
- Villar, J. W., and Dawe, G. A., 1975. “The Tilden mine-a new processing technique for iron ore,” *Mining Congress Journal*, 61 (10):40–48.
- Yang, S., Li, C., and Wang, L., 2017. “Dissolution of starch and its role in the flotation separation of quartz from hematite,” *Powder Technology*. vol. 320. pp. 346-357.
- Zhang, X., Gu, X., Han, Y., Parra-Álvarez, N., Claremboux, V., and Kawatra, S. K., 2019, “Flotation of Iron Ores: A Review”, *Mineral Processing and Extractive Metallurgy Review*, DOI: 10.1080/08827508.2019.1689494

## **4 Partially Substituting Amine with Frothers to Improve Iron Ore Flotation**

### **4.1 Abstract**

Most flotation processes use collectors and frothers to selectively float minerals. This is not the case of reverse flotation of hematite, where ether amine acts as both the collector and the frother. In flotation, hematite is commonly recovered in the froth by entrainment as particles are trapped by bubbles and recovered in the froth product. The level of entrainment can be reduced by controlling the bubble size and froth stability which is dependent on the frother type and dosage. In iron ore flotation it is very difficult to control the frothing and collecting characteristics separately as a suitable dose of ether amine as a collector may be an excessive dose as a frother and vice versa. Partially replacing amine with a frother not only could enhance process control and performance, but it could reduce reagent cost. Most frothers are less expensive than amines, so if amines can be partially replaced with frothers without losing separation efficiency it directly translates to cost savings overall. In this project, MIBC and PPG1012 were added as frothers at different amine replacement ratios. With a 10% amine replacement with MIBC the recovery improved by 2.5%. PPG 1012 can reduce the reagent cost, but considering the grade and recovery reduction and the high DFI, it cannot be easily recommended.

## 4.2 Introduction

The reverse cationic flotation process is the most common method to concentrate iron ores. In this process the gangue material primarily composed of silica is recovered in the froth or overflow product while the hematite concentrate is recovered in the sinks or underflow product. There are three main reagents used in hematite flotation: pH modifier, collector/frother, and depressant. Sodium hydroxide (NaOH) is used as a pH regulator in order to maintain the pH of the slurry around 10.5 which is key on establishing the zeta potential of minerals. Ether amine is used as a collector to render the quartz surface hydrophobic and as a frother to assist with froth formation and control froth stability. On the other side, modified corn starch is used as a depressant by adsorbing onto the hematite surface and preventing collector adsorption.

Entrainment of particles is one of the main problems encountered in flotation plants. This mechanism consists of particles trapped non-selectively by bubbles and transferred to the froth product. In iron ore flotation it is common to recover entrained hematite in the froth or tailings product, which translates to low grades and recoveries in the final concentrate. One of the main theories that explains the entrainment mechanism is the bubble swarm theory which states that as the bubbles come up to the surface, they start accumulating right underneath the froth/pulp interface where some of the water and suspended particles drain back and what is left is forced upward to the froth layer due to the buoyancy of bubbles (Wang et al., 2015; Smith and Warren, 1989).

Particles suspended in the water can either drain back to the pulp phase or be recovered by entrainment in the froth product. Cutting (1989) mentions that water and solids

drainage can happen due to froth collapsing in a specific area or by sedimentation through the Plateau borders which are channels that contain most of the liquid present in the froth as shown in Figure 4.1. The stability of the inter-bubble lamellae establishes the resistance of the bubble to further deformation and coalescence (Banford et al., 1998). As drainage continues the lamellae tends to increase in length and decrease in thickness (Banford et al., 1998).

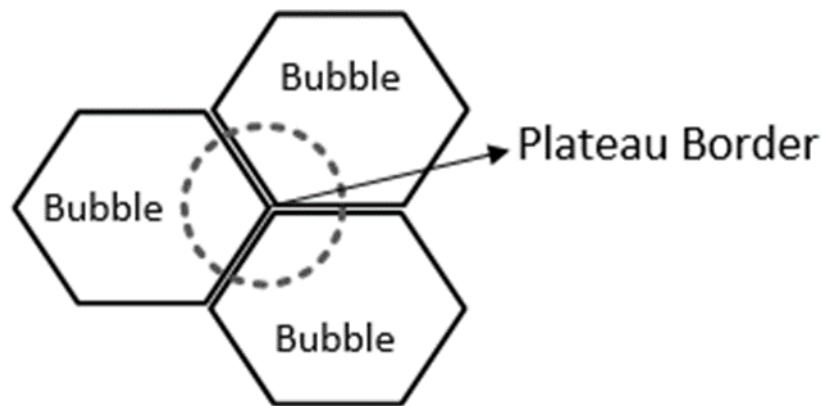


Figure 4.1: Plateau border depiction

Entrainment can be analyzed based on a classifying factor referred as the degree of entrainment which considers the degree of drainage of particles and water trapped in between bubbles (Johnson, 1972; Savassi, 1998; Zheng et al., 2006). The froth structure can greatly affect the degree of entrainment, however the froth structure itself depends on many other factors such as water content, bubble size, gas flow rate, ore mineralogy, and type and concentration of reagents (Savassi, 1998; Wang et al., 2015). This chapter focuses on the role of frothers and collectors in the recovery of hematite in iron ore flotation.

A high degree of hematite entrainment can be presented in the process due to an excess of frother. To achieve optimum results in iron ore flotation, it would be ideal to control the frothing and collecting characteristics independently. Since the ether amine behaves as both a frother and a collector, a suitable dose of ether amine as a collector may be an excessive dose as a frother or vice versa. Controlling frothing and collecting properties independently should make it easier to achieve optimal flotation conditions. Additionally, most frothers are less expensive than amines, so if amines can be partially replaced with frothers without losing separation efficiency it directly translates to cost savings overall. Selecting the right frother is key. The stability of a frother is particularly important as a stable froth assists the recovery of hydrophobic material while an unstable froth tends to be more selective (Morar et al., 2006). Processing plants commonly desire a surfactant that would allow the froth to be stable during flotation so that it can transfer the floated particles without collapsing, however, a frother that is too stable can be problematic after flotation when the froth needs to break down and filtered (Morar et al., 2006). This chapter presents a short review of amines and frothers in flotation and analyses the addition of non-collecting frothers to partially substitute the amine collector and reduce the entrainment of particles during the process.

#### **4.2.1 Amine Collectors in Flotation**

Selecting the ideal frother and the amine replacement ratio greatly depends on the ore mineralogy and the type of collector. Thus, it is important to understand the different types of amines and their frothing effect in flotation. Amines are defined as organic compounds derived from ammonia (NH<sub>3</sub>) by replacing one, two or three hydrogen atoms



with organic groups. The terms primary, secondary and tertiary amines refer to the number of hydrogen atoms from ammonia that were substituted by alkyl groups (see Figure 4.2). For instance:

- Ammonia:  $\text{NH}_3$
- Primary amine:  $\text{RNH}_2$
- Secondary amine:  $\text{R}_2\text{NH}$
- Tertiary amine:  $\text{R}_3\text{N}$
- Quaternary amine:  $\text{R}_4\text{N}^+$

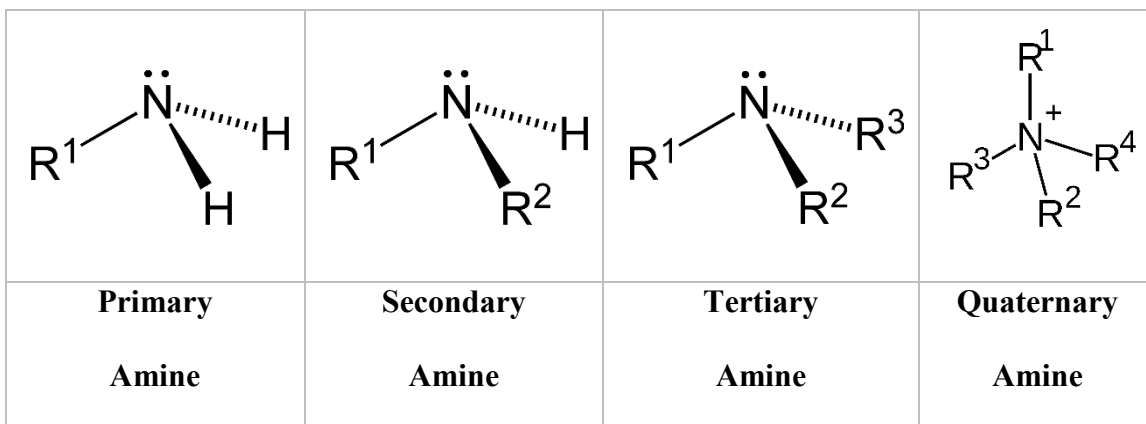
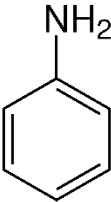
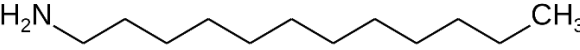
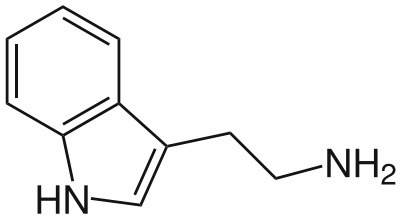


Figure 4.2: Primary, secondary, tertiary, and quaternary amine representation.

As shown in Table 4.1, amines can be classified based on whether the nitrogen atom is attached to a carbon atom belonging to a cyclic structure in the case of aryl amines, a chain in the case of alkyl amines, or to both in the case of alkyl-aryl amines (Nakhaei and Irannajad, 2018; Zhang et al., 2021). Additionally, based on the length of the alkyl chains and synthesis methods, amines can be classified as fatty amines, fatty diamines, ether amines, ether diamines, and condensates (Nakhaei and Irannajad, 2018). The greater the

alkyl chain, the greater the floatability and the lower the concentration required (Rao, 2004; Nakhaei and Irannajad, 2018; Zhang et al., 2021).

Table 4.1: Aryl amines, alkyl amines, and alkyl-aryl amines classification.

Amine Group	Example	Structure
Aryl amines	Aniline	
Alkyl amines	Dodecylamine	
alkyl-aryl amines	Tryptamine	

Fatty amine corresponds to any amine that is attached to an alkyl chain of 8-22 carbon atoms. They are derived from fatty acids as the acids are transformed to nitrates and then a catalytic hydrogenation of nitriles turns them into amines (Bulatovic, 2007; Nakhaei and Irannajad, 2018; Zhang et al., 2021). Fatty amines with alkyl chains of 16C or more show a low activity in the air-liquid interface and are usually utilized in flotation along with a frother (Papini et al. 2001). In past years, primary fatty amines (e.g. dodecylamine) were very common in reverse cationic flotation of iron ore, but nowadays ether amines are the most common collector in this industry despite the fact that they have a lower collecting power than fatty amines (Nakhaei and Irannajad, 2018; Zhang et al., 2021). Ether amine is produced when an aliphatic alcohol reacts with acrylonitrile and is then reduced. A second reaction with acrylonitrile produces an ether diamine. The oxygen gives a partial hydrophilic character to the hydrophobic chain, which makes it more soluble. Ether amines are known to have good frothing power and the use of separate frothers is not common. (Papini et al., 2001)

There is continuing work on analyzing and comparing the performance of amine collectors in iron ore flotation and on developing new collectors for commercial use around the world. In previous years, Papini et al. (2001) performed several iron ore experiments with different cationic collectors. The ore was obtained from the Iron Quadrangle in Brazil and the collectors used were: fatty monoamine, fatty diamine, ether monoamine, ether diamine, condensate, and kerosene combined with amine. From the study, Papini et al. (2001) concluded that ether monoamines were more efficient than ether diamines; fatty amines and condensates produced concentrates with high silica

contents making them poor collectors in the reverse cationic flotation of iron ore; and diamines were more effective than monoamines when combined with kerosene.

Similarly, Vieira and Peres (2007) studied the effect of ether monoamine and ether diamine in the reverse flotation of iron. It was determined that ether monoamine was more efficient than ether diamine in the flotation of fine (-74 to +38  $\mu\text{m}$ ) quartz at pH of 9, yet, at a higher pH, ether diamine showed better results when floating medium (-150 to +74  $\mu\text{m}$ ) and coarse (-297 to +150  $\mu\text{m}$ ) quartz with higher reagent dosages. (Parra-Alvarez et al., 2020)

Araujo et al. (2005) discusses that in some cases, the flotation performance is enhanced by combining ether diamines with ether monoamines or by partially substituting amines with fuel oil (e.g. fuel oil ASTM #5). The optimal amount of oil in the collector is around 20%, but the emulsification of the oil phase in the amine is necessary for successful results (Araujo et al., 2005). It was claimed by Araujo and Souza (1997) that the amine consumption is reduced without altering the metals recovery.

More recently, the use of quaternary ammonium surfactants has become appealing in reverse iron ore flotation due to its high selectivity, solubility, and collecting power (Weng et al., 2013; Nakhaei and Irannajad, 2018; Zhang et al., 2021). Weng et al. (2013) developed a quaternary ammonium surfactant (M-302) composed of ester bonds and hydrocarbon tails. This reagent was initially tested in the reverse cationic flotation of a Chinese magnetite ore and it showed stronger collecting power, a higher rate of foam collapse, and a wider effective temperature range than dodecylamine chloride (Zhang et al., 2021).

Gemini surfactants (GS) are compounds that consist of two polar tails and two polar heads that are chemically bonded by a spacer. These surfactants have superior properties than monomeric surfactants. In fact, their low critical micelle concentration (CMC) values make them more surface active, with stronger biological activity, greater solubilizing ability, and better foaming and wetting characteristics (Nakhaei and Irannajad, 2018; Zhang et al., 2021). Little work has been done regarding the use of gemini collectors in iron ore flotation, however Huang et al. (2014) proposed the use of ethane-1,2-bis(dimethyldodecylammonium bromide) (EBAB) as a collector in the reverse cationic flotation of quartz from a magnetite ore from the Gongchangling Iron Mine, Anshan Steel Company in China. The results showed that EBAB had a greater collecting power and selectivity for quartz than dodecylammonium chloride (DAC), a conventional monomeric surfactant.

Even though there is continuing work to develop new collectors for the reverse cationic flotation of iron ore, ether amines are still the dominant cationic collector in industry despite its low selectivity. Hence, the focus of this chapter is on partially replacing the ether amine with frothers. The next section includes a brief review of the different types of frothers used in flotation and their effect in froth formation and stability.

### **4.2.2 Frothers in Flotation**

Frothers play a very important role in flotation as they assist with the formation of fine bubbles, prevent bubble coalescence, decrease bubble rising rate, alter the action of the collector, increase bubble strength and stability during bubble-particle attachment, among other functions (Schlitt et al., 1992). Frothers are heteropolar surface-active compounds

with a hydrophilic (polar) group that reacts with water dipoles, and a hydrophobic (non-polar) hydrocarbon chain that is oriented towards the gas phase. The strength of the bubble wall increases due to the reaction between water dipoles and the polar group of the frother (Khoshdast and Sam, 2011; Schlitt et al., 1992; Parra-Alvarez et al., 2020). Most common frothers contain a hydrophobic group consisting of a hydrocarbon chain, and one of the following polar groups: (Schlitt et al., 1992)

- Hydroxyl group (OH)
- Carboxyl group (COOH)
- Carbonyl group (C=O)
- Amino group (NH<sub>2</sub>)
- Sulfo group (S(=O)<sub>2</sub>(OH))

Frothers can be classified based on their chemical and physical properties. Some examples include phenols which are aromatic alcohols such as ortho-cresol, meta-cresol, para-cresol, phenol, toluol, and naphthalene; aliphatic alcohols which are alcohol mixtures with 6-8 carbon atoms such as methyl isobutyl carbinol (MIBC), diacetone alcohol, n-propanol, n-butanol, n-pentanol, and t-butanol; natural oils and cyclic alcohol frothers which are blends of various terpinols, ketones, and ethers such as borneol, pinene, fenchone, anethol, and eucalyptol; and polyglycol ethers which are water soluble surfactants such as Dowfroth 250 produced by the reaction of methanol and propylene oxide, Dowfroth 1012, Aerofroth 65, and Aerofroth 67 (Bulatovic, 2007; Crozier, 1992; Hostynek et al., 1973; Harris et al., 2000; Laskowski, 2004; Tan et al., 2005). Polyglycol ether frothers vary significantly depending on the length of their carbon chain and

molecular weight. In general, a high molecular weight frother forms a more persistent froth but lower selectivity compared to a low molecular weight frother (Laskowski, 2004; Valluri and Kawatra, 2021).

The use of frothers improves flotation efficiency by increasing the rate of flotation (Khoshdast and Sam, 2011). Frothers can be characterized based on their power and selectivity. The power of the frother is related to the frothing capacity and how well the frother can increase flotation recovery and performance especially with coarse particles (Khoshdast and Sam, 2011). The term selectivity is related to hydrophobic particles adsorbing onto air bubbles, which is useful when dealing with fine particles (Khoshdast and Sam, 2011). These frothing characteristics can be defined based on the dynamic foamability index (DFI), the hydrophile-lipophile balance (HLB), and the critical coalescence concentration (CCC).

The dynamic foamability index (DFI) is related to the stability of the frother. It is defined as the limiting slope of the retention time  $t_r$  (average lifetime of a bubble) against concentration at  $c=0$  as seen in Equation 1 as stated by Cho and Laskowski (2002). The higher the DFI value, the greater the froth stability.

$$DFI = \left( \frac{\partial t_r}{\partial c} \right)_{c=0} \quad \text{Equation 4.1}$$

The hydrophilic-lipophilic balance (HLB), used to determine the suitability of a surfactant for a specific application, was originally proposed by Griffin (1949), though the most common method to determine the HLB was developed by Davies (1964). One equation for calculating this value is:  $HLB=7+1.3(O)+1.9(OH)-0.475(CxHy)$ , where OH is the number of hydroxyl functional groups present, O is the number of hydrophilic

oxygen functional groups present, and  $C_xH_y$  corresponds to the number of hydrophobic (lipophilic) groups present (Drzymala et al., 2018).

The HLB number for frothers ranges from 4-10, where 3.5-6 corresponds to frothers with emulsification properties, and 7-10 correspond to frothers with wetting properties (Drzymala et al., 2018; Tanaka and Igarishi, 2005). The HLB number defines the water affinity of frothers. The greater the HLB the higher the solubility in water (Kracht et al., 2016). For reference, aliphatic alcohols tend to have an HLB of 5-7.5, polypropylene glycols (PPG) an HLB of 7.4-9.3, and polypropylene glycol alkyl ethers an HLB of 6.5-8.3 (Laskowski, 2004). A summary of HLB values for different types of frothers can be found in Zhang et al. (2012).

Another important term when studying frothers is the mechanism of bubble coalescence, in other words, the mechanism by which bubbles merge into one single bubble during contact (see Figure 4.3). At a specific frother concentration known as critical coalescence concentration (CCC), bubble coalescence can be avoided (Castro et al., 2013). Frothers with a high CCC are commonly classified as weak frothers because it requires a higher dosage to reach the maximum frothing potential compared to frothers with a low CCC (Parra-Alvarez et al., 2020). A summary of CCC values for different types of frothers can also be found in Zhang et al. (2012).



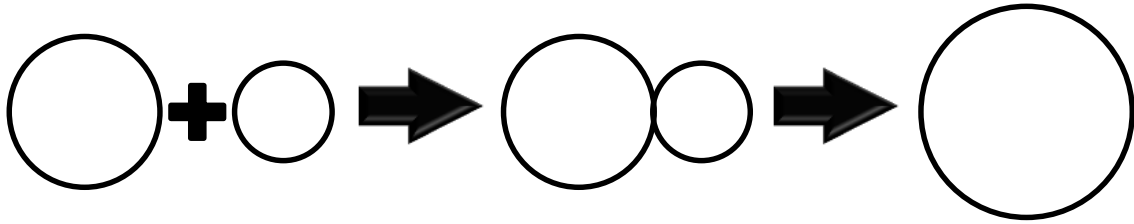


Figure 4.3: Bubble coalescence mechanism. The mechanism by which two bubbles merge into one single bubble during contact.

### 4.2.3 Frothing Ability of Amines and Frothers

Most flotation processes use collectors and frothers to selectively float minerals. This is not the case of reverse flotation of hematite where ether amine acts as both the collector and the frother (Uwadiale, 1992). Most frothers are simply short-chained surfactants which can present a hydrophobic group to the vapor phase while maintaining a strong orientation due to a hydrophilic group in the aqueous phase. MIBC certainly fits this condition: the isobutyl group is hydrophobic, the carbinol group is hydrophilic, and it is very short chained. The ether amines and ether diamines also fit into this category. If a shorter chained amine is used, such as ammonia, it has significantly less frothing power. If a longer chained amine is used, the surfactant ends up expressing more flocculating properties or collecting properties, based on where and how common the nitrogen groups are (Wang, 2016).

In general, low molecular weight frothers like the 400MW polypropylene glycols have consistent hydrophilic/hydrophobic groups. When the molecular weight of frothers starts increasing the frothing properties are reduced (Laskowski and Woodburn, 1998; Harvey et al., 2005). In essence, if the molecular weight is too high, it stops behaving too well as

a frother, but it still needs to be a surfactant or it behaves like water or ammonia (both very bad frothers by themselves), or ethanol (some frothing properties in water, but very limited).

Szczerkowska et al. (2016) studied the effect of the foamability index of short chain alkyl amines on the flotation of quartz. In this study, a method to determine amine foaming properties was developed. By plotting the initial froth and foam heights in a conventional flotation cell at different surfactant dosages, and utilizing an empirical equation, a parameter called foamability index (FI) was determined (Szczerkowska et al., 2016). The FI value was determined to be 92, 12 and 4 mg/(dm<sup>3</sup>) for butylamine, hexylamine and octylamine respectively. It was concluded that a higher amine concentration is required as the length of the alkyl amine decreases in order to obtain a similar quartz recovery (Szczerkowska et al., 2016).

Zhou et al. (2019) performed tests using an air-water system in a mini flotation cell setup. The purpose of the study was to determine water overflow and bubble size for a primary amine (dodecylamine), two ether amines (Flotigam® EDA and Flotigam® 2835-2L), and the combination of each of these collectors with two frothers (MIBC and PPG 425). It was found that amines reduce bubble size less effectively than frothers. Ether amines showed bubble coalescence at low dosages, but when blended with frothers, the bubble coalescence was eliminated. It was also observed that as the amine concentration increases, amines start dominating bubble size at fixed frother dosages. From these results, Zhou et al. (2019) concluded that blending amine with frothers helps eliminate bubble coalescence if residual concentrations of ether amines are below 10 ppm. It was

also concluded that water overflow strongly depends on reagent type. The combination of MIBC and Flotigam® EDA was the only blend that did not cause water overflow.

Vidyadhar et al. (2002) performed a series of experiments to determine the influence of long-chain alcohols on the adsorption of a mixture of amines and alcohols on feldspars. From spectroscopy results it was concluded that compared to results with only amine cations, the adsorption of the amine/alcohol mixture forms a close-packed surface layer which improves flotation recovery. Different alkyl amines (C8, C12 and C16) and alcohols of different alkyl chain lengths (C8, C10, C12, C14 and C16) were tested, and it was discovered that the maximum flotation recovery was obtained when the alkyl chain length of the alcohol and the amine were the same.

Similarly, Monte and Oliveira (2004) studied the addition of long chain alcohols in the flotation of sylvite with dodecylamine. The results showed that the addition of hexanol could significantly improve the adsorption of dodecylamine on potassium chloride (KCl). Other alcohols such as octanol and decanol showed improvements, whereas dodecanol inhibited adsorption. The study discussed how the addition of alcohols could not be the only reason why the recovery was enhanced. Thus, Monte and Oliveira (2004) suggested that due to the low solubility of alcohols in the saturated salt solution, the formation of a second phase at the liquid-gas interface is likely. One thing to keep in mind is that frothers may also act as collectors, activators, or depressants if their chemistry allows it on a given surface.

Filippov et al. (2010) proposed that one method to increase collector effectiveness in oxide ores flotation is mixing reagents with different molecular structures and adding

non-ionic surfactants. For instance, the presence of alcohols in the quartz-amine system lowers the electrostatic repulsion of amines and forms hemimicelles on the quartz surface, which means a close-packed adsorption layer will form at the surface, facilitating silicate flotation and lowering collector dosages. By performing tests with a magnetite ore, Filippov et al. (2010) concluded that the adsorption of a mixture of ether diamine and primary monoamine or a mixture of ether diamine with alcohol gives a more stable layer of adsorption due to variations in the surface energy. It may also be that the greater mobility of the alcohol frothers helps facilitate the adsorption of collector onto portions of silicates that were not accessible with only ether amine. Thus, the frother and collector show a synergistic effect in collector effectiveness Filippov et al. (2010).

Silva et al. (2008) performed laboratory, pilot plant, and industrial tests where the amine collector was partially replaced with a frother mixture in a Brazilian iron ore concentrator. The blend of ester and aldehyde, were used as the frother mixture for these tests. The collector used was a 20% - 30% neutralized ether amine. While the percent amine replacement with a frother was varied throughout the experiments, the other flotation variables were kept constant, such as the starch dosage, pulp pH, and water chemistry. The results for these tests showed that 10% replacement of collector by the selected frother can be achieved with improved overall results. Silva et al. (2008) reported that with a 10% replacement the iron recovery improved from 67.96% to 80.78%, the iron grade improved from 64.92% to 65.43%, resulting in extra revenues of approximately \$3 million per year.

The studies reviewed so far provide a better understanding on the advantages of partially replacing amines with frothers in flotation. These studies explored mixing amines and frothers in 2-phase systems and in the flotation of feldspar, sylvite, and magnetite ores (Zhou et al., 2019; Vidyadhar et al., 2002; Monte and Oliveira, 2004; Filippov et al., 2010; Silva et al., 2018). However, limited work has been performed with hematite ores commonly beneficiated following the reverse cationic flotation process. It is clear that selecting the right frother and the adequate amine replacement ratio greatly depends on process variables, especially ore mineralogy, water chemistry, and the type and concentration of reagents used during the process. The focus of the experimental work in this chapter is to evaluate the feasibility of partially substituting the ether amine with frothers in the reverse cationic flotation of hematite to reduce entrainment and improve recovery.

### **4.3 Materials**

The hematite ore was collected from the autogenous mill screen underflow at an iron ore processing plant in the North American Iron range in the U.S. An X-ray diffraction (XRD) analysis for this ore is shown in Figure 4.4. From this analysis it was determined that the ore is composed of quartz (65.15%), hematite (21.45%), magnesioferrite (7.7%), and goethite (5.7%). The 80% passing size was determined to be 8 mm with a liberation size of 25  $\mu\text{m}$ .

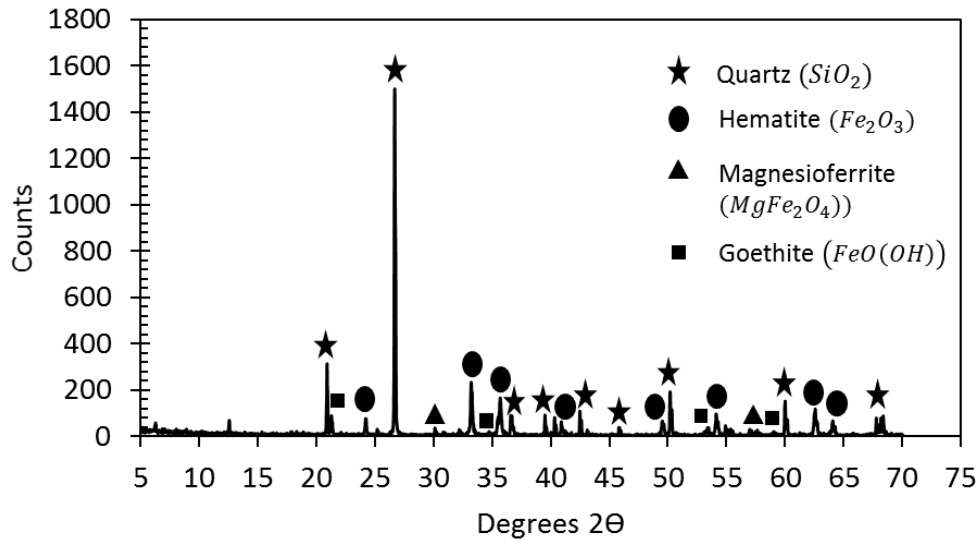


Figure 4.4: XRD results for the hematite sample used. Quartz: 65.15%, Hematite: 21.45%, Magnesioferrite: 7.7%, Goethite: 5.7%.

Two frothers were selected for this study: methyl isobutyl carbinol (MIBC) and polypropylene glycol (PPG 1012). These frothers were selected due to their great differences in strength and stability, identified by their CCC and DFI values. As shown in Table 4.4, MIBC has a lower CCC value than PPG 1012, meaning that a higher dosage of MIBC is required to avoid bubble coalescence compared to PPG 1012. From this it is considered that MIBC is weaker than PPG 1012. Regarding the DFI values, the high DFI value of PPG 1012 explains why this frother produces a more stable froth than MIBC.

Table 4.2: CCC and DFI values for MIBC and PPG 1012 (Gupta et al., 2007)

<b>Parameters</b>	<b>MIBC</b>	<b>PPG 1012</b>
Critical Coalescence Concentration - CCC (ppm)	11.5	6.5
Dynamic Foamability Index – DFI $\left(\frac{s * dm^3}{mmol}\right)$	35.02	267.25

For pH control a 10% caustic soda solution was prepared with sodium hydroxide (NaOH) acquired from Sigma Aldrich. For desliming a 10% dispersant solution was prepared using an anionic polyacrylamide (Cyquest 3223 antiprecipitant) dispersant provided by Solvay. Acid modified corn starch provided by Cleveland Cliffs was used during desliming as a flocculant (0.3% solution) and during flotation as a depressant (3% solution). The starch was gelatinized and causticized in the lab prior to every experiment. A 1% ether amine solution was used as the collector/frother in flotation. This solution was prepared with a primary ether monoamine 30% neutralized with acetic acid which was also provided by Solvay.

## **4.4 Methods**

### **4.4.1 Baseline of Flotation Experiments**

A “control” flotation test was performed in the laboratory following a typical flotation process at an iron ore concentration plant. In this case the ore was ground to approximately 25 μm at 80% passing in a rod mill, deslimed with corn starch flocculant (0.0625 lb/ton) and anionic polyacrylamide dispersant (3 lb/ton), and floated with corn

starch depressant (1.5 lb/ton) and ether amine collector (1.5 lb/ton) in a 2-liter Denver Flotation cell. The pH was maintained at 10.5 along the process with sodium hydroxide (NaOH) and the water used contained 7.5 ppm of calcium and 1.5 ppm of magnesium. No frother was added during the baseline. This test was performed in triplicate for reproducibility.

#### 4.4.2 Maximum Tolerable Froth Dosage Determination

Directly replacing a percentage of amine with methyl isobutyl carbinol (MIBC) and polypropylene glycol (PPG 1012) would most likely cause froth overflow during flotation. For this reason, the maximum tolerable frother dosage at which the froth does not overflow without scraping was determined for MIBC and PPG 1012. Figure 4.5 shows the transition from no frother dosage to the maximum tolerable frother dosage at which the froth starts overflowing. These experiments were performed at a constant pH of 10.5 and a constant starch dosage of 1.5 lb/ton, but amine was not added to the system due to its frothing effects. 5 g/ton of frother were added at a time until the froth started to overflow.

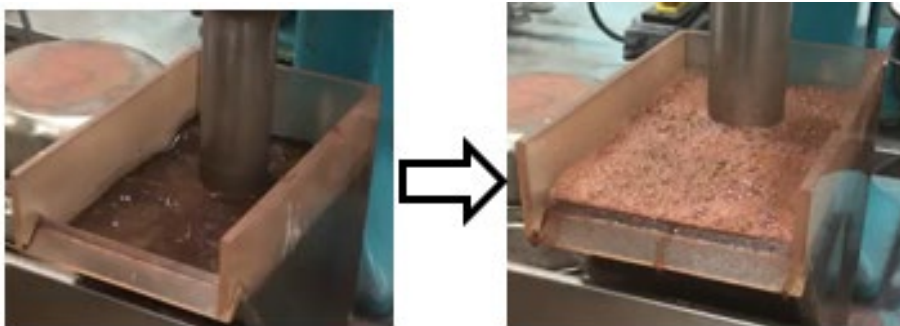


Figure 4.5: Visual transition from no frother dosage to the maximum tolerable frother dosage at which the froth starts overflowing without scraping.



### **4.4.3 Flotation Tests by Partially Replacing Amine with a Frother**

The laboratory procedure was similar to the one described for the baseline experiments except for the reagent's addition during the flotation process. The grinding and desliming procedures were not altered. For all the flotation experiments the pH was maintained at 10.5 adjusted with sodium hydroxide (NaOH) and the starch depressant dosage was kept constant at 1.5 lb/ton. After the starch addition the slurry was conditioned for 3 minutes. Then the desired amount of ether amine was added and conditioned for 1 minute followed by the addition of the selected frother and conditioning for 1 more minute. After all the reagents were added, the air was turned on and the froth product was collected in a tailings pan. Then, both products were filtered, dried and taken for iron ore analysis using a UV-VIS spectrophotometer with a 1,10-phenanthroline indicator.

For each frother (MIBC and PPG 1012), the ether amine was replaced by 5, 10 and 15%. The specific dosages for each experiment are shown in Section 4.5.2. Three replicates were performed per test to ensure reproducibility and all experiments were randomized.

## **4.5 Results and Discussion**

### **4.5.1 Baseline of Flotation Experiments**

The final flotation performance obtained for a single stage of flotation without frother in the laboratory was of  $63.2 \pm 1.7\%$  iron grade and  $54.4 \pm 2.1\%$  iron recovery. The final iron product in a concentrator plant in the United States with similar ore characteristics has been reported to average 64-67% grade, with 5% silica and a recovery of around 75% iron after four stages of scavenging (Zhang et al., 2021). Keeping in mind that the

laboratory tests only include one stage of flotation, the results can be used as a baseline for this project. Thus, this data was used as a point of reference for the flotation experiments with frother addition.

#### 4.5.2 Maximum Tolerable Froth Dosage Determination

The maximum tolerable frother dosages recorded for MIBC and PPG 1012 were 0.11 and 0.17 lb/ton respectively. These values were used to determine the amine and frother dosages for each experiment as shown in Table 4.3 and 4.4.

Table 4.3: Dosage determination for partial amine replacement with MIBC

<b>Amine Replacement (%)</b>	<b>Starch Dosage (lb/ton)</b>	<b>Amine Dosage (lb/ton)</b>	<b>MIBC Dosage (lb/ton)</b>
0	1.5000	1.5000	0.0000
5	1.5000	1.4250	0.0055
10	1.5000	1.3500	0.0110
15	1.5000	1.2750	0.0165
100	1.5000	0.0000	0.1100

Table 4.4: Dosage determination for partial amine replacement with PPG 1012

<b>Amine Replacement (%)</b>	<b>Starch Dosage (lb/ton)</b>	<b>Amine Dosage (lb/ton)</b>	<b>PPG 1012 Dosage (lb/ton)</b>
0	1.5000	1.5000	0.0000
5	1.5000	1.4250	0.0085
10	1.5000	1.3500	0.0170
15	1.5000	1.2750	0.0255
100	1.5000	0.0000	0.1700

### 4.5.3 Flotation Tests by Partially Replacing Amine with a Frother

Table 4.5: Flotation results after partially substitution the ether amine collector with MIBC frother

<b>Amine Replacement (%)</b>	<b>Iron Grade (%Fe)</b>	<b>Iron Recovery (%)</b>
0	63.2 ± 1.7	54.4 ± 2.1
5	62.6 ± 3.1	56.0 ± 5.4
10	63.7 ± 2.0	57.1 ± 1.3
15	63.5 ± 2.0	54.8 ± 4.0

Table 4.6: Flotation results after partially substitution the ether amine collector with PPG1012 frother

<b>Amine Replacement (%)</b>	<b>Iron Grade (%Fe)</b>	<b>Iron Recovery (%)</b>
0	63.2 ± 1.7	54.4 ± 2.1
5	57.8 ± 5.7	53.8 ± 1.6
10	63.2 ± 1.0	52.8 ± 0.1
15	60.3 ± 1.3	57.3 ± 3.7

The final product for the baseline tests without a frother resulted in a grade of 63.2 ± 1.7% and a recovery of 54.4 ± 2.1%. As it is observed in Table 4.5, with a 10% ether amine replacement with MIBC frother, the recovery improved by approximately 2.5wt% while maintaining the iron grade. As shown in Table 4.6, partially replacing the collector with PPG 1012 resulted in lower grades and recoveries for all the replacement ratios tested, in comparison to the baseline tests. This could be attributed to the high DFI value of PPG 1012 which translates to the formation of very stable froths that are no longer beneficial to the process.

As stated earlier in the chapter, the froth product is composed of material that has been recovered by true flotation and material that has been recovered by entrainment. The recovery of particles by entrainment is known to be proportional to the water recovery (Engelbrech and Woodburn, 1975). As stable froths increase the viscosity of bubble

films and lower the coalescence, they tend to collect more entrained water compared to unstable froths (Morar et al., 2006). This could explain why partially replacing the ether amine with PPG 1012 resulted in a lower iron recovery in the concentrate due to a higher entrainment of hematite compared to the performance obtained with MIBC.

Comparing the iron grade results with both frothers it is evident that MIBC is able to produce a concentrate with a higher iron grade compared to PPG 1012, which tells us that in this process MIBC shows a greater selectivity than PPG 1012. This data agrees with a study performed by Gupta et al. (2007) with coal flotation. Furthermore, previous research shows that froth stability is greatly dependent on the type and concentration of frothers (Gupta et al., 2007). MIBC is considered a weaker frother, but as its concentration increases it can increase the froth stability significantly. This could explain why a 15% replacement of ether amine with MIBC resulted in a lower iron recovery in the concentrate than the results obtained with a 10% replacement.

With a 10% amine replacement with MIBC the recovery improved by 2.5wt% which corresponds to millions of dollars in extra revenue in industry as a whole. Note that a few percentage points of improvement in iron recovery can be millions of dollars in savings (Zhang et al., 2021). Moreover, most commercially used frothers are less expensive than the amine collectors used in industry which provides another reason why partially substituting amines with frothers such as MIBC can be efficient and profitable (Silva et al., 2008). Using PPG 1012 could reduce the reagent cost but based on the results obtained in this study it can reduce earnings in production. Frothers with very high DFI values such as PPG 1012 tend to be undesirable in industry as they are difficult to handle

and consume more energy during the filtration process. It is recommended to test alternative frothers and possibly other collectors with less frothing properties so the frothing and collecting power can be independently controlled.

## **4.6 Conclusions**

In the reverse flotation of hematite, entrainment can be reduced and the iron recovery can be improved by partially substituting the amine with a frother. Selecting the right frother and amine combination for this purpose is greatly dependent on the ore mineralogy and the type and concentration of the reagents used during the process. This chapter provided a brief review of the different types of amines and frothers used in flotation and previous studies on mixing amines with frothers. Additionally, experiments were performed using a hematite ore from the North American iron range, a primary ether monoamine and two different frothers. With a 10% amine replacement with MIBC the recovery improved by 2.5% which corresponds to millions of dollars in extra revenue in industry as a whole. PPG 1012 can reduce the reagent cost but considering the grade and recovery reduction and the high DFI, it cannot be easily recommended.

## **4.7 References**

- Araujo, A.C., Souza, C.C., 1997. “Partial replacement of amine in reverse column flotation of iron ores: 1—Pilot plant studies.” In: Proceedings of the 70th Annual Meeting Minnesota Section SME and 58th Annual University of Minnesota Mining Symposium, Duluth, Minnesota, pp. 111–112

- Araujo, A. C., Viana, P. R. M., and Peres, A. E. C., 2005, “Reagents in iron ores flotation.” *Minerals Engineering*, 18(2). pp. 219-224.
- Banford, A. W., Aktas, Z., and Woodburn, E. T., 1998. “Interpretation of the effect of froth structure on the performance of froth flotation using image analysis,” *Powder Technology*, 98, pp. 61-73.
- Bulatovic, S. M. 2007. “Flotation reagents: Chemistry, theory and practice”, Netherlands: Elsevier Science. 3–99.
- Castro, S., Miranda, C., Toledo, P. and Laskowski, J.S., 2013. “Effect of frothers on bubble coalescence and foaming in electrolyte solutions and seawater,” *International Journal of Mineral Processing*, 124, pp.8-14.
- Cho, Y.S. and Laskowski, J.S., 2002. “Effect of flotation frothers on bubble size and foam stability,” *International Journal of Mineral Processing*, 64(2-3), pp.69-80.
- Crozier, R.D., 1992. “Flotation: theory, reagents and ore testing,” Oxford: Pergamon.
- Cutting, G. W., 1989, “Effect of froth structure and mobility on plant performance”, *Mineral Processing and Extractive Metallurgy Review*. 5, pp. 169-201.
- Davies, J.T., 1964. “Mass-transfer and interfacial phenomena,” In *Advances in Chemical Engineering*, Academic Press. Vol. 4, pp. 1-50.
- Drzymala, J., and Kowalczyk, P.B., 2018. “Classification of flotation frothers,” *Minerals*, 8(2), p.53.

- Engelbrethc, J. A., and Woodburn, E. T., 1975. “The effects of froth height, aeration rate and gas precipitation of flotation,” *Journal of the South African Institute of Mining and Metallurgy*, pp. 125-132.
- Filippov, L. O., Filippova, I. V., and Severov, V. V., 2010, “The use of collectors mixture in the reverse cationic flotation of magnetite ore: The role of Fe-bearing silicates.” *Minerals Engineering*, 23, pp. 91-98.
- Gupta, A. K., Banerjee, P. K., Mishra, A., Satish, P., and Pradip, P., 2007, “Effect of alcohol and polyglycol ether frothers on foam stability, bubble size and coal flotation,” *International Journal of Mineral Processing*, Vol. 82, pp. 126-137.
- Griffin, W.C., 1949. “Classification of Surface-Active Agents by “HLB”,” *Journal of Cosmetic Science*, 1, pp. 311-326.
- Harris, G.H. and Jia, R., 2000. “An improved class of flotation frothers,” *International journal of mineral processing*, 58(1-4), pp.35-43.
- Harvey, P. A., Nguyen, A. V., Jameson, G. J., and Evans, G. M., 2005. “Influence of sodium dodecyl sulphate and dowfroth frothers on froth stability,” *Minerals Engineering*, Vol. 18, Issue 3, pp. 311-315.
- Hostynek, J. and Collins, D., and Dow Chemical Co, 1973. “Frothing agents for the floatation of ores,” U.S. Patent 3,710,939.
- Huang, Z., Zhong, H., Wang, S., Xia, L., Zou, W., and Liu, G., 2014, “Investigations on reverse cationic flotation of iron ore by using a Gemini surfactant: ethane-1, 2-bis (dimethyl-dodecyl-ammonium bromide).” *Chemical Engineering Journal*, 257. pp. 218-228.



- Johnson, N.W., 1972. “The flotation behaviour of some chalcopyrite ores,” University of Queensland Press.
- Khoshdast, H. and Sam, A., 2011. “Flotation frothers: review of their classifications, properties and preparation,” *The Open Mineral Processing Journal*, 4, pp.25-44.
- Kracht, W., Orozco, Y. and Acuña, C., 2016. “Effect of surfactant type on the entrainment factor and selectivity of flotation at laboratory scale,” *Minerals Engineering*, 92, pp.216-220.
- Laskowski, J.S., 2004. “Testing flotation frothers,” *Physicochemical Problems of Mineral Processing*, (38), pp.13-22.
- Laskowski, J. S., and Woodburn, E. T., 1998. “Frothing in flotation II,” Gordon and Breach Science Publishers, Amsterdam, The Netherlands.
- Monte, M. B. M., and Oliveira, J. F., 2004, “Flotation of sylvite with dodecylamine and the effect of added long chain alcohols”, *Minerals Engineering*, 17, pp. 425-430.
- Morar, S. H., Hatfield, D. P., Barbian, N., Bradshaw, D. J., Cilliers, J. J., and Triffett, B., 2006. “A comparison of flotation froth stability measurements and their use in the prediction of concentrate grade,” *IMPC 2006, Proceedings of 23rd International Mineral Processing Congress*.
- Nakhaei, F., and Irannajad, M., 2018. “Reagents types in flotation of iron oxide minerals: a review,” *Mineral Processing and Extractive Metallurgy Review*. 39:2. pp. 89-124.

- Papini, R. M., Brandao, P. R. G., and Peres, A. E. C., 2001, “Cationic flotation of iron ores: amine characterization and performance.” *Mining, Metallurgy & Exploration*, 18(1). pp. 5-9.
- Parra-Alvarez, N., Claremboux, V., and Kawatra, S. K., 2020, “Improving hematite flotation by partially replacing amine with frothers”, 2020 SME Annual Conference & Expo, Phoenix, AZ, Conference proceedings. No. 20-070.
- Rao, S.R., 2004. “Electrical characteristics at interfaces,” In *Surface Chemistry of Froth Flotation*, 2nd ed.; Kluwer Academic/Plenum Publishers, New York, NY, USA, pp. 209–256.
- Savassi, O. N., 1998, “Direct estimation of the degree of entrainment and the froth recovery of attached particles in industrial cells”, The University of Queensland, Australia.
- Schlitt, W.J. et al. (1992). “Mineral processing,” *Mining Engineering Handbook*,
- SME/AIME, NY., Vol. 1, pp. 2232-2234.
- Silva, R. R. R., Correa de Araujo, A., and Farias de Oliveira, J., 2008, “Frother assisted amine flotation of iron ores”, 2nd International Iron Symposium.
- Smith, C. A., 1984, “Dynamic simulation of sulphide flotation circuits”, The University of Queensland, Australia.
- Szczerkowska, S., Siedlarz, M., Wojcik, M., and Kowalczyk, P. B., 2016. “Effect of foamability index of short chain alkyl amines on flotation of quartz,” *Mineral Engineering Conference MEC2016*, Vol. 8, Issue E3S. Wroclaw University of

Science and Technology, Faculty of Geoengineering, Mining and Geology,  
Wybrzeze Wyspianskiego 27, 50-370 Wroclaw, Poland.

- Tan, S.N., Pugh, R.J., Fornasiero, D., Sedev, R. and Ralston, J., 2005. “Foaming of polypropylene glycols and glycol/MIBC mixtures,” *Minerals Engineering*, 18(2), pp.179-188.
- Tanaka, K.O.S.U.K.E., and Igarashi, A.K.I.N.O.R.I., 2005. “Determination of nonionic surfactants” CRC Press: Boca Raton, FL, USA. pp. 149-214.
- Uwadiae, G. G. O. O., 1992, “Flotation of iron oxides and quartz – A review”, *Mineral Processing and Extractive Metallurgy Review*, Issue 3, Vol. 11, pp. 129-161.
- Valluri, S., and Kawatra, S.K., 2021. “Use of frothers to improve the absorption efficiency of dilute sodium carbonate slurry for post combustion CO<sub>2</sub> capture,” *Fuel Processing Technology*, Vol. 212, 106620.
- Vidyadhar, A., Rao, K. H., and Chernyshova, I. V., 2002, “Mechanisms of amine-feldspar interaction in the absence and presence of alcohols studied by spectroscopic methods”, *Colloids and Surfaces, Aspects* 214, pp.127-142.
- Vieira, A. M, and Peres, A. E. C., 2007. “The effect of amine type, pH, and size range in the flotation of quartz,” *Minerals Engineering*, 20(10):1008-1013.  
DOI:10.1016/j.mineng.2007.03.013
- Wang, D., 2016. “Flotation reagents: applied surface chemistry on minerals flotation and energy resources beneficiation,” *Metallurgical Industry Press*, Springer, Beijing, China. Vol. 1, pp. 127-133.

- Wang, L., Peng, Y., Runge, K., and Bradshaw, D., 2015. “A review of entrainment: Mechanisms, contributing factors and modelling in flotation”, *Minerals Engineering*. 70, pp. 77-91.
- Weng, X., Mei, G., Zhao, T., and Zhu, Y., 2013. “Utilization of novel ester-containing quaternary ammonium surfactant as cationic collector for iron ore flotation,” *Separation and Purification Technology*, Vol. 103, pp. 187-194.
- Zhang, W., Nasset, J.E., Rao, R. and Finch, J.A., 2012. “Characterizing frothers through critical coalescence concentration (CCC) 95-hydrophile-lipophile balance (HLB) relationship,” *Minerals*, 2(3), pp.208-227.
- Zhang, X., Gu, X., Han, Y., Parra-Álvarez, N., Claremboux, V., and Kawatra, S. K., 2021, “Flotation of Iron Ores: A Review”, *Mineral Processing and Extractive Metallurgy Review*, DOI: 10.1080/08827508.2019.1689494
- Zheng, X., Johnson, N. W., and Franzidis, J. P., 2006, “Modelling of entrainment in industrial flotation cells: water recovery and degree of entrainment”, *Minerals Engineering*, Vol. 19, Issue 11, pp. 1191–1203.
- Zhou, X., Tan, Y. H., and Finch, J. A., 2019. “Frothing Properties of Amine/Frother Combinations,” *Mining, Metallurgy & Exploration*, 36, pp. 81-88.

## 5 Specifically Adsorbed Ions in the Reverse Cationic Flotation of Iron Ore<sup>1</sup>

### 5.1 Abstract

Although extensive research has been conducted on the effect of water chemistry in flotation, no single study exists which describes the effect of calcium and magnesium on the adsorption of starch onto the hematite in iron ore flotation. In this work flotation, entrainment, zeta potential, and settling tests were performed to determine the differing impact of calcium and magnesium in iron ore flotation. Results showed that magnesium is more detrimental to the flotation process at far lower concentrations than calcium. Performing flotation with 45 ppm of calcium resulted in a comparable impact on the process as performing flotation with 7 ppm of magnesium. While calcium promotes the adsorption of starch onto the hematite and reduces entrainment, past an optimal dosage magnesium is promoting the adsorption of starch to everything in solution causing low grades and recoveries. It was found that the starch adsorption onto the hematite is strongly impacted by the presence of magnesium, suggesting that starch is collecting the magnesium and self-flocculating prior to adsorption onto the hematite. Thus, the presence

---

<sup>1</sup> The material contained in this chapter was previously published in the journal “Mineral Processing and Extractive Metallurgy Review”.

Citation:

Parra-Álvarez, N., Haselhuhn, H. J., Claremboux, V., and Kawatra, S. K., 2021, “Specifically Adsorbed Ions in the Reverse Cationic Flotation of Iron Ore,” *Mineral Processing and Extractive Metallurgy Review*, DOI: 10.1080/08827508.2021.2018314

of magnesium can significantly reduce the flotation performance far more than what would be expected from calcium.

## 5.2 Introduction

Potential-determining, indifferent, and specifically adsorbed ions are the main types of ions found in process water in iron ore flotation plants. Potential-determining ions such as  $\text{H}_3\text{O}^+$  and  $\text{OH}^-$  affect the sign and magnitude of the surface potential (Leja and Rao, 2004). The presence and concentration of these ions is defined by the pH of the solution. Hematite reverse flotation often takes place at pH values near 10.5, which causes both hematite and silica to have negative surface charges in the absence of modifiers (Zhang et al., 2021).

Indifferent ions can only affect the magnitude of the zeta potential which makes them less likely to cause problems in flotation. These ions can only adsorb to the mineral surface by Coulombic forces, which means that they are attracted by opposite charges and repelled by like charges (Delgado et al., 2007). The most common indifferent ions present in iron ore flotation are monovalent ions such as sodium ( $\text{Na}^+$ ), potassium ( $\text{K}^+$ ), and chloride ( $\text{Cl}^-$ ). However, specifically adsorbed ions chemically bind to the surface of minerals and can neutralize functional groups of reagents, affecting both the sign and magnitude of the zeta potential. This means that specifically adsorbed ions can have a much more detrimental effect on flotation. Calcium and magnesium are the main specifically adsorbed ions present in iron ore flotation, thus the focus of this paper.

The hematite ore mined in the North American Iron Range has very low iron grades (~30wt% Fe) and is very fine, with a liberation size of approximately 25  $\mu\text{m}$  at 80%

passing (Haselhuhn and Kawatra, 2015; Zhang et al, 2021). The most effective way to concentrate this ore is via selective flocculation and dispersion, also called desliming, to remove the ultrafine silica particles, followed by reverse cationic flotation, where silica is floated with an etheramine collector and hematite is depressed with corn starch (Nakhaei and Irannajad, 2018). This process is like that employed in Brazil except that, due to the fine liberation, deslime thickeners are used instead of cyclones for removing siliceous slimes. Both desliming and flotation are performed at alkaline conditions and heavily rely on water chemistry (Haselhuhn and Kawatra, 2015). Note that magnetite operations are not nearly as sensitive to water hardness.

To minimize the usage of freshwater, it is common practice to recirculate water and access multiple water sources in flotation plants (Liu et al., 2013). This recirculation can cause great variations in water chemistry and increase the concentrations of calcium and magnesium in solution. The recirculation of the water allows the ions to build up due to water evaporation and other effects leading to concentration. Furthermore, the water can acquire additional ions from sparingly soluble minerals during the process (Duarte and Lima, 2021). Water variations can also originate from within the process as chemical reagents are added and separation processes take place. Table 5.1 shows concentrations of important ionic species present in process water at three different locations in an iron ore concentration plant based on Haselhuhn and Kawatra (2015). Chloride, potassium, and sodium are indifferent ions that can only alter the magnitude of the zeta potential of minerals as they stop interacting with the surface once a neutral charge is reached. On

the contrary, divalent cations such as calcium and magnesium form chemical bonds directly with the surface and alter both magnitude and sign of the zeta potential.

Table 5.1: Ionic species concentration in process water at various locations in an iron ore concentration plant (Haselhuhn and Kawatra, 2015)

	<b>After Comminution</b>	<b>Flotation Feed</b>	<b>Flotation Concentrate</b>
pH	10.59	10.67	10.59
Magnesium (mg/L)	2.67	8.49	0.23
Calcium (mg/L)	4.47	9.2	4.36
Chloride (mg/L)	110	110	100
Potassium (mg/L)	11.4	11.9	10.9
Sodium (mg/L)	455	448	433

As shown in Table 5.1, calcium and magnesium concentrations vary throughout the process. Calcium concentrations are usually higher than magnesium, but even at lower concentration magnesium is more detrimental. Even though both ions have the same charge (+2), they behave differently due to atomic size differences. While magnesium has a covalent diameter of 278 pm, calcium has a covalent diameter of 342 pm (Pyykkö and Atsumi, 2009). The smaller size of magnesium allows it to penetrate the electrical double layer much faster than calcium.



Using the covalent diameter of the ions as an indicator of the typical distance at which they interact with other atoms, one finds that magnesium with its smaller covalent diameter is capable of interacting with minerals at shorter distances. Since the electrostatic interactions between cations are governed by an inverse square law, this means the forces binding magnesium to a mineral surface should be stronger than the forces binding calcium or another larger atom to the same surface. If these cations are idealized as spheres with sizes corresponding to their typical interaction diameters, then magnesium has a higher surface charge than calcium (or barium or strontium) due to its typically smaller interaction distance.

Strontium and barium are also divalent ions with a +2 charge and have greater covalent diameters than both calcium and magnesium. Strontium has a covalent diameter of 370 pm and barium has a covalent diameter of 392 pm (Pykkö and Atsumi, 2009). The average hydroxyl group distance in the [100] plane of hematite is 285 pm (Zhang et al., 2021). As shown in Figure 5.1, since the covalent diameter of magnesium is less than 285 pm, magnesium can form complexes at every hydroxyl group in the hematite. However, the covalent diameters of calcium, strontium, and barium are greater than 285 pm, thus they can only form complexes at every other hydroxyl group in the hematite.

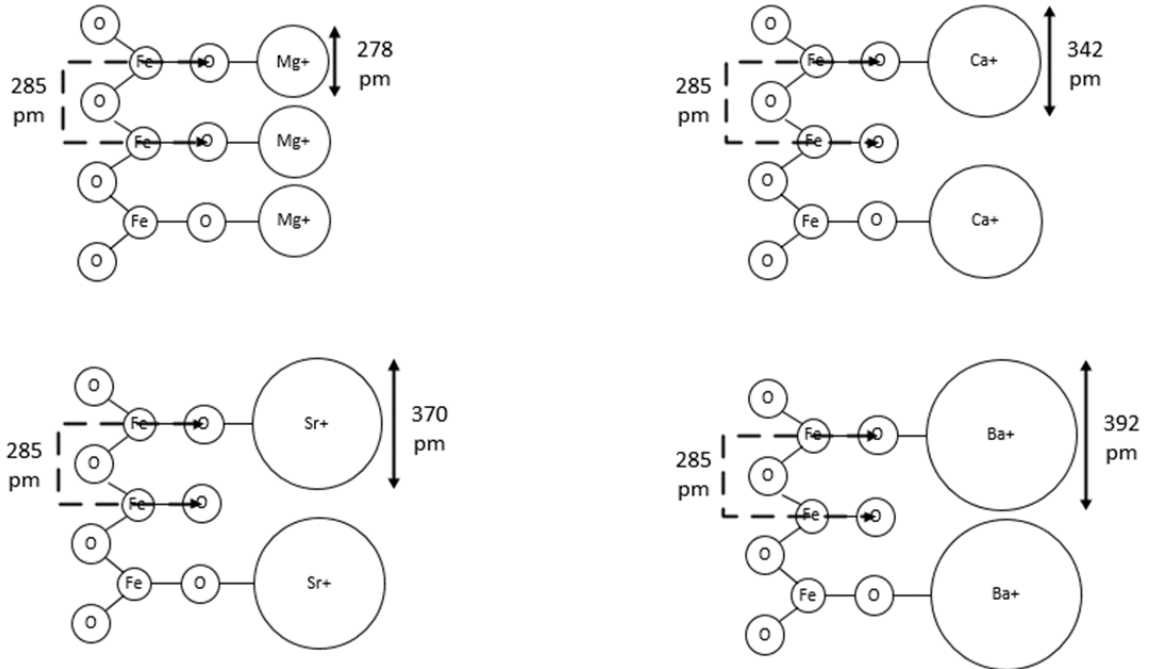


Figure 5.1: Divalent ions complexes with the hydroxyl groups in the [100] plane of hematite.

Based only on site spacing, the maximum extent of adsorption should be the same for calcium, strontium, and barium. However, Figure 5.2 clearly shows that calcium has a greater impact on the zeta potential than strontium and barium. Therefore, surface charge density also plays a key role in the interaction of these ions with the mineral surface. Calcium has a greater surface charge density than strontium and barium. Figure 5.2 confirms that magnesium has a stronger impact on the zeta potential of hematite than calcium in line with its greater surface charge density and site spacing.

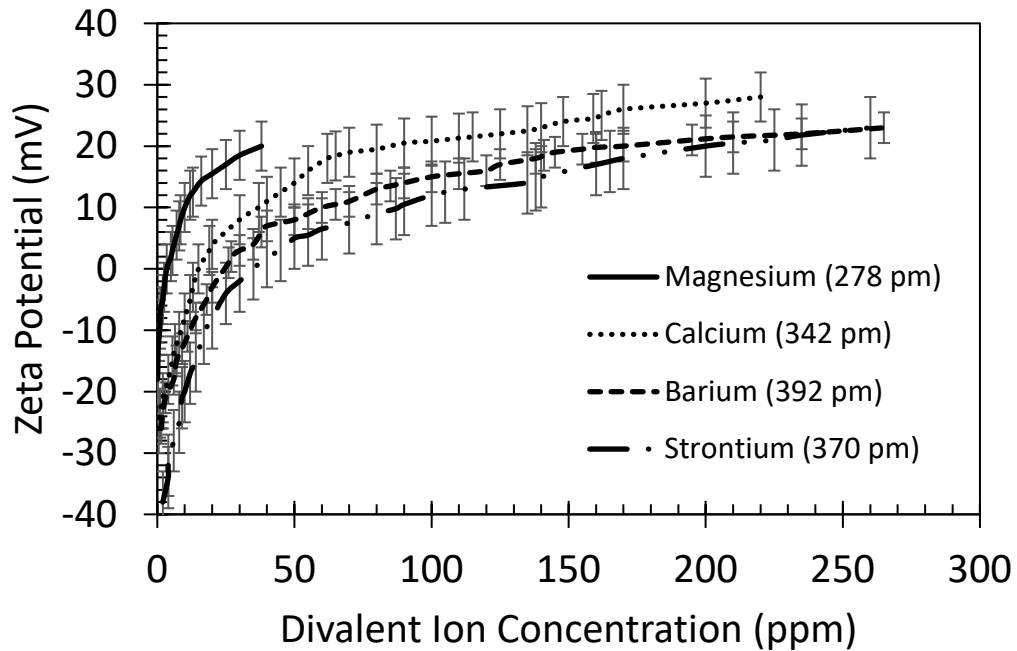


Figure 5.2: Zeta Potential of hematite ore at increasing concentrations of Magnesium, Calcium, Barium, and Strontium.

Solids can be recovered in the froth product by two main mechanisms: true flotation and entrainment (Nykänen et al., 2020; Matos et al., 2021). In true flotation, hydrophobic particles attach to air bubbles and float to the surface. Silica is expected to be recovered in the froth by true flotation while hematite is expected to be recovered in the underflow product. If starch does not depress the hematite, then the cationic collector can adsorb to it and collect it alongside the silica in the hydrophobic froth product. In entrainment, particles that are suspended in the water near the pulp/froth interface get trapped in between bubbles and are transferred to the froth product (Smith and Warren, 1989). Elevated levels of entrainment of hematite result in low iron recoveries in the final

concentrate. If the starch does not depress the hematite properly, these particles will stay suspended in solution and will most likely be trapped within bubbles.

The effect of divalent cations in flotation varies based on the ore, type of reagents, valency and concentration of ionic species, among other factors (Tang and Wen, 2018). The effect of calcium and magnesium in the reverse cationic flotation of iron ore is not fully understood. Previous studies have shown that high concentrations of calcium and magnesium cause a sign reversal on the zeta potential of silica, making it positively charged and preventing the adsorption of the cationic collector which adsorbs onto the silica primarily by electrostatic interactions (Fuerstenau and Palmer, 1976; Lelis et al., 2019; Lelis et al., 2020; Rao, 2004; Ren et al., 2018).

Other studies have shown that these ions can also be problematic in the depression activity as they are themselves strong depressants (Lelis et al., 2020; Li et al., 2018; Laskowski and Castro, 2012). Calcium and magnesium can be depressants due to their strong impact on zeta potential, due to their flocculating effects, or due to their ability to activate the adsorption of otherwise selective depressants onto non-selective flocculants. Shortridge et al. (1999) determined that calcium and magnesium improve the depression activity of long chain polysaccharide depressants like CMC (carboxymethylcellulose) used in talc flotation. Additionally, researchers have found that magnesium could have a stronger depression effect than calcium due the precipitation of  $Mg(OH)_2$  species at pH 10, forming a hydrophilic coating around the particles and preventing flotation (Lelis et al., 2020; Li et al., 2018; Laskowski and Castro, 2012).

Although extensive research has been conducted on the effect of water chemistry in flotation, no single study exists which describes the effect of calcium and magnesium on the adsorption of starch onto the hematite in iron ore flotation. In this research we have determined that while calcium promotes the adsorption of starch onto the hematite and reduces entrainment, past an optimal dosage magnesium is promoting the interaction of starch with everything in solution, reducing depressant selectivity and yielding low iron grades and recoveries. Although this work only deals with acid modified corn starch as a depressant, reviews of the interactions of multiple types of starches (Rath and Sahoo, 2020) would suggest that other natural starches would behave similarly.

### **5.3 Materials**

The hematite ore used for this study was obtained from an iron ore beneficiation plant from the North American Iron Range in the U.S. The samples were collected at the autogenous mill screen underflow, right before dispersant addition as depicted in Figure 5.3. At this location there are no surface-active reagents previously added, and fresh surface sites are guaranteed as the ore needs to be ground in the lab prior to flotation. Figure 5.4 shows the X-Ray diffraction (XRD) results for the hematite ore used. In summary, the iron ore sample was composed of 65% of quartz, 21% of hematite, with the remainder being other iron oxides and gangue minerals.

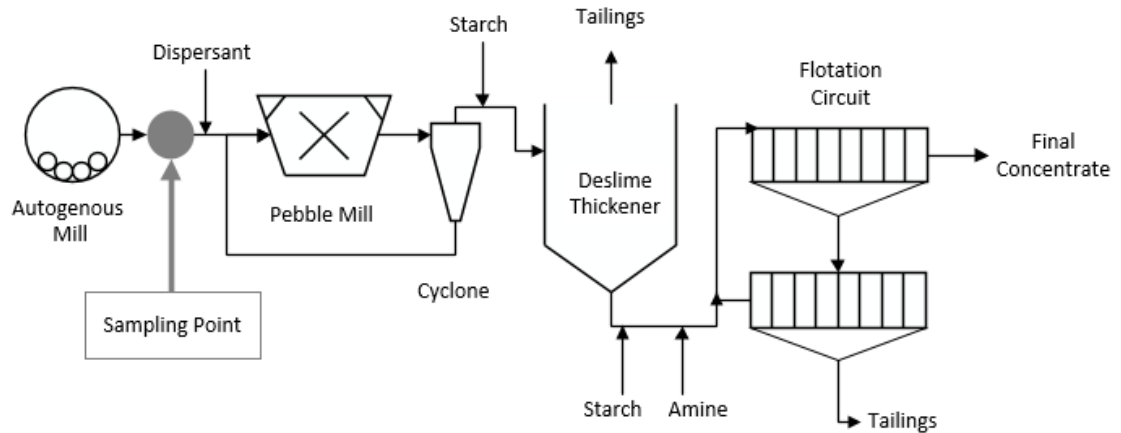


Figure 5.3: Sampling location at the iron ore concentrator plant: autogenous mill screen underflow, right before dispersant addition. Particle size: 0.8 mm at 80% passing.

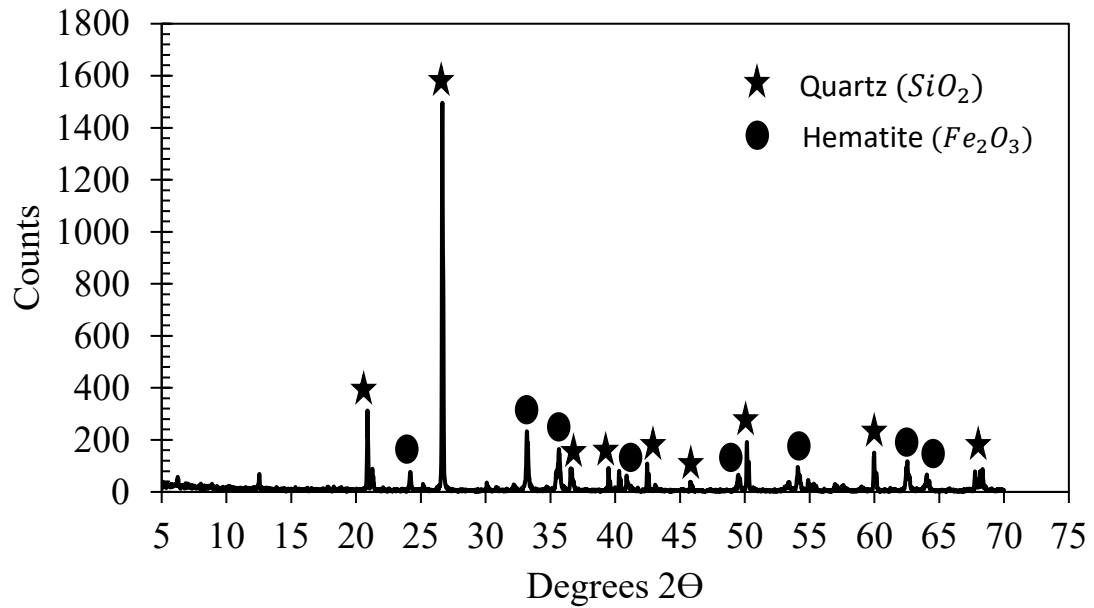


Figure 5.4: X-Ray diffraction for the hematite ore used. Quartz: 65%, Hematite: 21%

The reagents used during the experiments were: sodium hydroxide as a pH modifier, 10% solution; Cyquest 3223 anionic polyacrylamide as a dispersant, 10% solution; ether monoamine as a collector in flotation, 1% solution; and acid modified corn starch as a flocculant in desliming, 0.3% solution, and as a depressant in flotation, 3% solution. The

acid modified corn starch was gelatinized in water at 240°C for 30 minutes and causticized with sodium hydroxide before use. This starch gelatinization step is very important as stated by Yang et al. (2017) and Tang et al. (2016).

## **5.4 Methods**

### **5.4.1 Sample Preparation**

Due to the sampling point being located so early in the process, the hematite ore must undergo grinding and desliming in the lab prior to flotation. To obtain similar grade and recovery targets as the plant for the preliminary steps, it was important to use a similar water chemistry as the plant's process water. Table 5.2 shows that municipal water available in the Michigan Technological University laboratory has a much higher water hardness than the water used during flotation at the concentrator plant. For this reason, it was decided to mix municipal water with deionized water at a specific ratio to lower the water hardness. Water hardness levels can vary daily in each location, so titration tests were performed on the city water every time a new batch of water was prepared to accurately determine the necessary mixing ratio. As shown in Table 5.2, the mixed water used for grinding and desliming contained 5.7 ppm of calcium and 1.1 ppm of magnesium per ICP results. The calcium concentration was still higher than the plant's flotation water but it can be countered by higher additions of dispersant in the preliminary steps.

Table 5.2: Water chemistry comparison between municipal water available at Michigan Tech, flotation process water at the plant, and the feed water used for grinding and desliming at the Michigan Tech Laboratory

	<b>Municipal Water available at MTU Lab</b>	<b>Plant's Flotation Water</b>	<b>Feed Water used in MTU Lab</b>
Calcium (mg/L)	63.4	3.2	5.7
Magnesium (mg/L)	13.4	1.4	1.1
Total Water Hardness (mg/L of CaCO <sub>3</sub> )	298.9±5	18.7±0.02	16.6±0.0

Prior to flotation feed slurry composed of 60% solids was prepared and adjusted to a pH of 10.5 with sodium hydroxide (NaOH). Then it was treated with 3 lb/ton of Cyquest 3223 Anionic Polyacrylamide dispersant and ground in a rod mill to an 80% passing size of 25 µm. Subsequently, the slurry was transferred to a deslime cell where it was diluted to a 7% solids solution and conditioned for 1 minute at a pH of 10.5 and 0.0625 lb/ton of starch flocculant. Once the solution was conditioned and left to settle for 30 seconds the slimes were removed to achieve a grade of 40-45wt% Fe.



### 5.4.2 Flotation Tests and Iron Content Analysis

The concentrate from the deslime step was placed in a 2 L Denver flotation cell and flotation water was added to prepare a 15% solids slurry. The flotation water used was prepared by adding a specific amount of calcium chloride dihydrate or magnesium chloride hexahydrate with deionized water. The slurry was adjusted to a pH of 10.5 with sodium hydroxide (NaOH), followed by the addition of 1.5 lb/ton of starch depressant and conditioned for 3 minutes. Then, 1.5 lb/ton of 30% neutralized etheramine were added and conditioned for 1 more minute. Afterwards, the air was turned on and the froth product was collected. The froth collection pan was swapped at intervals of 15, 30, 60, 120, and 165 seconds for entrainment analysis.

After floating for 165 seconds, the air was turned off and all the tailings and concentrate products were weighed, filtered, and dried overnight. The next day all samples were weighed again and prepared for iron content analysis using a Hach DR5000™ UV-VIS spectrophotometer at 510 nm. This procedure consisted of digesting a representative sample of each product in hydrochloric acid (HCl), diluting with distilled water, and adding ammonium acetate (pH buffer), hydroxylamine hydrochloride (reductant), and 1,10-phenanthroline (indicator solution). The iron concentration correlates to light absorbance using Beer-Lambert's law (Day and Underwood, 1991).

Tests were performed at 0, 45, 60, 100, and 200 ppm of calcium and at 0, 7, 15, and 30 ppm of magnesium. Each test was performed in triplicate to ensure reproducibility.

### **5.4.3 Zeta Potential Analysis**

First, 1-gram samples of freshly ground ore were hydrated with deionized water at a pH of 10.5 and sealed for 24 hours. Then, each sample was placed in a plastic beaker with 200 ml of deionized water previously adjusted to pH 10.5 with sodium hydroxide (NaOH). The calcium and magnesium concentrations were controlled by adding a certain amount of calcium chloride dihydrate or magnesium chloride hexahydrate solutions depending on the experimental design. Tests were performed at 25, 50, 100, and 200 ppm of calcium and magnesium both with and without starch. For the tests with starch, 1.5 lb/ton of previously cooked causticized corn starch was added after the addition of the calcium or magnesium chloride solution. A magnetic stirrer was used to keep the particles suspended in solution. Only plastic instruments were used to avoid surface adsorption of minerals and critical ions to lab equipment.

The zeta potential was measured using a Malvern Zetasizer Nano ZS. The sample was inserted into a DTS1070 folded capillary cell with a syringe, followed by the placement of the cell in the Zetasizer. Each measurement was divided into three runs and each sample was measured in triplicate for accuracy.

### **5.4.4 Settling Tests**

The settling rate of solids (both silica and hematite) was determined by measuring the total suspended solids in solution over a period of time using a Hach DR5000™ UV/VIS spectrophotometer at 810 nm properly calibrated (Krawczyk and Gonglewski, 1959). As the solids settle the total suspended solids concentration in solution will decrease. The

absorbance at 810 nm was calibrated with the gravimetric method at various concentrations of the iron ore samples in deionized water at 10.5 pH.

Samples were prepared and conditioned in the same way than the zeta potential analysis samples. These tests were performed at 25, 50, 100, and 200 ppm of calcium and magnesium added as calcium chloride dihydrate or magnesium chloride hexahydrate solutions, along with 1.5 lb/ton of starch. Once all the reagents were added, the sample was inserted into a 10 mm light path cuvette which was then placed inside the UV/VIS cell. Settling rate plots were obtained by measuring the total suspended solids concentration in solution every 10 seconds for 5 minutes. Each measurement was performed in triplicate to ensure reproducibility and determine accuracy.

## **5.5 Results and Discussion**

Given that the focus of this research is the differing effect of calcium and magnesium in flotation, it is important to identify all the sources of calcium and magnesium in the laboratory setup, including grinding, desliming, and flotation. Figure 5.5 depicts the chemical analysis of calcium and magnesium for nine different streams in the flow diagram. This data can be used to perform a calcium and magnesium balance for the overall system. Note that in the magnesium balance, a small margin of error can be attributed to ICP-OES analysis and/or losing some material containing magnesium during the grinding process.

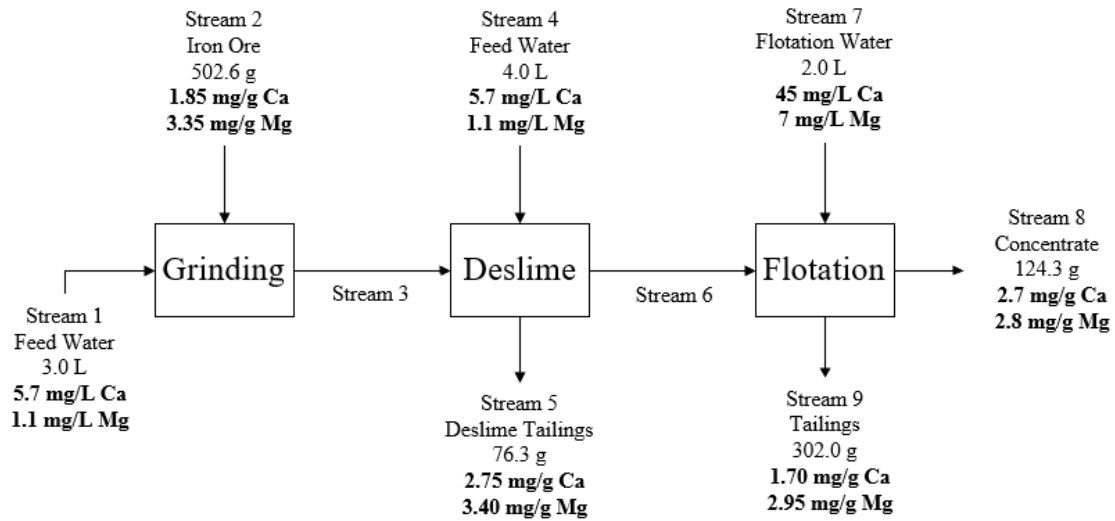


Figure 5.5: Chemical analysis of calcium and magnesium throughout grinding, desliming, and flotation in the laboratory setup.

### 5.5.1 Flotation and Entrainment Analysis

In the reverse cationic flotation of iron ore, silica is rendered hydrophobic by the amine collector and is transferred to the froth by true flotation. Meanwhile, hematite is depressed by starch and collected in the underflow product. The depression action of starch is key in the process because, at 10.5 pH, both hematite and silica are negatively charged. If starch does not adsorb onto the hematite, then the cationic amine collector can adsorb non-selectively resulting in poor iron recovery during flotation. Additionally, low depressant performance can promote entrainment of hematite in the froth.

The purpose of this study was to investigate the effect of calcium and magnesium on starch adsorption during flotation. Analyzing entrainment plots at various concentrations of calcium and magnesium helped identify the differing behavior of these ions in the

depressing activity of starch. The simple correlation method described by Lynch et al. (1981) was chosen for entrainment analysis. A plot of the percent water recovered in the froth versus the percent of hematite recovered in the froth provides a visual indication of the level of entrainment. Hematite particles recovered in the froth via entrainment mechanism follow a straight line in the plot. As the slope of the line decreases, the level of entrainment decreases.

As observed in Figure 5.6, as the calcium concentrations increase, the level of hematite entrainment reduced. In other words, calcium is promoting the depression of hematite by the starch, which enhances the collector selectivity towards the silica and reduces the amount of hematite particles suspended near the pulp/froth interface so that they are not accidentally trapped in the bubbles (entrained) and recovered in the froth product. If the depressant is excessively active, selectivity drops and the majority of the material does not float. This results in high recoveries in the tailings, but low grades as very little separation occurs.

Figure 5.7 shows the grade and recovery plot at various concentrations of calcium to determine the optimum calcium concentration for this flotation setup. Typically, when analyzing grade and recovery curves the point located higher up and farther to the right would indicate the best performance (Kawatra, 2009). In this case 45 ppm of calcium yielded the best performance with a grade of 58.9 +/- 0.3wt% Fe and an iron recovery of 62.8 +/- 0.5wt%. Note that 45 ppm of calcium was added during the flotation step depicted as stream 7 in Figure 5.5. Accounting for the calcium concentration coming

from desliming, the actual calcium dosage that yielded the best performance was 46.85 +/- 0.07 ppm.

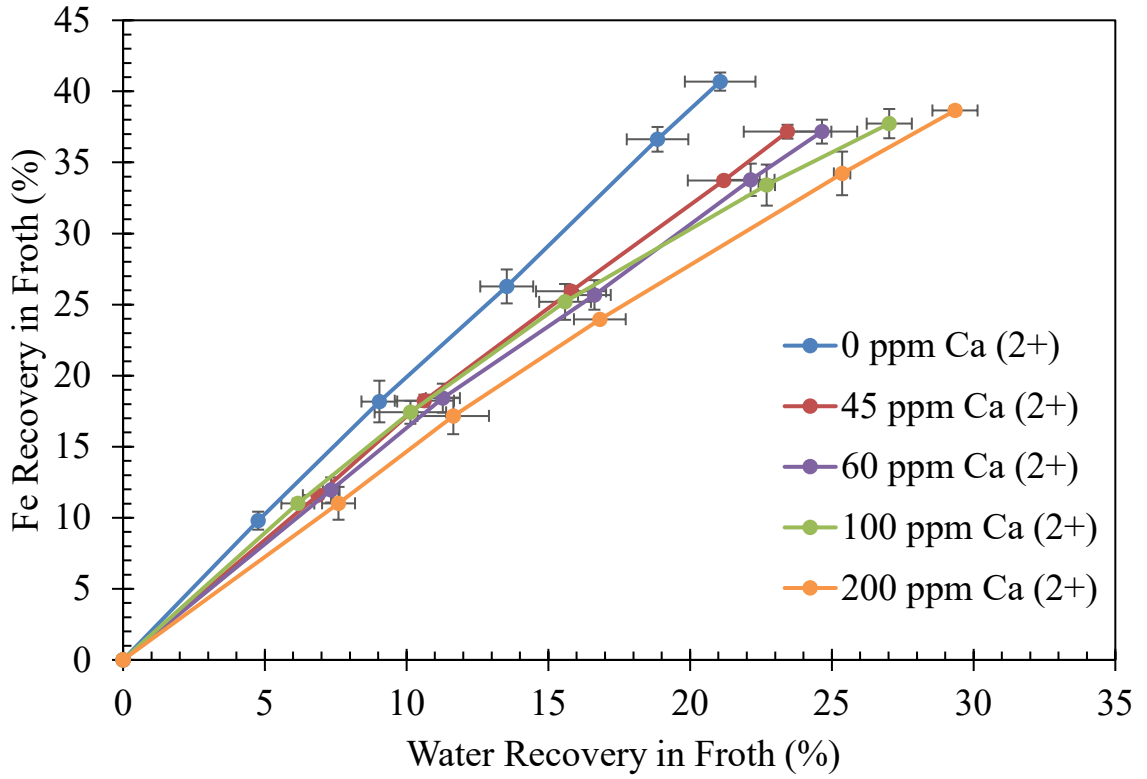


Figure 5.6: Entrainment tests for hematite ore at various concentrations of calcium. For these tests, the magnesium concentration added was 0 ppm.

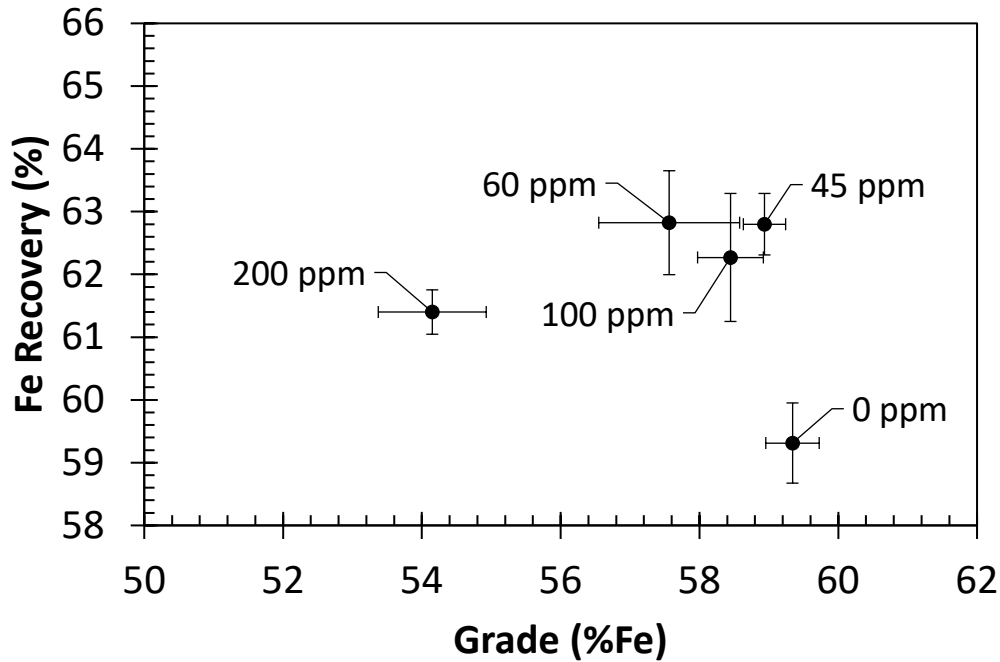


Figure 5.7: Grade/Recovery curve at various concentrations of calcium. For these tests, the magnesium concentration added was 0 ppm. Slight reductions in zeta potential can cause flocculation of slimes thereby increasing recovery. Higher concentrations of calcium coat surfaces and activate both silicates and hematite for starch adsorption. The optimum flotation performance was obtained at 45 ppm calcium. Past this dosage both grade and recovery decreased.

As shown in Figure 5.8, an increase in the magnesium concentration does not seem to affect the level of entrainment initially. However, a decrease in the level of entrainment is observed at 30 ppm of magnesium just as observed in the case of calcium. Furthermore, the grade and recovery plot shown in Figure 5.9 shows that 7 ppm of magnesium yielded the best performance with a grade of 58.0 +/- 1wt% Fe and an iron recovery of 63.8 +/- 1wt%. Note that 7 ppm of magnesium was added during the flotation step depicted as

stream 7 in Figure 5.5. Accounting for the magnesium concentration coming from desliming, the actual magnesium dosage that yielded the best performance was 9.95 +/- 0.07 ppm. This confirms that even at lower concentrations, magnesium is more detrimental than calcium in the system. As observed in Figure 5.7 and 5.9, increasing calcium and magnesium concentrations over the optimal dosages reduce both recovery and grade which can be attributed to the calcium and magnesium lowering the charge difference between silica and hematite.

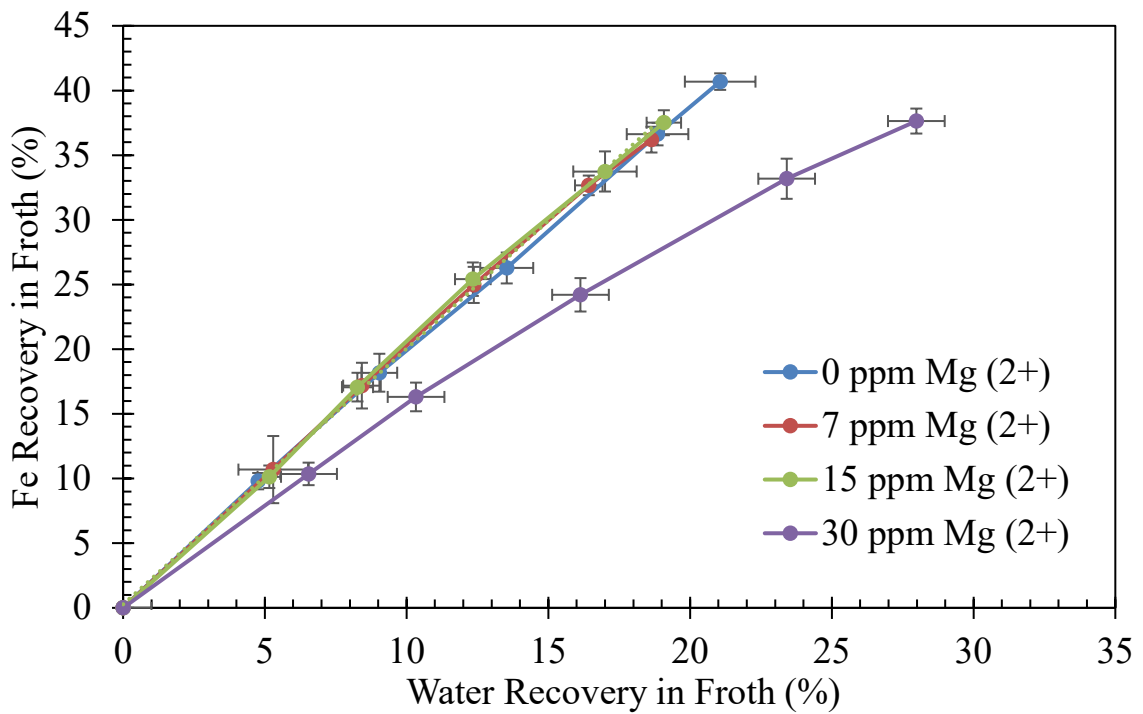


Figure 5.8: Entrainment tests for hematite ore at various concentrations of magnesium.

For these tests, the calcium concentration added was 0 ppm.



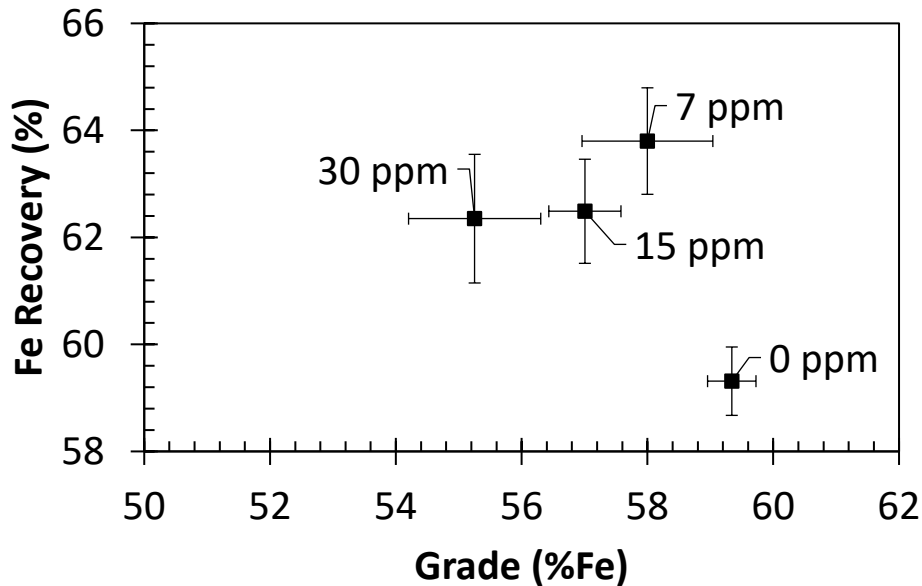


Figure 5.9: Grade/Recovery curve at various concentrations of magnesium. For these tests, the calcium concentration added was 0 ppm. Slight reductions in zeta potential can cause flocculation of slimes thereby increasing recovery. Higher concentrations of magnesium coat surfaces and activate both silicates and hematite for starch adsorption. The optimum flotation performance was obtained at 7 ppm magnesium. Past this dosage both grade and recovery decreased.

When analyzing both entrainment and grade and recovery graphs for both calcium and magnesium it is observed that past the optimal dosages the iron recovered in the froth and the iron recovered in the concentrate are both reduced. This could only be possible if the water recovery in the froth is increased. Flocs of particles tend to hold water, though the closer the particles get the less water they can hold. The addition of calcium and magnesium could be pulling the flocs more tightly together, driving the water to the froth product. Moreover, flocs of silica may also be carrying water with them to the froth.

In addition to the flotation data presented above, a flotation test combining the optimal dosages of calcium (45 ppm) and magnesium (7 ppm) was performed. The obtained results showed an iron grade of 55.47 +/- 1.1wt% and an iron recovery of 71.31 +/- 0.2wt%. Table 5.3 compares this result with the performance obtained using the optimal dosages of calcium and magnesium independently. Evidently, when combining 45 ppm of calcium with 7 ppm magnesium, the grade decreased and the recovery increased due to non-selective flocculation of hematite and silica.

Table 5.3: Summary of flotation performance with only deionized water and at optimal dosages of calcium and magnesium separately and combined.

<b>Calcium Concentration (ppm)</b>	<b>Magnesium Concentration (ppm)</b>	<b>Iron Grade (wt%)</b>	<b>Iron Recovery (wt%)</b>
0	0	59.34 +/- 0.4	59.30 +/- 0.6
45	0	58.90 +/- 0.3	62.80 +/- 0.5
0	7	58.00 +/- 1	63.80 +/- 1
45	7	55.47 +/- 1.1	71.31 +/- 0.2

### 5.5.2 Zeta Potential Analysis

The zeta potential analysis of iron ore flotation feed confirmed that starch affects the impact of magnesium in the zeta potential of hematite at 10.5 pH. In the absence of starch (Figure 5.10) it is shown that magnesium has a stronger impact in the zeta potential of

fully-hydrated hematite than calcium. Even though both are divalent cations attracted to the negatively charged surface of hematite, magnesium causes the zeta potential sign to change from negative to positive at around 90 ppm, whereas calcium did not cause a sign reversal in the range of concentrations studied. As mentioned earlier, the stronger impact of magnesium could be attributed to its smaller atomic size and greater surface charge density.

Figure 5.11 depicts the data obtained after the addition of calcium or magnesium followed by 1.5 lb/ton of starch and maintaining the pH at 10.5. In the presence of starch, it is observed that magnesium no longer caused a charge reversal on the zeta potential of fully-hydrated hematite within the concentrations studied. Considering that the only difference from Figure 5.10 is the starch addition, starch is limiting the effect of magnesium on the surface of the hematite. The most probable mechanism is that starch is capturing the magnesium before either the starch or the magnesium can adsorb onto the hematite surface. This could explain why magnesium was more detrimental than calcium in the flotation / entrainment results.

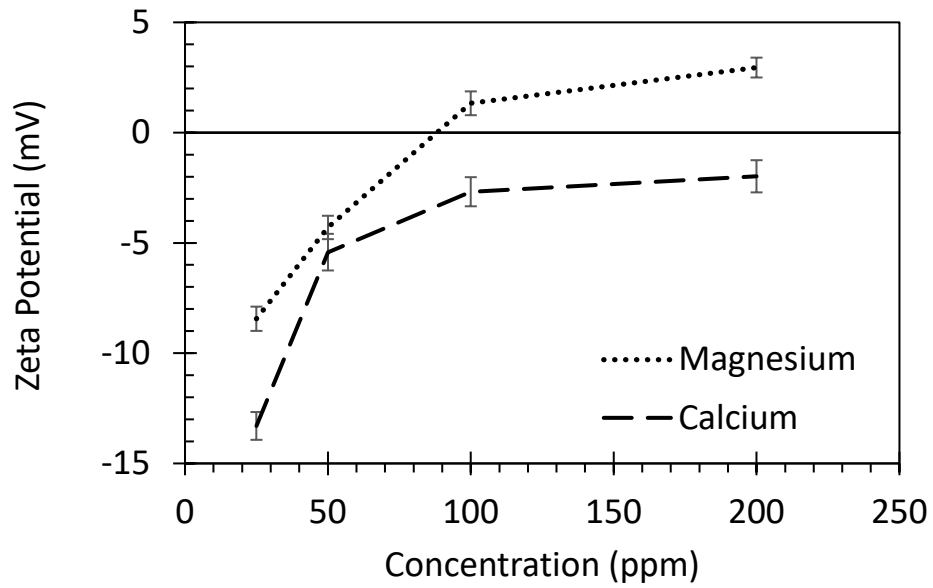


Figure 5.10: Zeta potential of flotation feed sample conditioned with increasing concentrations of magnesium or calcium at a pH of 10.5 (no starch added). Concentration expressed in ppm.

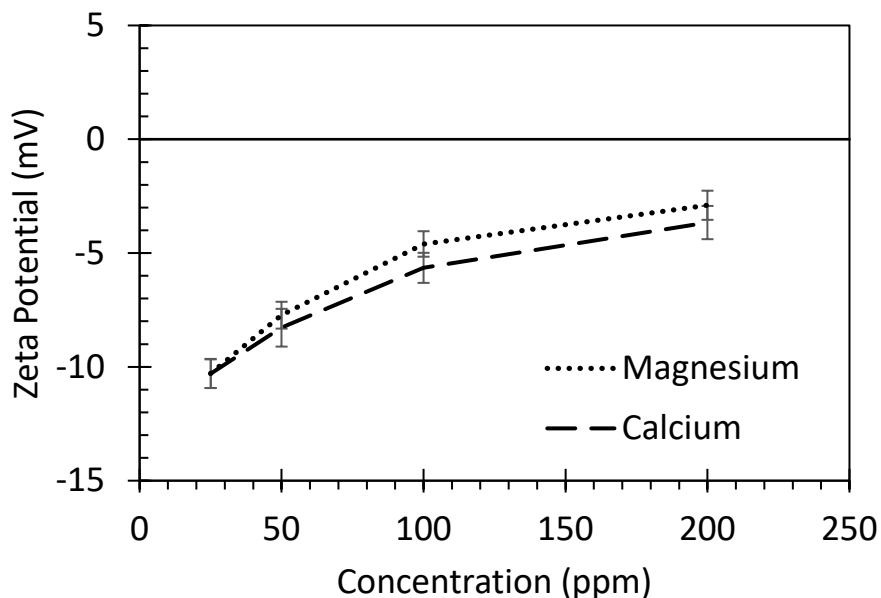


Figure 5.11: Zeta potential of flotation feed sample conditioned with increasing concentrations of magnesium or calcium, followed by 1.5 lb/ton of starch at a pH of 10.5. Concentration expressed in ppm.

Figures 5.12 and 5.13 show the same data as Figures 5.10 and 5.11 except the concentration is expressed in terms of molarity. From these figures it is clear that both lines come closer together at first until all available sites have filled with calcium. Without the presence of starch the magnesium then crosses the isoelectric point because it has a smaller size and can adsorb to more surface sites (Figure 5.12). In the presence of starch the calcium behaves similarly compare to the tests without starch, whereas magnesium does not cross the isoelectric point indicating that magnesium is more readily interacting with the starch than calcium (Figure 5.13).

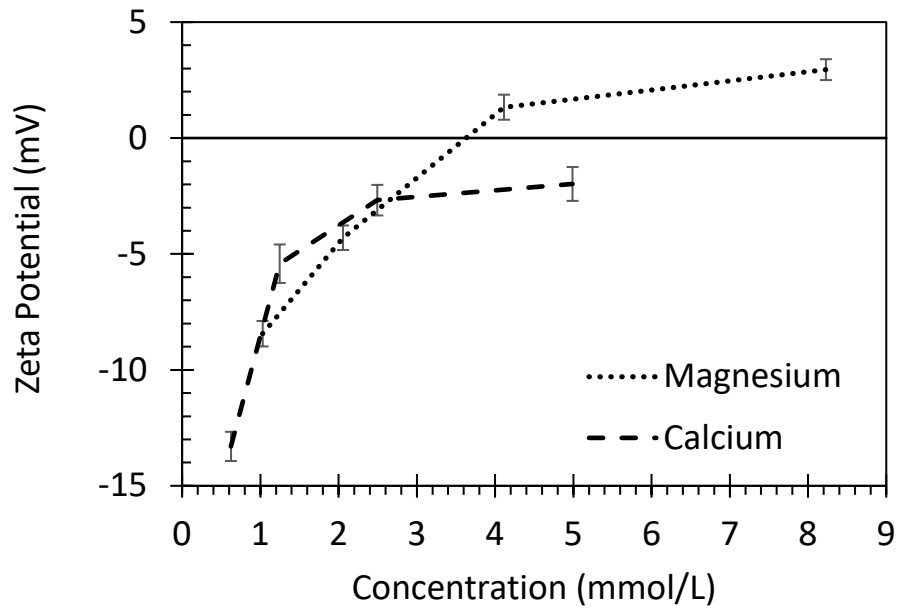


Figure 5.12: Zeta potential of flotation feed sample conditioned with increasing concentrations of magnesium or calcium at a pH of 10.5 (no starch added). Concentration expressed in molarity (mmol/L).

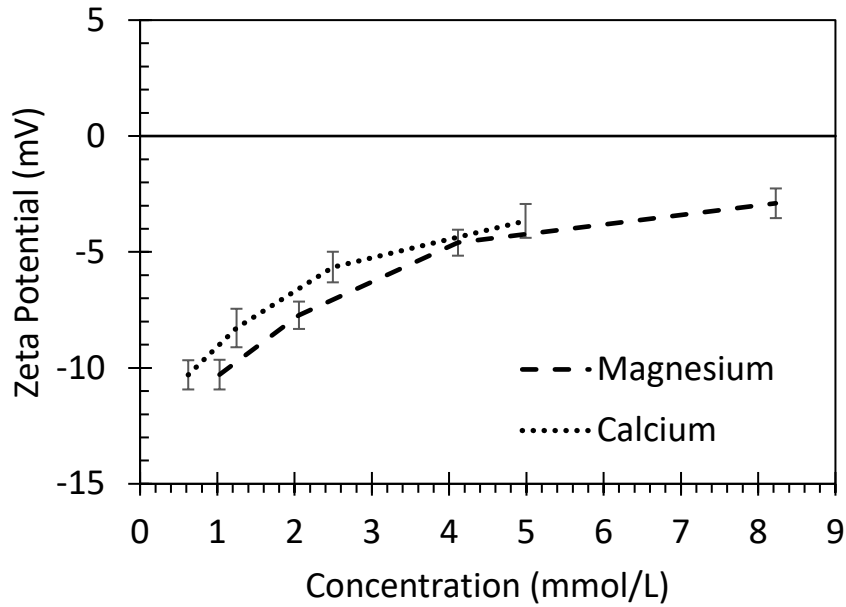


Figure 5.13: Zeta potential of flotation feed sample conditioned with increasing concentrations of magnesium or calcium, followed by 1.5 lb/ton of starch at a pH of 10.5. Concentration expressed in molarity (mmol/L).

### 5.5.3 Settling Tests

Settling tests were performed with a fully-hydrated hematite ore to analyze the effect of calcium and magnesium on the settling rate of solids in flotation. These tests show the total suspended solids (hematite and silica) in solution over a period of time. As the solids settle in solution, the total suspended solids concentrations will decrease. Particles that are flocculated will settle faster.

As shown in Figure 5.14 and 5.15, when 50 ppm of calcium or magnesium are added to the solution followed by the addition of 1.5 lb/ton of starch, the settling rate improves in contrast to the settling with no calcium, no magnesium, and no starch, only calcium, only

magnesium, and only starch. This means that initially both calcium and magnesium activate the adsorption of starch onto the solids. As the divalent cations adsorb onto the hematite and silica particles, they create positively charged surface sites that will attract the starch. Modified starch is slightly negative due to the presence of the carboxylate group (Green and Colombo, 1984). The starch is more selective towards hematite surfaces than silica surfaces due to more similar site spacing and more favorable degree of hydration, but as the divalent ions increase in solution starch may be adsorbing non-selectively and flocculating both hematite and silica.

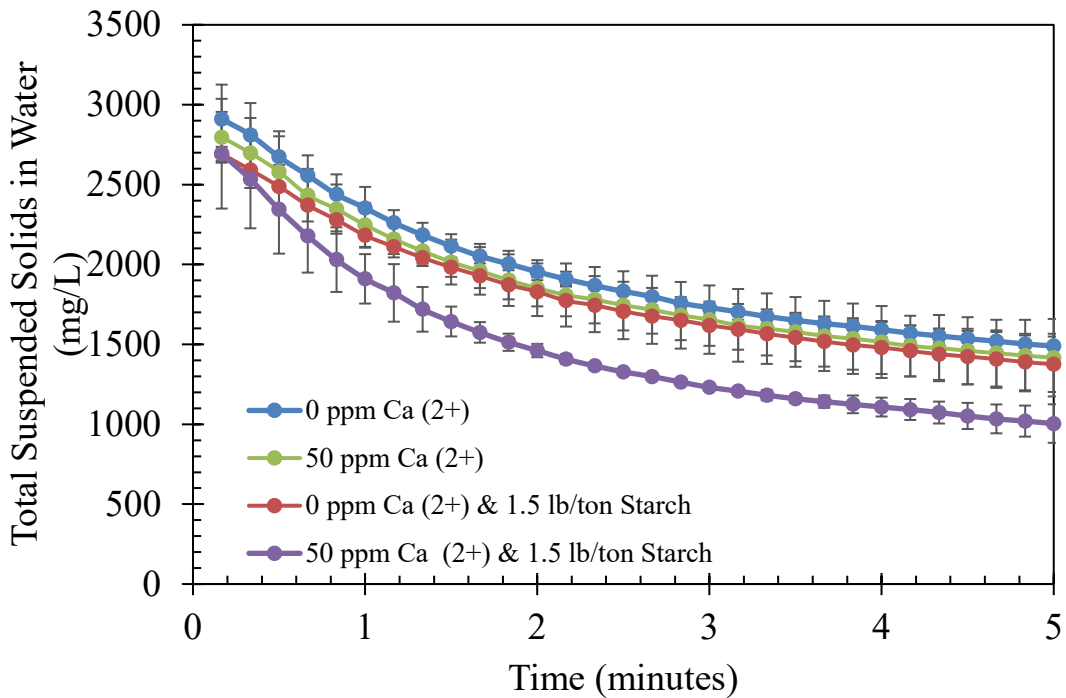


Figure 5.14: Settling tests for a fully hydrated iron ore at 10.5 pH with varying concentrations of calcium and starch. Calcium activates the starch for adsorption and increases flocculation of particles.



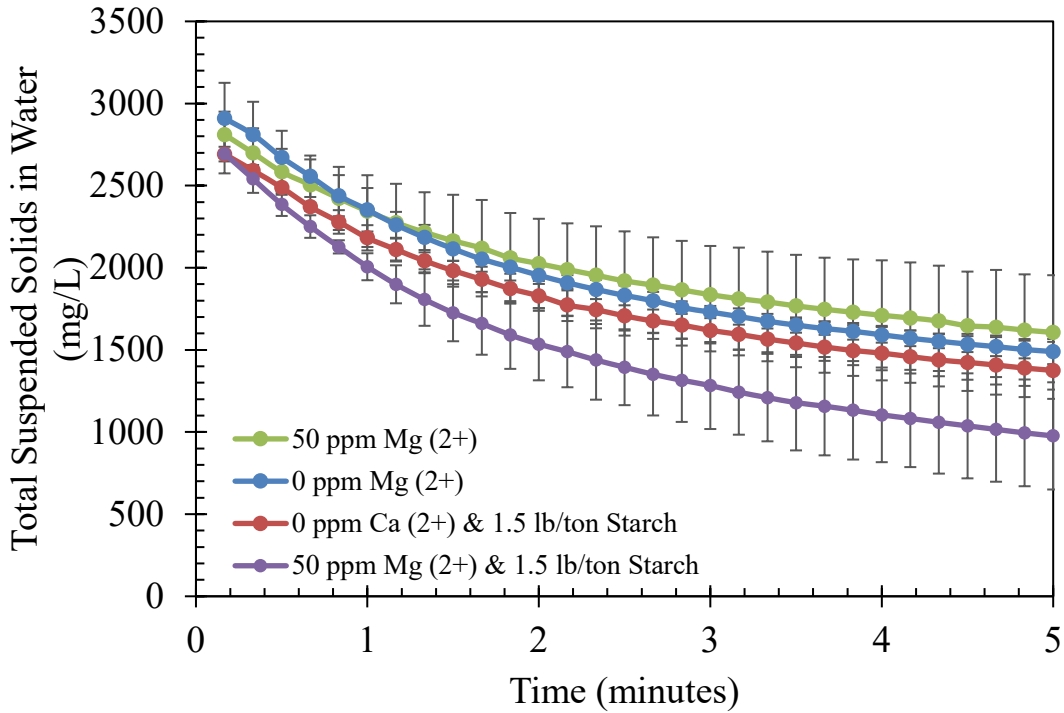


Figure 5.15: Settling tests for a fully hydrated iron ore at 10.5 pH with varying concentrations of magnesium and starch. Magnesium activates the starch for adsorption and increases flocculation of particles.

Figure 5.16 shows the settling rate as the calcium concentration increases from 25 ppm to 200 ppm in the presence of 1.5 lb/ton of starch. For these tests starch was added after the addition of calcium. The settling rate was not significantly affected by increasing calcium concentrations, but a slight increase in the settling rate is observed at 200 ppm. This could be attributed to the starch flocculating the ore even further as the calcium ions are reducing repulsion or activating more sites for starch adsorption.

Figure 5.17 shows the settling rate as the magnesium concentration increases from 25 ppm to 200 ppm in the presence of 1.5 lb/ton of starch. For these tests starch was added after the addition of magnesium. Contrary to calcium, as the concentration of magnesium

increases, the settling rate is reduced. This result confirms what it was concluded with the flotation tests and zeta potential results. Magnesium is preventing the starch adsorption onto the hematite while calcium is promoting adsorption. One theory to explain this behavior is that magnesium is adsorbing onto the starch and making it self-flocculate before starch gets the chance to adsorb onto the mineral surface.

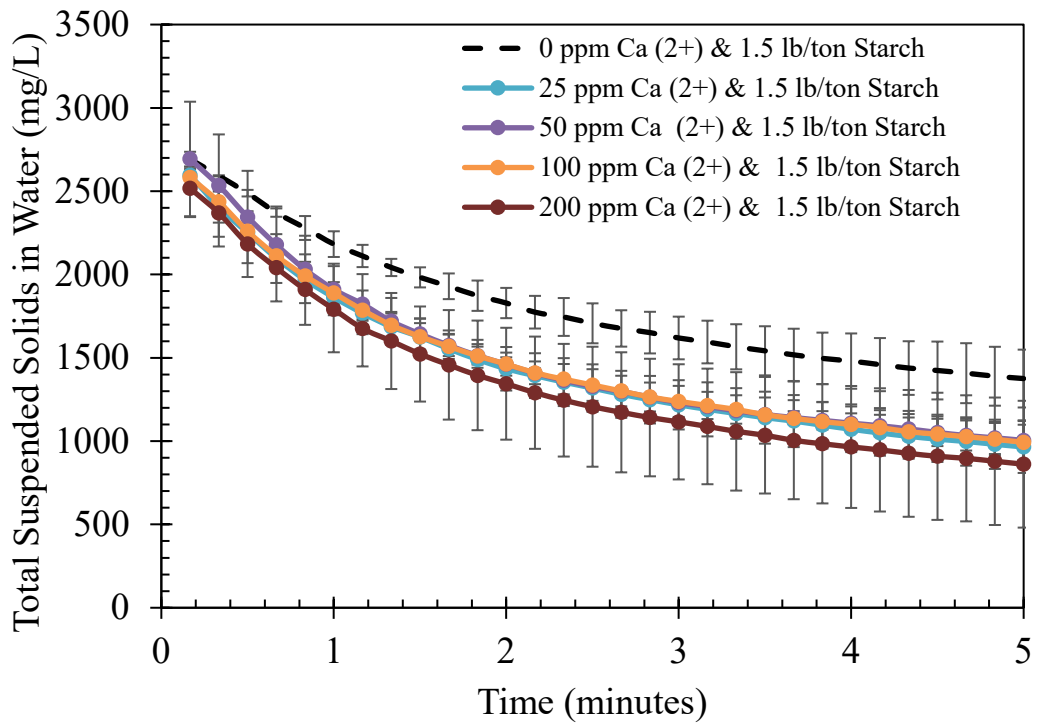


Figure 5.16: Settling tests for a fully hydrated iron ore at 10.5 pH conditioned with 1.5 lb/ton of starch and increasing calcium concentrations. An increase in calcium will not change the settling rate of solids significantly.

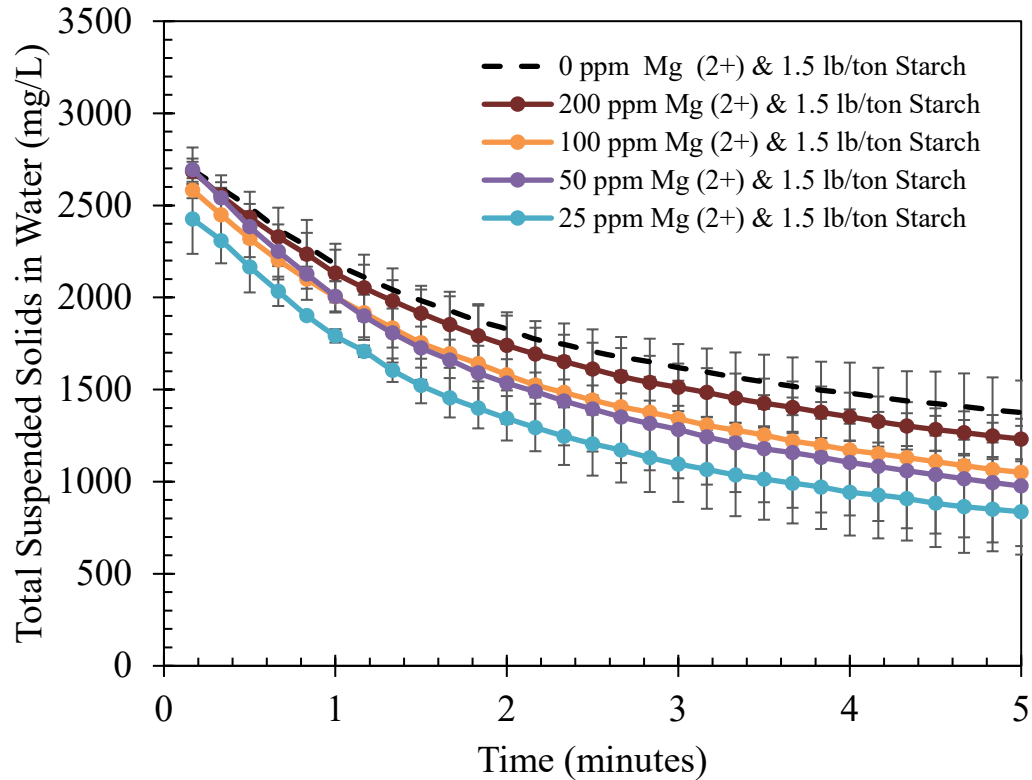


Figure 5.17: Settling tests for a fully hydrated iron ore at 10.5 pH conditioned with 1.5 lb/ton of starch and increasing magnesium concentrations. As magnesium increases, it affects the adsorption of starch to the ore.

## 5.6 Conclusions

Prior literature of calcium and magnesium has largely treated them as interchangeable species in iron ore flotation. However, the impact of magnesium species on flotation is far more detrimental at far lower concentrations than calcium species. Flotation tests were performed to evaluate the difference in these effects using a hematite ore body:

- A concentration of 7 ppm of magnesium was found to have a comparable impact on flotation as 45 ppm of calcium

- A concentration of 7 ppm magnesium or 45 ppm calcium were found to have optimal results for this flotation
- A concentration of 7 ppm magnesium and 45 ppm calcium was found to perform worse than either cation individually, suggesting that these effects combine to push the flotation beyond its optimum value
- The optimum values will naturally be different for different ore bodies

The adsorption of magnesium onto the hematite surface was found to be strongly impacted by the presence of starch, suggesting that starch collects the magnesium and self-flocculates more rapidly than it adsorbs to hematite. Since starch plays a vital role in depressing hematite during reverse cationic flotation, the presence of magnesium can greatly reduce the effectiveness of the flotation process beyond what would be expected from calcium.

## 5.7 References

- Day, R. A., and Underwood, A. L., 1991. "Quantitative analysis," In Determination of iron with 1,10-Phenanthroline, 6th ed. Englewood Cliffs, NJ: Prentice Hall. pp. 645-646.
- Delgado, A. V., González-Caballero, F., Hunter, R. J., Koopal, L. K., and Lyklema, J., 2007. "Measurement and interpretation of electrokinetic phenomena," Journal of Colloid and Interface Science, Vol. 309, Issue 2, pp. 194-224.
- Duarte, G. M. P., and Lima, R. M. F., 2021. "Quartz and Hematite Activation by Zn, Ca and Mg Ions in the Cationic Flotation Route for Oxidized Zinc Ore,"

Mineral Processing and Extractive Metallurgy Review, DOI:

10.1080/08827508.2021.1931175

- Fuerstenau, M. C., and Palmer, B. R., 1976. “Anionic flotation of oxides and silicates,” Society of Mining Engineers of AIME, Mineral Processing Division, Gaudin, A. M., Fuerstenau, M. C., Eds.; American Institute of Mining, Metallurgical, and Petroleum Engineers, New York, NY, USA, pp. 148-196.
- Green, R. E., and Colombo, A. F., 1984. “Dispersion-Selective Flocculation-Desliming characteristics of oxidized taconites,” Bureau of Mines, United States Department of Interior.
- Haselhuhn, H. J., and Kawatra, S. K., 2015. “Effects of Water Chemistry on Hematite Selective Flocculation and Dispersion,” Mineral Processing and Extractive Metallurgy Review, Vol. 36, Issue 5, pp. 305-309. DOI: 10.1080/08827508.2014.978318
- Kawatra, S. K., 2009. “Froth Flotation – Fundamental Principles,” SME mining engineering handbook. Vol. 2, 3rd Edition.
- Krawczyk, D., and Gonglewski, N., 1959. “Determining Suspended Solids Using a Spectrophotometer,” Sewage and Industrial Wastes, Vol. 31, No. 10, pp. 1159-1164.
- Laskowski, J.S., and Castro, S., 2012. “Hydrolyzing ions in flotation circuits: seawater flotation,” In: Proceedings of the 13th International Mineral Processing Symposium, Bodrum (Turkey), pp. 219–228.

- Leja, J., and Rao, S.R., 2004. “Surface Chemistry of Froth Flotation,” Plenum Press, 2nd Edition, Vol. 1, pp. 211-217.
- Lelis, D. F., da Cruz, D. G., and Lima, R. M. F., 2019, “Effects of calcium and chloride ions in iron ore reverse cationic flotation: Fundamental studies,” *Mineral Processing and Extractive Metallurgy Review*. Issue 6, Vol. 40, pp. 402-409.
- Lelis, D. F., Lima, R. M. F., Rocha, G. M., and Leão, V. A., 2020. “Effect of magnesium species on cationic flotation of quartz from hematite,” *Mineral Processing and Extractive Metallurgy Review*. Doi: 10.1080/08827508.2020.1864362
- Li. W., Li, Y., Wei, Z., Xiao, Q., and Song, S., 2018. “Fundamental studies of SHMP in reducing negative effects of divalent ions on molybdenite flotation,” *Minerals*, 8(9), 404.
- Liu, W., Moran, C. J., and Vink, S., 2013. “A review of the effect of water quality on flotation,” *Minerals Engineering*, 54, pp. 91-100. doi: 10.1016/j.mineng.2013.07.011
- Lynch, A. J., Johnson, N. W., Manlapig, E. V., and Thorne, C. G., 1981, “Mineral and coal flotation circuits: Their simulation and control”, Elsevier, Amsterdam.
- Matos, V. E., Nogueira, S. C. S., Silva, G., Kowalczyk, P., and Peres, A. E. C., 2021. “Differences in Etheramines Froth Properties and the Effects on Iron Ore Flotation. Part II: Three-Phase Systems,” *Mineral Processing and Extractive Metallurgy Review*. DOI: 10.1080/08827508.2021.1888725

- Nakhaei, F., and Irannajad, M., 2018. “Reagent types in flotation of iron oxide minerals: a review,” *Mineral Processing and Extractive Metallurgy Review*, 39:2. pp. 89-124.
- Nykänen, V. P. S., Braga, A. S., Pinto, T. C. S., Matai, P. H. L. S., Lima, N. P., Filho, L. S. L., and Monte, M. B. M., 2020, “True flotation versus entrainment in reverse cationic flotation for the concentration of iron ore at industrial scale”, *Mineral Processing and Extractive Metallurgy Review*, Issue 1, Vol. 41, pp. 11-21.
- Pyykkö, P., and Atsumi, M., 2009. "Molecular Single-Bond Covalent Radii for Elements 1–118," *Chemistry – A European Journal*, Vol. 15, No. 1, pp. 186-197.
- Rao, S.R., 2004. “Electrical characteristics at interfaces,” In *Surface Chemistry of Froth Flotation*, 2nd ed.; Kluwer Academic/Plenum Publishers, New York, NY, USA, pp. 209–256.
- Rath, S. S., and Sahoo, H., 2020. “A review on the application of starch as depressant in iron ore flotation,” *Mineral Processing and Extractive Metallurgy Review*, DOI: 10.1080/08827508.2020.1843028
- Ren, L., Qiu, H., Zhang, Y., Nguyen, A., Zhang, M., Wei, P., and Long, Q., 2018. “Effects of alkyl ether amine and calcium ions on fine quartz flotation and its guidance for upgrading vanadium from stone coal,” *Powder Technology*, 338, pp. 180–189.

- Smith, P. G., and Warren, L. J., 1989. “Entrainment of Particles into Flotation Froths,” *Mineral Processing and Extractive Metallurgy Review*, 5:1-4, 123-145, DOI: 10.1080/08827508908952647
- Shortridge, P.G., Harris, P.J., Bradshaw, D.J, 1999. “The influence of ions on the effectiveness of polysaccharide depressants in the flotation of talc,” In *Proceedings of the 3rd UBC-McGill Bi-Annual International Symposium on Fundamentals of Mineral Processing*, Canadian Institute of Mining, Metallurgy and Petroleum, Quebec City, QC, Canada, pp. 155–169.
- Tang, M., and Wen, S., 2018. “Effects of cations/anions in recycled tailing water on cationic reverse flotation of iron oxides,” *Minerals*, 9, 161. Doi: 10.3390/min9030161
- Tang, M., Wen, S., and Liu, D., 2016. “Effects of heating- or caustic-digested starch on its flocculation on hematite,” *Mineral Processing and Extractive Metallurgy Review*, 37:1, 49-57, DOI: 10.1080/08827508.2015.1115986
- Yang, S., Li, C., and Wang, L., 2017. “Dissolution of starch and its role in the flotation separation of quartz from hematite,” *Powder Technology*. vol. 320. pp. 346-357.
- Zhang, X., Gu, X., Han, Y., Parra-Álvarez, N., Claremboux, V., and Kawatra, S. K., 2021, “Flotation of Iron Ores: A Review”, *Mineral Processing and Extractive Metallurgy Review*, Vol. 42, Issue 3. DOI: 10.1080/08827508.2019.1689494



## 6 Hydration of Hematite<sup>2</sup>

### 6.1 Abstract

The flotation of iron ore strongly depends on the surface charge. When hematite is ground fresh surfaces are created which have never been exposed to water. These surfaces differ from weathered hematite surfaces until they undergo hydration. This work seeks to determine if this effect is measurable in the zeta potential of the hematite, and investigates how long it takes for the hematite hydration to reach a stable equilibrium once water is added. Zeta potential measurements were performed on a dehydrated pure hematite sample which was added to water to determine the magnitude and time scale of the zeta potential changes during the hydration process. This investigation determined that the hydration of hematite occurs in 5-20 minutes. Silica was also investigated, and it was found that the zeta potential of silica did not change meaningfully over the course of an hour. This work concludes that the hydration of hematite proceeds rapidly enough that it is unlikely to play a meaningful role in the industrial flotation of iron ore.

### 6.2 Introduction

In an iron ore concentration plant, flotation is often used to separate iron oxides from gangue materials. Flotation depends on differences between the surfaces of the hematite

---

<sup>2</sup> The material contained in this chapter is in preparation for submission to the journal “Mineral Processing and Extractive Metallurgy Review”.

Citation:

Parra-Álvarez, N., Claremboux, V., and Kawatra, S. K., 2022, “Hydration of Hematite,” *Mineral Processing and Extractive Metallurgy Review*.

or magnetite from gangue materials like silica or alumina. It is known that hematite surfaces can undergo hydration when submerged in water (Parks, 1967). A review of the literature however has not clearly indicated how rapidly this hydration occurs. Does this hydration occur on a time scale relevant to the industrial flotation of iron ore? It takes about 30 minutes to 2 hours for iron ore to pass through the iron ore concentration process (Carlson and Kawatra, 2013).

When hematite is first mined from the ground, the surfaces of this hematite have typically already been exposed to groundwater or other natural weathering processes. When hematite is crushed and ground fresh surfaces are created, which have never been exposed to water. These surfaces have different chemistries, and should present different zeta potentials and flotation behavior until they have undergone the same hydration processes.

Hydration of an oxide mineral involves adding hydroxyl groups to exposed metal cations. Water will dissociate into  $H^+$  and  $OH^-$  ions, with the  $OH^-$  attaching to the metal ion and  $H^+$  associating with an existing oxygen ion to form a hydroxyl coating on the oxide surface (Parks, 1967). This process is usually believed to be rapid, but the authors have heard concerns related to an aging of iron ore after crushing from operating plants and other researchers.

If the hydration of these fresh surfaces takes place during the  $\frac{1}{2}$  to 2 hours that the hematite is expected to reside in the concentration process, then this sort of aging could have a significant impact on the flotation process. For example, the extent of dispersion demonstrated by recirculated material could be reasonably expected to differ from fresh

material. It would mean that the recirculated material should probably be treated as a different material than the fresh ore because of its different surface properties. On the other hand, if hydration takes less than half an hour or more than two hours, then it would suggest that there is no need to change current practices in response to ore aging behavior.

To investigate this effect, the zeta potential provides a key measure of the electrokinetic behavior of a particle's surface. The zeta potential measures the effective surface charge that determines the motion of a mineral surface in a fluid. Any significant changes in the flotation behavior of hematite are expected to be highlighted by changes in the zeta potential of the hematite and vice versa. Since zeta potential connects the hydration process to flotation behavior, zeta potential measurement was chosen as the primary method of investigating this phenomenon.

If the hydration of hematite is to be meaningful to the industrial flotation of iron ore then the zeta potential of the freshly ground hematite should vary significantly between half an hour and several hours after the introduction of water.

### **6.3 Materials and Methods**

The zeta potential evolves from the arrangement of ions within the solution. As such, a constant ionic strength was chosen so that zeta potential results could be compared directly between experiments. Table 1 indicates that 0.4 g of sodium chloride (NaCl) in 50 ml of deionized water gave the most consistent zeta potential measurements. Since NaCl is monovalent in both ions, this gives an ionic strength equal to its concentration:

0.137 mol/L. This ionic strength was maintained for all other zeta potential tests performed, using NaCl as a source of relatively inactive ions as necessary.

Table 6.1: Zeta potential variability of hematite in 50 ml of deionized water at increasing ionic strength conditions controlled by NaCl additions. Tests performed in triplicate.

<b>Sodium Chloride (NaCl) added (g)</b>	<b>Zeta potential of hematite (mV)</b>	<b>St. deviation (mV)</b>
0.1	5.32	8.71
0.2	-0.41	1.66
0.3	0.50	1.32
0.4	-0.83	0.39
0.5	0.22	1.40

The synthetic hematite used was an Iron(III) oxide, powder, <5 micron, ≥99%, obtained from Sigma Aldrich. Prior to each experiment, 10 grams of hematite were placed in a furnace at 600°C for 30 minutes to remove any water present in the sample. Once the hematite was removed from the furnace and cooled for a couple of minutes, it was added into 500 ml of the prepared solution. Three different solutions were used for these tests. One with a sodium bicarbonate/sodium carbonate buffer, one with an ammonium hydroxide/ammonium chloride buffer, and one with sodium hydroxide (NaOH) mixed with sodium chloride (NaCl) to maintain ionic strength.

As soon as the hematite was in contact with the solution, the sample was agitated with a magnetic stirrer at 600 RPM and the first zeta potential measurement was performed

immediately. For the experiments with buffer solutions, the next zeta potential measurements were performed every hour for the first 6 hours, and at 12, 24, 36, and 48 hours from the starting point. For the experiments with NaOH, the zeta potential was measured as many times as possible over a one-hour period. The zeta potential was measured using a Malvern Zetasizer Nano ZS. The sample was inserted into a DTS1070 folded capillary cell with a syringe and placed in the Zetasizer. The analysis consisted on three measurements each divided into 50 runs. Each sample was measured in triplicate and the exact time was recorded.

The synthetic silica used was a SIL-CO-SIL 40, composed of 99.7% silica, 44 microns, obtained from U.S. Silica, Ottawa, IL. Due to low loss on ignition, there was no need to place the silica samples in a furnace prior to experiments. The zeta potential of silica in a solution containing deionized water, NaOH, and NaCl, was measured continuously over a one-hour period.

## 6.4 Results and Discussion

Figures 1 and 2 show the zeta potential of hematite as it is submerged in deionized water with two kinds of alkaline buffers. As it is observed, both graphs show a similar pattern. At the first measurement (time = 0hrs) the zeta potential appeared to be negative. With the sodium bicarbonate/sodium carbonate buffer solution the initial measurement for hematite was  $-32.69 \pm 1.6$  mV (Figure 1), and with the ammonium hydroxide/ammonium chloride buffer solution the initial measurement for hematite was  $-10.79 \pm 0.6$  mV (Figure 2). After the first hour the zeta potential for both cases started to approach zero and remained near it for the rest of the experiments. This could indicate an increase in the

degree of surface hydration based on Parks (1967) who states that the IEP of oxides increases as hydration proceeds. A more basic IEP could explain why the zeta potential of hematite became less negative as the hydration time increased. Nevertheless, the use of buffers could have also altered the zeta potential of hematite. When the buffer was added, the cations and anions provided by the buffer may have reacted with the hematite surface to neutralize the surface charge.

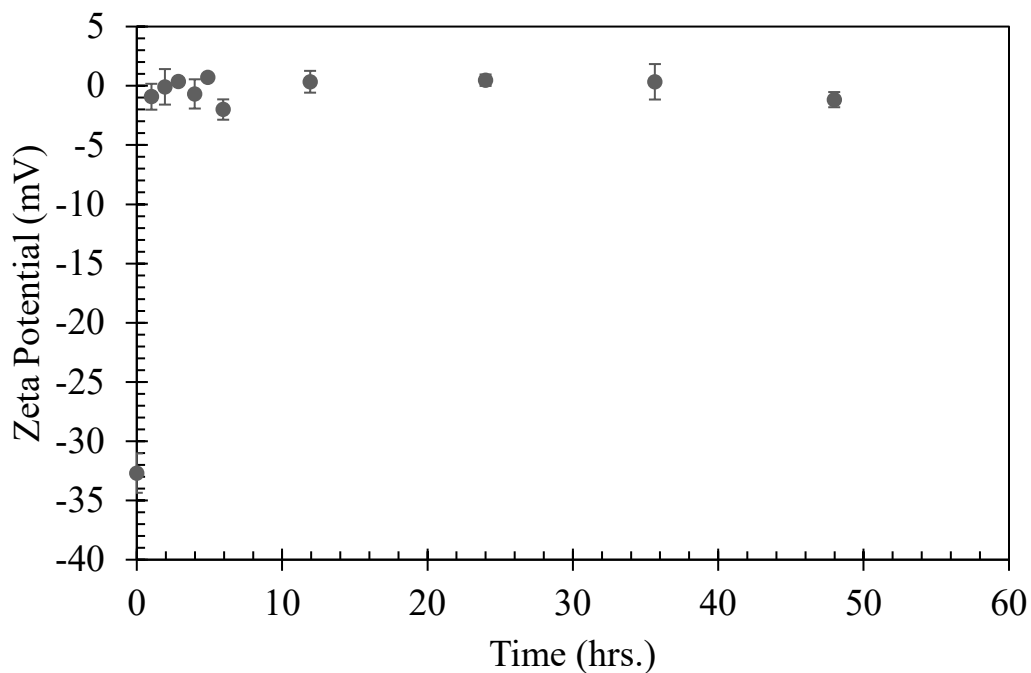


Figure 6.1: Zeta potential of hematite in a sodium bicarbonate/sodium carbonate buffer solution over a period of 48 hours. Initial pH of 10.43 and final pH of 10.27.

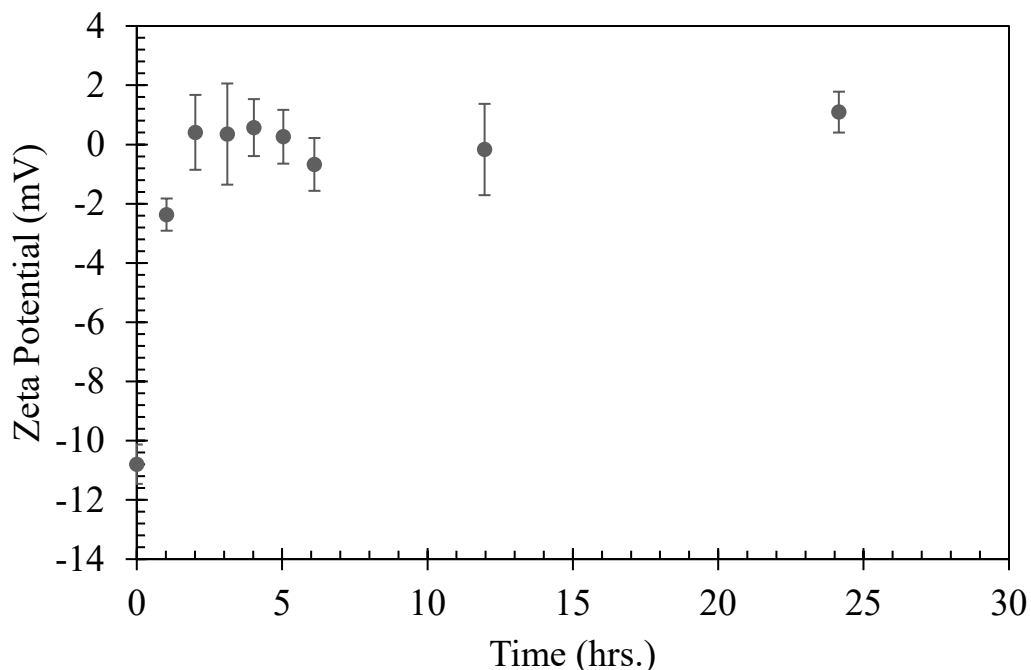


Figure 6.2: Zeta potential of hematite in an ammonium hydroxide/ammonium chloride buffer solution over a period of 24 hours. Initial pH of 10.95 and final pH of 9.18.

To rule out the possibility of the buffer neutralizing the zeta potential of hematite, tests were performed with NaOH to maintain alkaline pH levels. Continuous zeta potential measurements were taken over a period of one hour. These tests were not performed over 48 hours as the absorption of carbon dioxide from the atmosphere would affect the pH significantly. Figure 3 shows the obtained results. As it is observed, the graph followed a pattern similar to the one observed in Figure 1 and 2. The initial zeta potential of hematite was recorded to be  $-10.7 \pm 0.9$  mV but after a few minutes of the hematite submerged in solution, the zeta potential started becoming less negative and remained near zero for the next 40+ minutes. Now that this behavior cannot be attributed to the presence of a buffer,

it is clear that as soon as the hematite becomes submersed in solution, the surface hydration process takes place.

In the reverse cationic flotation of hematite, the goal is to separate hematite from silica and other impurities. Zeta potential measurements on the silica were performed continuously with NaOH over a period of one hour. Results are shown in Figure 4. No significant change was observed on the zeta potential of silica over the period studied. Given that the zeta potential averaged approximately -36 mV it is inferred that the silica hydrated immediately as it became in contact with the solution. Perhaps even faster than what was observed with the hematite.

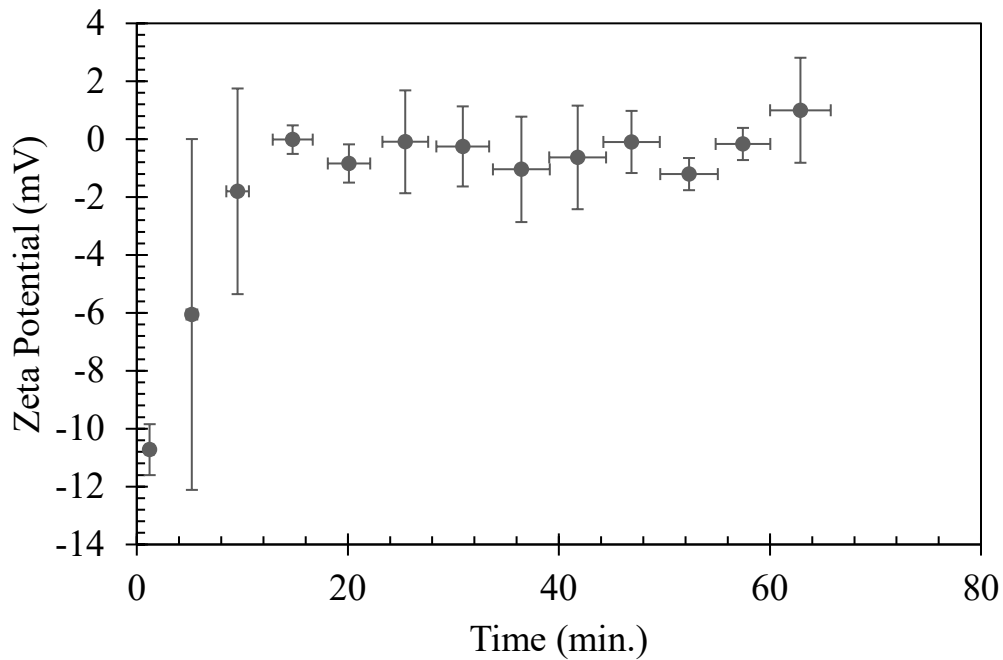


Figure 6.3: Zeta potential of hematite in a solution containing sodium hydroxide (NaOH) mixed with sodium chloride (NaCl) over a period of 1 hour. Initial pH of  $9.9 \pm 0.1$  and final pH of  $9.3 \pm 0.2$ .



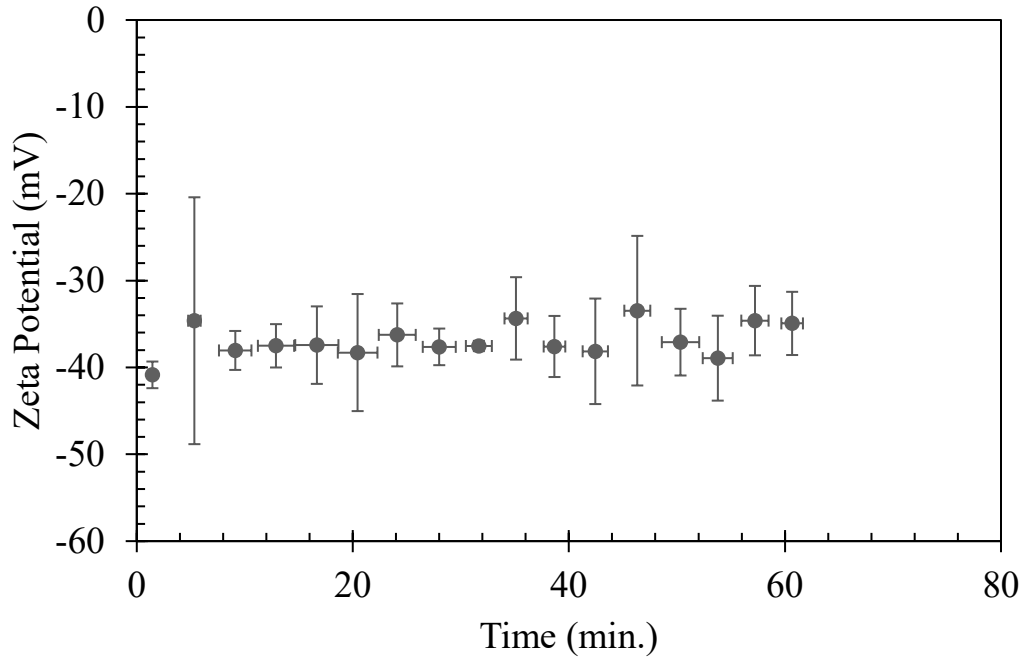


Figure 6.4: Zeta potential of silica in a solution containing sodium hydroxide (NaOH) mixed with sodium chloride (NaCl) over a period of 1 hour. Initial pH of  $10.1 \pm 0.05$  and final pH of  $7.8 \pm 0.8$ .

Prior to this research, no single study defined the rate at which the hematite becomes hydrated in a flotation system. It was unknown whether the rate of hydration could affect the adsorption of reagents and thus the process performance. In general, the average period that it takes for the ore to pass through the plant is from 30 minutes to 2 hours (Carlson and Kawatra, 2013). With this research it was determined that the hematite hydrates within 5 to 20 minutes of being immersed in water, thus studying the effect of degree of hydration on the adsorption of reagents in flotation becomes irrelevant.

## 6.5 Conclusion

The time scale of the hydration of pure hematite was determined to be on the order of 5 to 20 minutes. Conversely, the zeta potential of silica was found to be effectively constant over the course of the same experiments. From these conclusions, we determine that in a plant-scale operation, it is very likely that the hydration of hematite is entirely completed before it reaches flotation.

## 6.6 References

- Carlson, J. J, and Kawatra, S. K., 2013. “Factors affecting zeta potential of iron oxides,” *Mineral Processing and Extractive Metallurgy Review*, 34:5, 269-303, DOI: 10.1080/08827508.2011.604697
- Parks, G. A., 1967. “Aqueous surface chemistry of oxides and complex oxide minerals.” *Advances in Chemistry Series*, 67, pp. 115–123.
- Zhang, X., Gu, X., Han. Y, Parra-Álvarez, N., Claremboux, V., and Kawatra, S.K., 2021. “Flotation of iron ores: A review,” *Mineral Processing and Extractive Metallurgy*, 42(3), pp. 184-212.

## A Copyright documentation

Figure 4.2 and the figures found in Table 4.1 are from Wikipedia. They are all public domain. Please see below for full citations.

Figure 4.2:

- “Primary amine” by Kes47. Licensed under Public domain via Wikimedia Commons - <https://commons.wikimedia.org/wiki/File:Primary-amine-2D-general.svg>. Accessed March 2022.
- “Secondary amine” by by Kes47. Licensed under Public domain via Wikimedia Commons - <https://commons.wikimedia.org/wiki/File:Secondary-amine-2D-general.svg>. Accessed March 2022.
- “Tertiary amine” by by Kes47. Licensed under Public domain via Wikimedia Commons - <https://commons.wikimedia.org/wiki/File:Amine-2D-general.svg>. Accessed March 2022.
- “Quaternary ammonium cation” by Fvasconcellos. Licensed under Public domain via Wikimedia Commons - [https://commons.wikimedia.org/wiki/File:Quaternary\\_ammonium\\_cation.svg](https://commons.wikimedia.org/wiki/File:Quaternary_ammonium_cation.svg). Accessed March 2022.

Table 4.1 – Figure citations:

- “Structural formula of aniline” by Chem Sim 2001. Licensed under Public domain via Wikimedia Commons - [https://commons.wikimedia.org/wiki/File:Structural\\_formula\\_of\\_aniline.svg](https://commons.wikimedia.org/wiki/File:Structural_formula_of_aniline.svg). Accessed March 2022.

- “Dodecylamin” by Kopiersperre. Licensed under Public domain via Wikimedia Commons - <https://commons.wikimedia.org/wiki/File:Dodecylamin.svg>. Accessed March 2022.
- “Tryptamine” by Harbin. Licensed under Public domain via Wikimedia Commons - <https://commons.wikimedia.org/wiki/File:Tryptamine.svg>. Accessed March 2022.

All other material in this document is the author’s original work.